

Supporting Information:
**Mechanistic Insights into the Hydrolysis of Organophosphorus
Compounds by Paraoxonase 1: Exploring the Limits of Selectivity of a
Promiscuous Enzyme**

Sivaramakrishnan Muthukrishnan,¹ Vivekanand S. Shete,¹ Toby. T. Sanan,^{1,1}
Shameema Oottikkal,¹ Lauren M. Porter,¹ Thomas J. Magliery*^{1,2}, Christopher M.
Hadad*¹

Departments of Chemistry¹ and Biochemistry², The Ohio State University, 100 W. 18th
Avenue, Columbus, Ohio 43210

*To whom correspondence should be addressed:

TJM: magliery@chemistry.ohio-state.edu, phone (614) 247-8425

CMH: hadad.1@osu.edu, phone (614) 688-3141

Table of Contents

1. General synthetic procedures for OP substrates and inhibitors	S2
2. Complete Library of ligands studied	S2-S4
3. ¹ H NMR, ¹³ C NMR, IR spectroscopic and Mass Spectrometric data	S4-S48
4. Results of Enzyme Kinetics	S49-S50
5. Selected Poses from docking of ligands in G2E6	S50-S54
6. Selected Poses from MD simulations of ligand-G2E6 complex	S54-S60
7. Thermochemistry for the hydrolysis of ligands (without enzyme)	S61-S62
8. References	S62-S63

1. General synthetic procedures for OP substrates and Inhibitors:

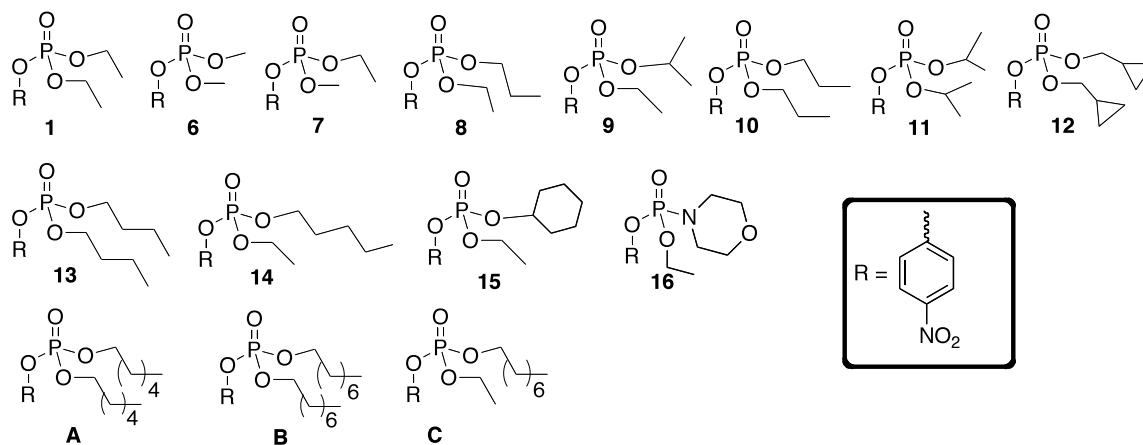
The general reaction for the preparation of the photoaffinity labels (PAL-Group ID) was the addition of a phosphoryl dichloridate (1 equivalent) to the corresponding alcohol (1 equivalent) in the presence of toluene at 0°C. A solution of triethylamine (1 equivalent) in toluene was added dropwise, and the reaction was brought to room temperature and stirred overnight. The reaction mixture was filtered and the supernatant was evaporated. The solid residue was then re-suspended in dry acetone. Upon cooling the mixture to 0°C, sodium azide (1 equivalent) was added and the reaction was stirred for 8 hours. The reaction mixture was filtered, and the solvent was evaporated. The crude product was purified by silica gel column chromatography (hexane:ethyl acetate 80:20 as the eluent). Compounds were obtained in 40–80% yield. The purified compounds were analyzed by IR, ¹H and ¹³C NMR as well as HRMS.

The general reaction for the formation of the SAR substrates/inhibitors was the addition of a phosphoryl dichloridate (1 equivalent) to the corresponding alcohol (2 equivalents) in the presence of toluene at 0°C. A solution of triethylamine (2 equivalents) in toluene was added dropwise, and the reaction was stirred at room temperature overnight. The reaction mixture was filtered, and the solvent was then evaporated. The crude product was purified by silica gel column chromatography (hexane:ethyl acetate 80:20 as the eluent). Compounds were isolated in 50–80% yield. The purified compounds were analyzed by IR, ¹H and ¹³C NMR as well as HRMS.

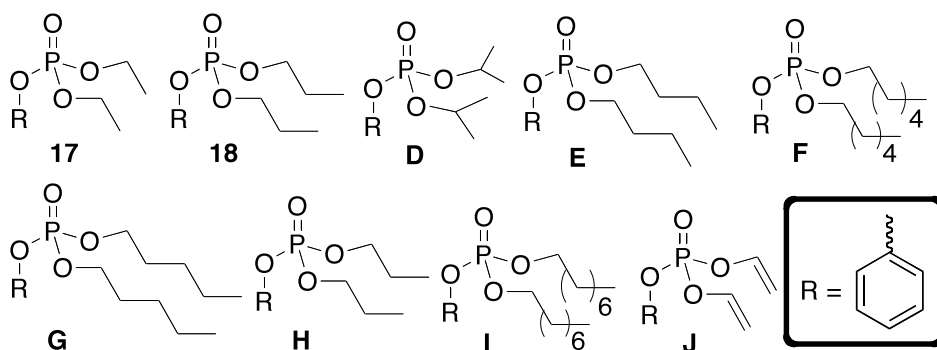
2. Complete Library of ligands studied

Compounds A-P were also synthesized and screened; since they had no hydrolytic activity against G2E6 PON1, these molecules were not discussed in the manuscript.

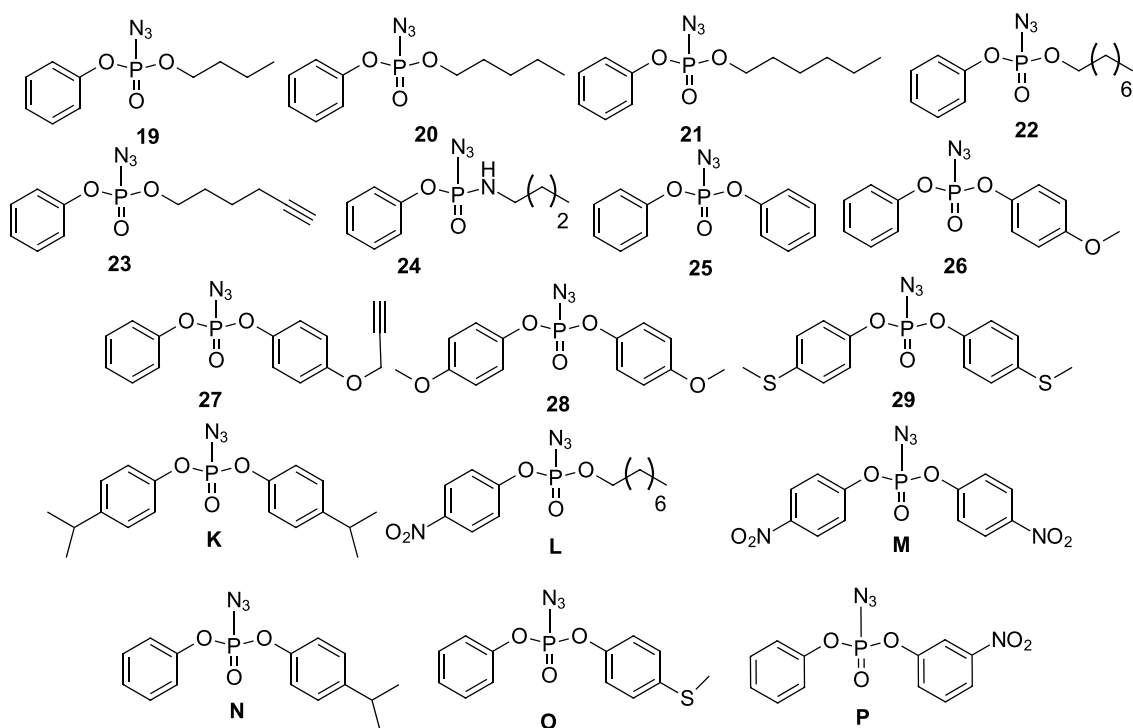
Group I



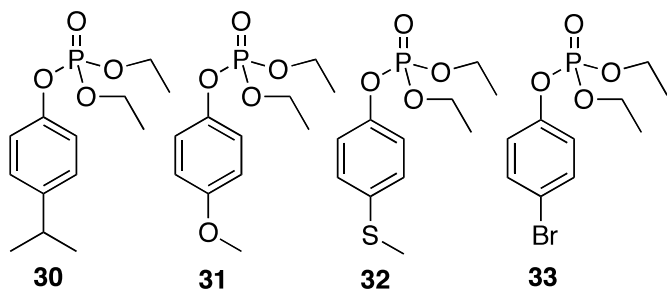
Group II



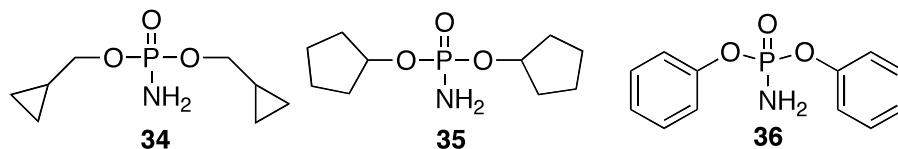
Group III



Group IV



Group V

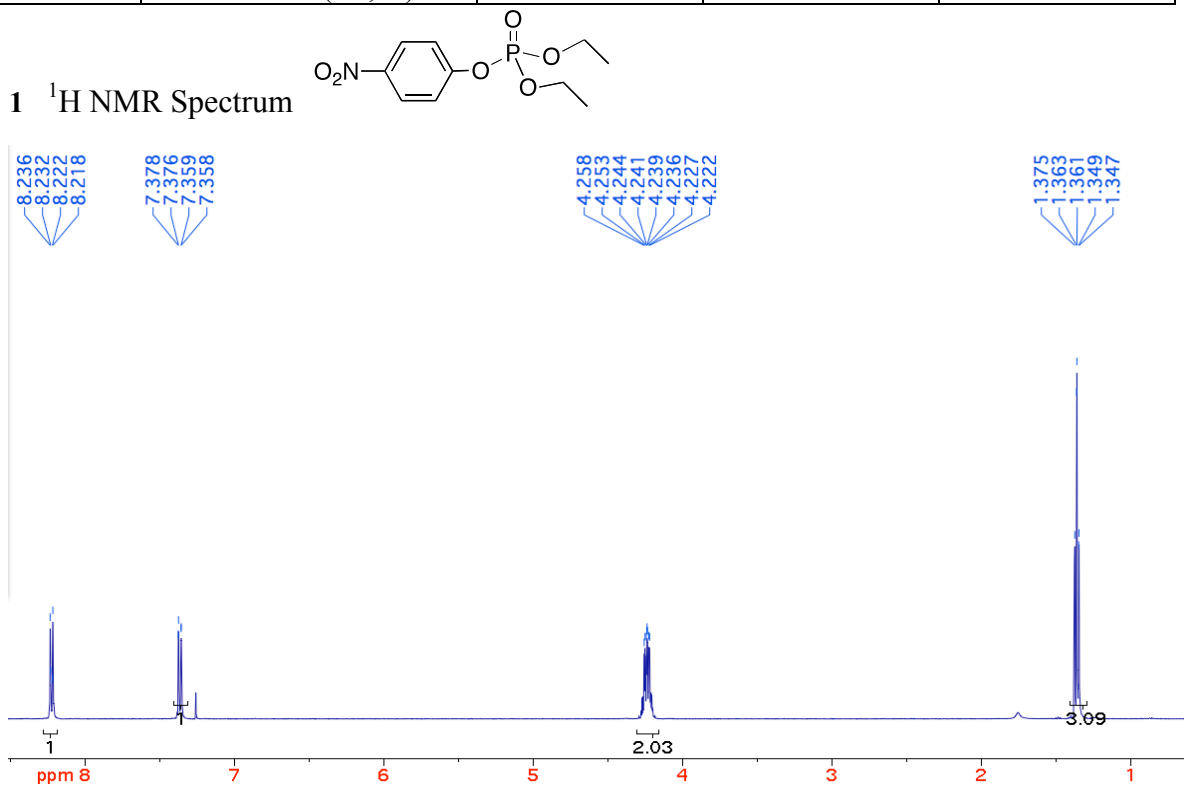


3. ¹H NMR, ¹³C NMR, IR spectroscopic and Mass Spectrometric data of newly synthesized molecules.

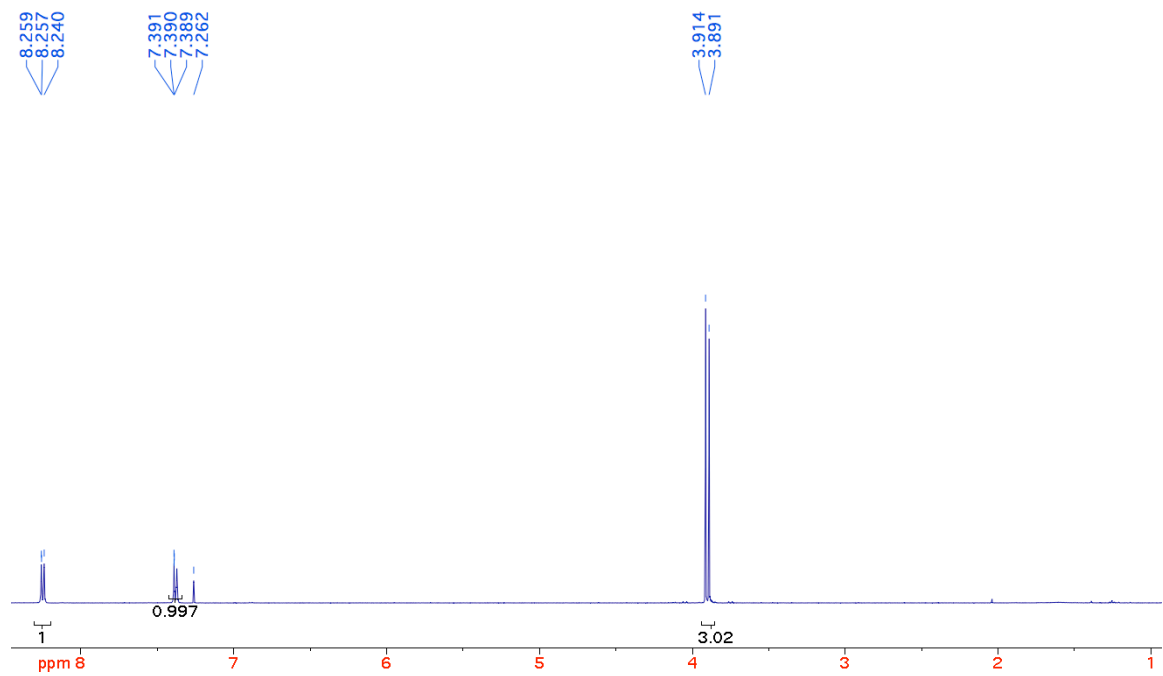
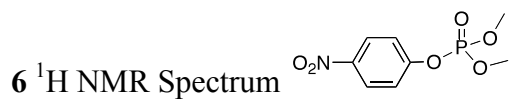
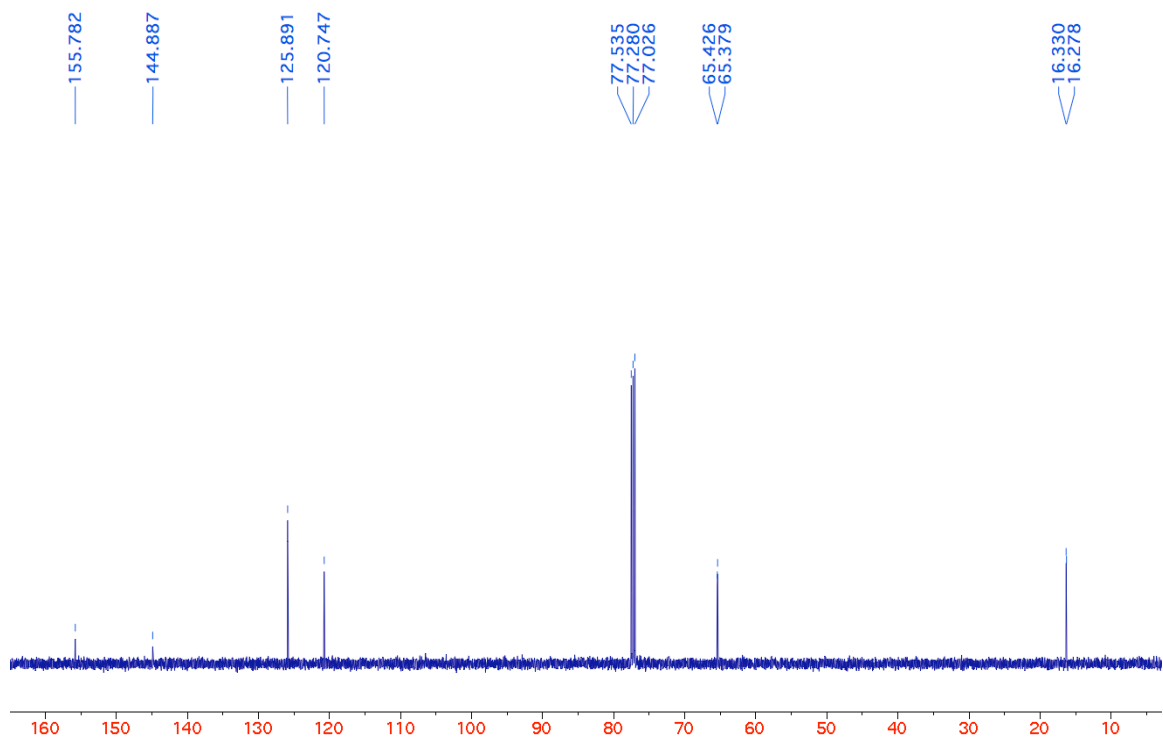
Molecule	¹ H NMR	¹³ C NMR	IR	MS
1	8.22 (2H, d, <i>J</i> 10 Hz), 7.36 (2H, d, <i>J</i> 10 Hz), 4.23 (4H, q, <i>J</i> 5 Hz), 1.35 (6H, t, <i>J</i> 5 Hz)	155.8, 144.8, 125.9, 120.7, 65.4, 16.3	2988, 29840, 1590, 1345	Calc. (M+Na) ⁺ 298.0456 Expt 298.0449
6	8.25 (2H, d, <i>J</i> 10 Hz), 7.38 (2H, d, <i>J</i> 10 Hz), 3.91 (6H, d, <i>J</i> 10 Hz)	155.3, 144.8, 125.7, 120.5, 55.3	3017, 2914, 2860, 1252, 1045	Calc (M+Na) ⁺ 270.0143 Expt 270.0141
7	8.25 (2H, d, <i>J</i> 10 Hz), 7.38 (2H, d, <i>J</i> 10 Hz), 4.28-4.25 (2H, m), 3.90 (6H, d, <i>J</i> 10 Hz), 1.40- 1.37 (3H, m),	155.8, 145.1, 126.0, 120.9, 65.8, 55.5, 16.5	2928, 2846, 1048	Calc (M+Na) ⁺ 284.0300 Expt 284.0301
8	8.20 (2H, d, <i>J</i> 10 Hz), 7.35 (2H, d, <i>J</i> 10 Hz), 4.24-4.22 (2H, m), 4.11- 4.09 (2H, m), 1.72-1.68 (2H, m), 1.36-1.33 (3H, m), 0.94-0.92 (3H, m)	155.6, 144.6, 125.6, 120.5, 70.6, 65.2, 23.5, 16.1, 9.9	2987, 1591, 1342, 1290, 1023,	Calc (M+Na) ⁺ 312.0613 Expt 312.0610
9	8.18 (2H, d, <i>J</i> 10 Hz), 7.33 (2H, d, <i>J</i> 10 Hz), 4.76-4.74 (1H, m), 4.20- 4.17 (2H, m), 1.29-1.34 (9H, m),	155.7, 144.5, 125.5, 120.5, 74.6, 65.0, 50.4, 23.4, 16.0	2980, 1580, 1349, 1256, 1025	Calc (M+Na) ⁺ 312.0613 Expt 312.0611
10	8.22 (2H, d, <i>J</i> 10 Hz),	155.9, 144.8,	2960, 1590,	Calc (M+H) ⁺

	7.37 (2H, d, <i>J</i> 10Hz), 4.13 (4H, q, <i>J</i> 5Hz), 1.74- 1.71 (4H, m), 0.95 (6H, q, <i>J</i> 5Hz)	125.8, 120.7, 70.7, 23.8, 10.1	1339, 1236, 1015	304.0950 Expt 304.0965
11	8.20 (2H, d, <i>J</i> 10 Hz), 7.34 (2H, d, <i>J</i> 10 Hz), 4.74 (2H, q, <i>J</i> 5Hz), 1.32 (12H, d, <i>J</i> 5 Hz)	156.4, 144.6, 125.7, 120.6, 74.4, 14.3	2984, 2938, 1592, 1347, 1008	Calc. (M+Na) ⁺ 326.0769 Expt 326.0739
12	8.23 (2H, d, <i>J</i> 10Hz), 7.38 (2H, d, <i>J</i> 10Hz), 4.04 (4H, q, <i>J</i> 10Hz), 1.19-1.21 (2H, m), 0.60 (4H, d, <i>J</i> 10Hz), 0.32 (4H, d, <i>J</i> 10Hz)	151.2, 130.0, 125.2, 120.4, 73.7, 11.5, 3.8	3114, 2894, 1522, 1347, 1036	Calc (M+Na) ⁺ 350.0769 Expt 350.0786
13	8.25 (2H, d, <i>J</i> 10Hz), 7.38 (2H, d, <i>J</i> 10Hz), 4.18 (4H, q, <i>J</i> 5Hz), 1.72- 1.68 (4H, m), 1.44-1.41 (4H, m), 0.94 (6H, t, <i>J</i> 5Hz)	155.8, 144.8, 125.8, 120.7, 69.0, 32.3, 18.8, 13.7	2956, 1591, 1523, 1346, 1233	Calc (M+Na) ⁺ 354.1082 Expt 354.1078
14	8.23 (2H, d, <i>J</i> 10Hz), 7.35 (2H, d, <i>J</i> 10Hz), 4.25-4.24 (2H, m), 4.18- 4.15 (2H, m), 1.71-1.70 (2H, m), 1.39-1.35 (7H, m), 0.89-0.88 (3H, m)	155.8, 144.8, 125.8, 120.6, 69.3, 65.3, 29.5, 27.6, 22.2, 16.2, 14.0	2950, 1601, 1388, 1295, 1101	Calc (M+Na) ⁺ 340.0926 Expt 340.0923
15	8.25 (2H, d, <i>J</i> 10Hz), 7.39 (2H, d, <i>J</i> 10Hz), 4.54-4.52 (1H, m), 4.26- 4.24 (2H, m), 1.96-1.93 (2H, m), 1.77-1.74 (2H, m), 1.39-1.30 (3H, m), 1.28 (3H, t, <i>J</i> 5Hz), 1.27- 1.26 (3H, m)	155.8, 144.5, 125.6, 120.6, 79.2, 65.0, 33.2, 24.9, 23.4, 16.0	2921, 2866, 1259, 1045	Calc (M+Na) ⁺ 352.1395 Expt 352.1390
16	8.20 (2H, d, <i>J</i> 10Hz), 7.34 (2H, d, <i>J</i> 10Hz), 4.19-4.17 (2H, m), 3.61- 3.60 (4H, m), 3.21-3.19 (4H, m), 1.35 (3H, t, <i>J</i> 5Hz),	156.0, 144.4, 125.6, 120.6, 66.8, 63.7, 44.6, 16.1	3010, 2921, 2860, 1255, 1048	Calc (M+Na) ⁺ 339.0722 Expt 339.0722
A	8.18 (2H, d, <i>J</i> 10Hz), 7.34 (2H, d, <i>J</i> 10Hz), 4.12 (4H, q, <i>J</i> 5Hz), 1.65 (4H, t, <i>J</i> 5Hz), 1.31 -1.24 (12H, m), 0.82 (6H, t, 5Hz)	155.6, 144.6, 125.5, 120.5, 69.1, 31.1, 30.1, 24.9, 22.4, 13.8	2928, 1593, 1346, 1023, 936	Calc (M+Na) ⁺ 410.1708 Expt 410.1724
B	8.15 (2H, d, <i>J</i> 10Hz), 7.31 (2H, d, <i>J</i> 10Hz), 4.10-4.09 (4H, m), 4.02-	155.6, 144.5, 125.5, 120.5, 69.0, 60.2, 31.6,	2957, 1593, 1346, 1295,	Calc (M+Na) ⁺ 466.2334

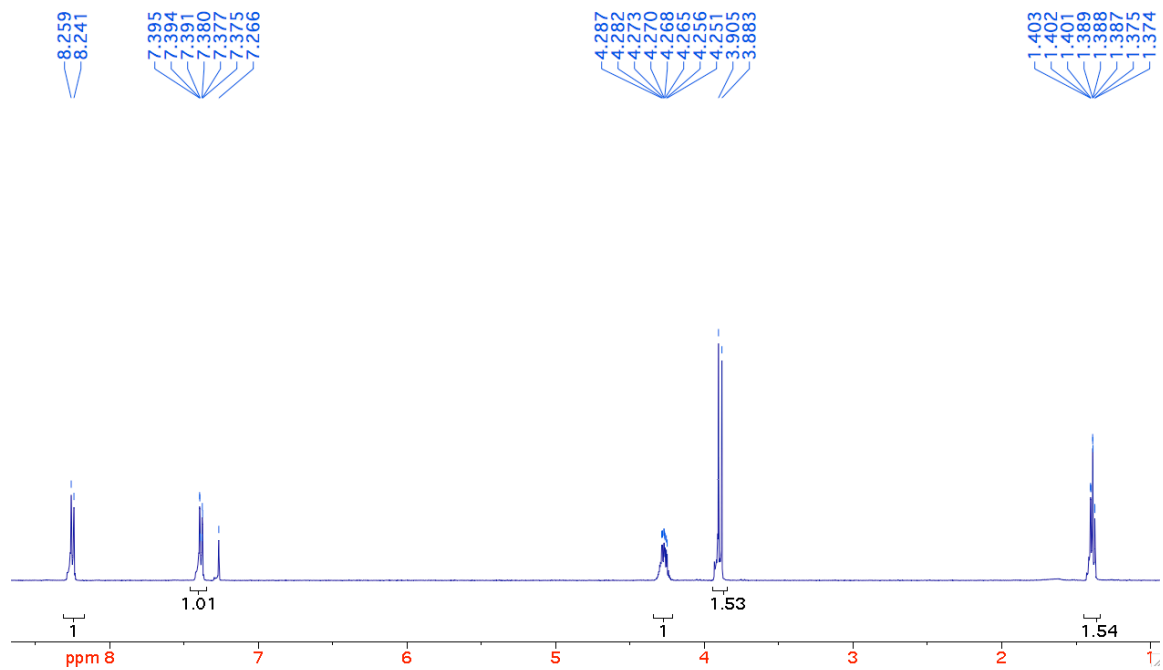
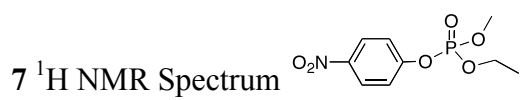
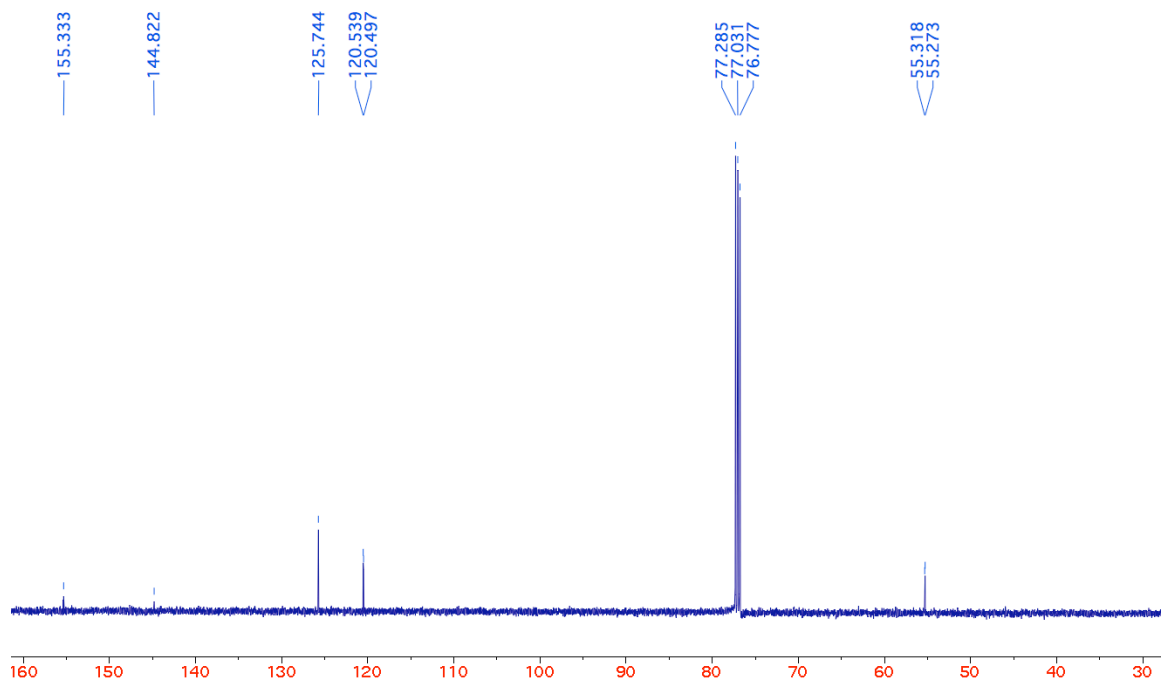
	4.01(4H,m), 1.63-1.61(4H, m), 1.27-1.14 (16H, m), 0.8-0.6 (6H, m)	30.2, 29.1, 25.3, 22.5, 13.9	1023,	Expt 466.2292
C	8.24 (2H, d, <i>J</i> 10Hz), 7.38 (2H, d, <i>J</i> 10Hz), 4.26-4.24 (2H, m), 4.18-4.17(2H, m), 1.71-1.70 (2H, m), 1.40-1.37 (3H, m), 1.28-1.25 (10H, m), 0.89-0.86 (3H, m)	155.8, 144.8, 125.8, 120.7, 69.4, 65.4, 31.9, 30.4, 29.3, 25.5, 22.8, 16.3, 14.2	2955, 1590, 1346, 1295, 1028,	Calc (M+Na) ⁺ 382.1395 Expt 382.1390



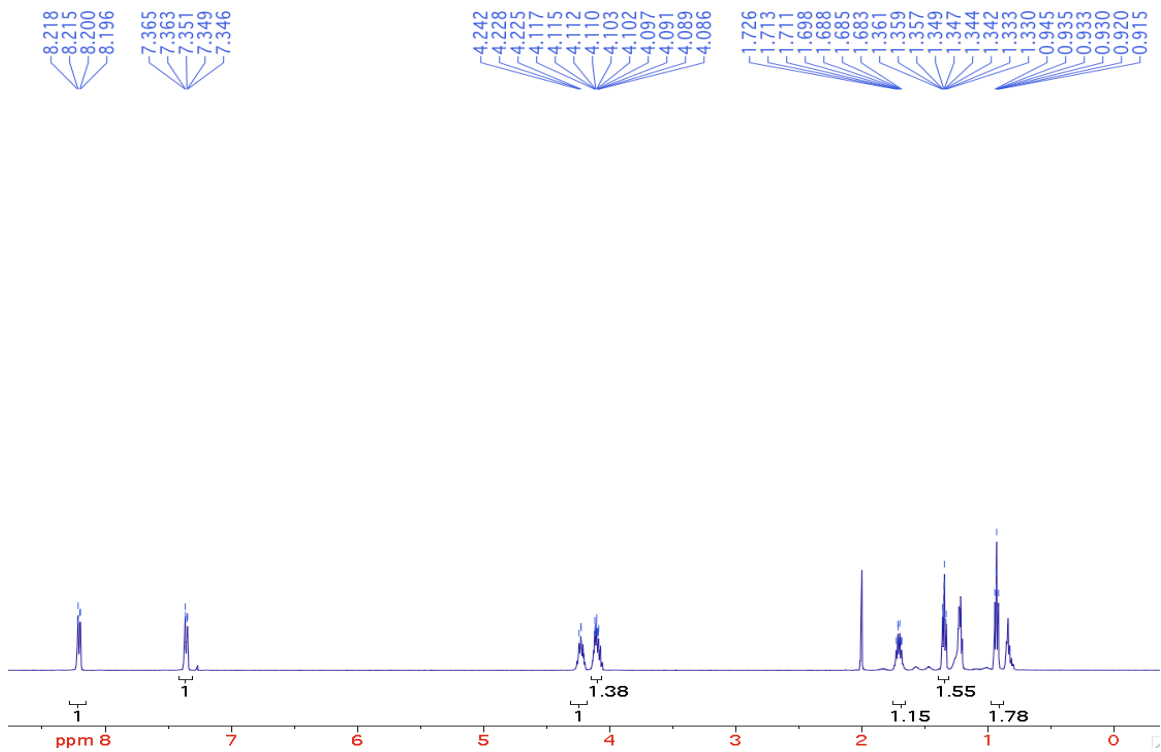
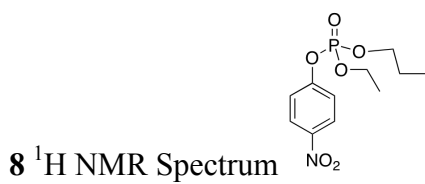
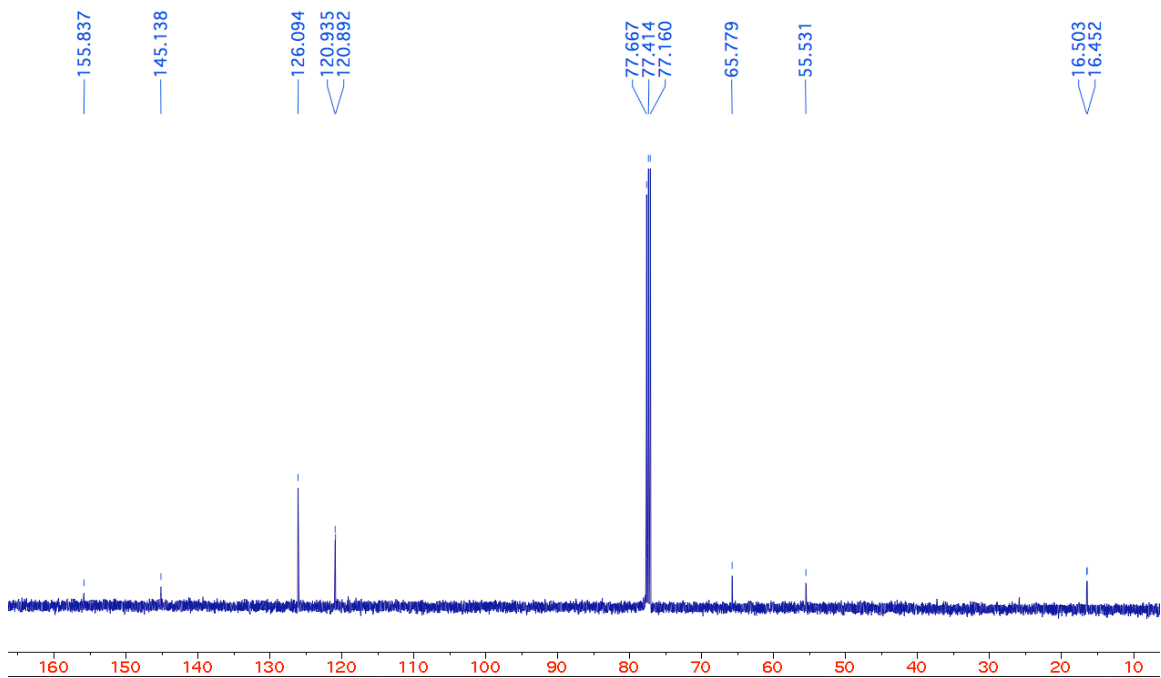
¹³C NMR Spectrum



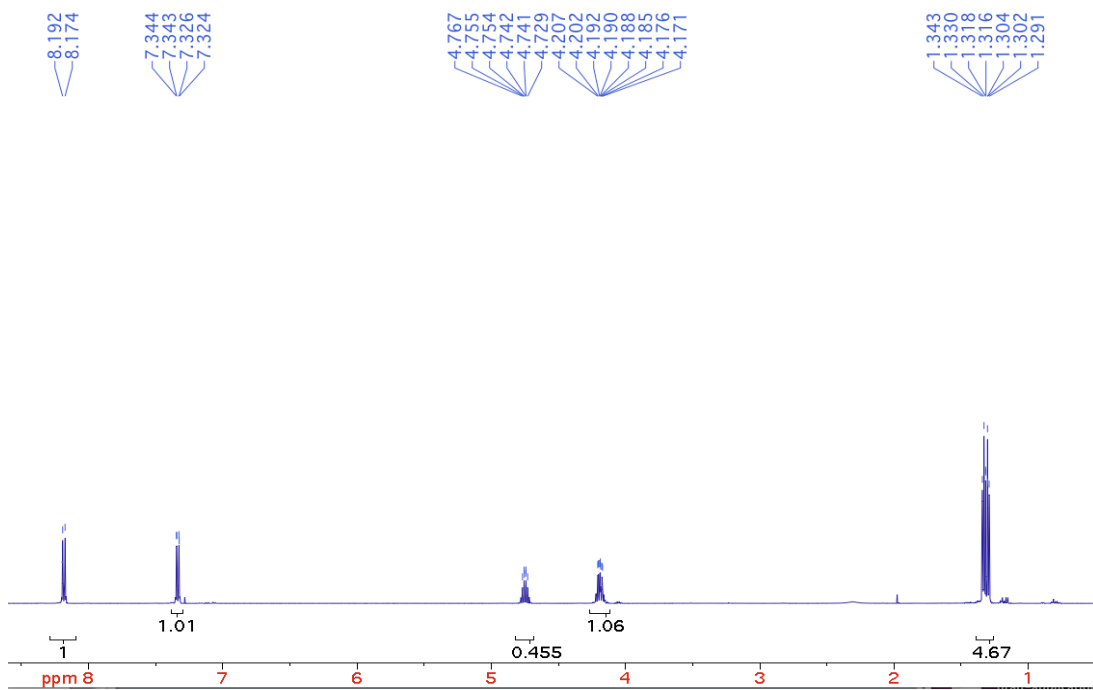
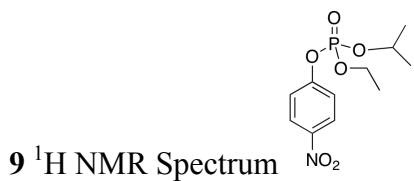
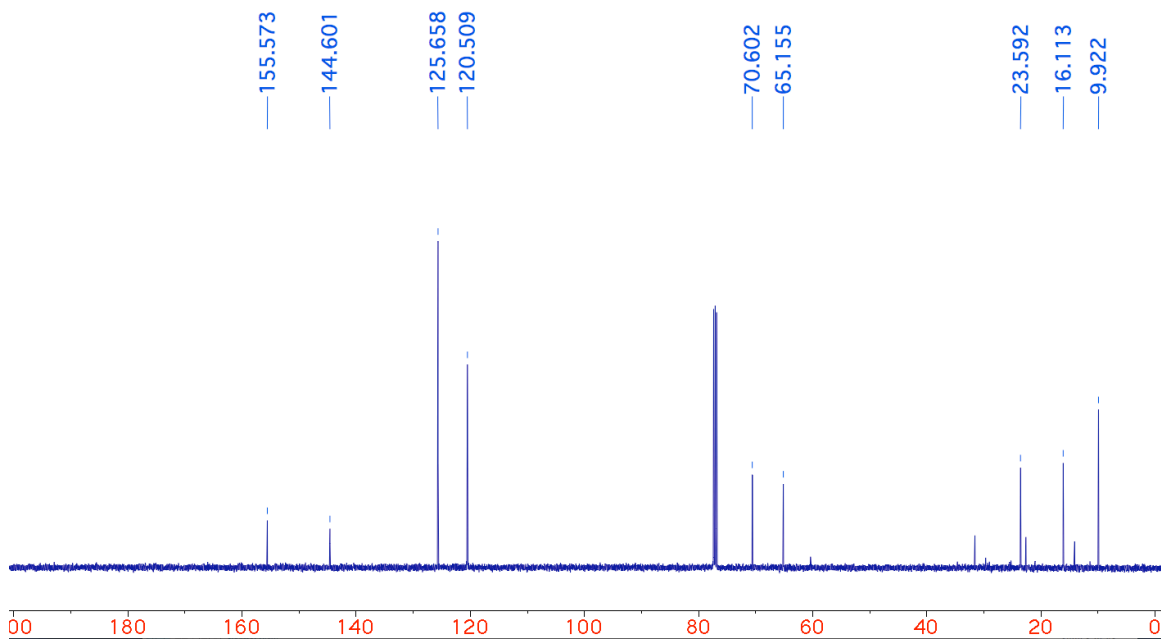
^{13}C NMR Spectrum



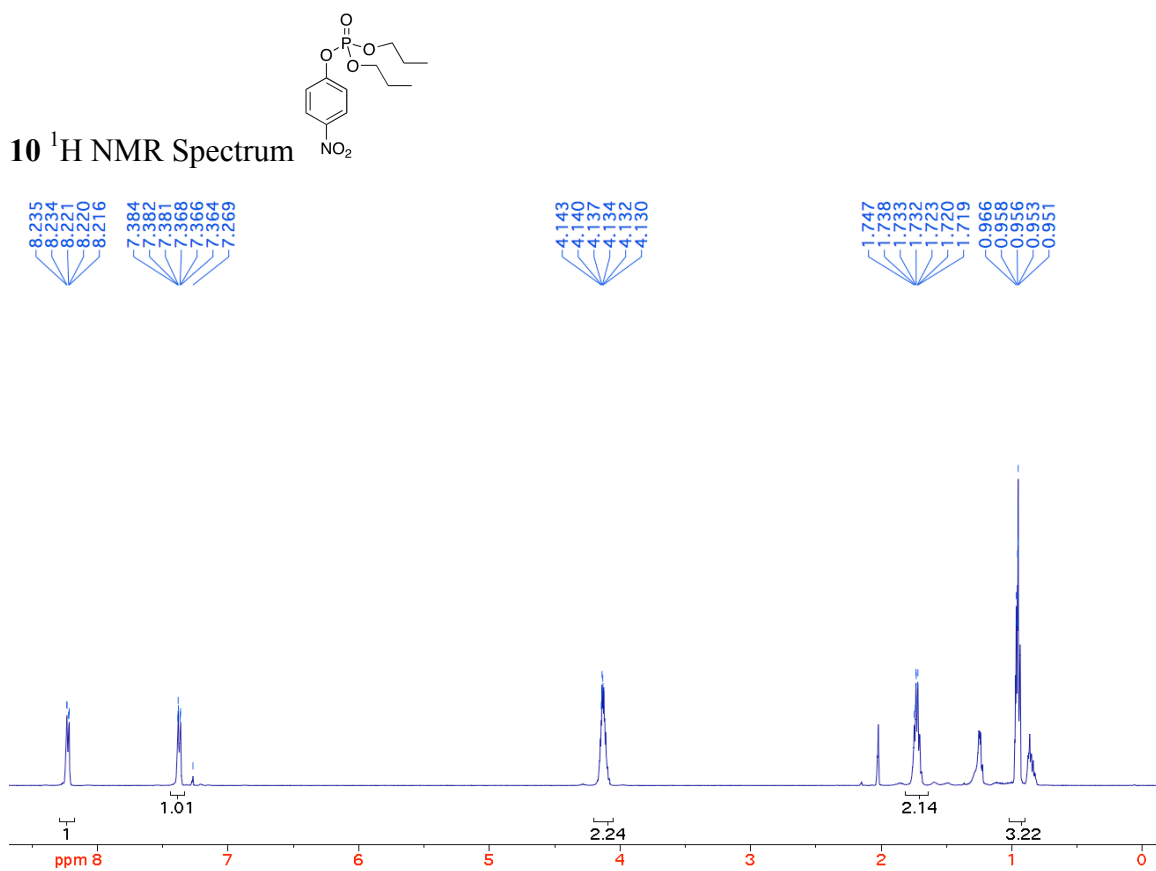
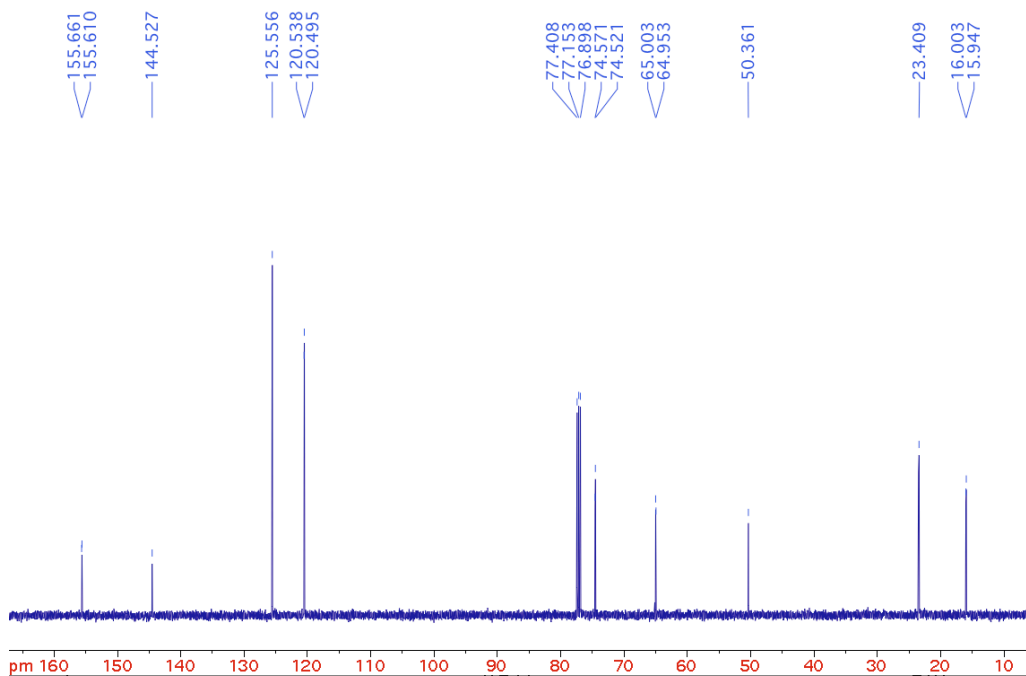
^{13}C NMR Spectrum



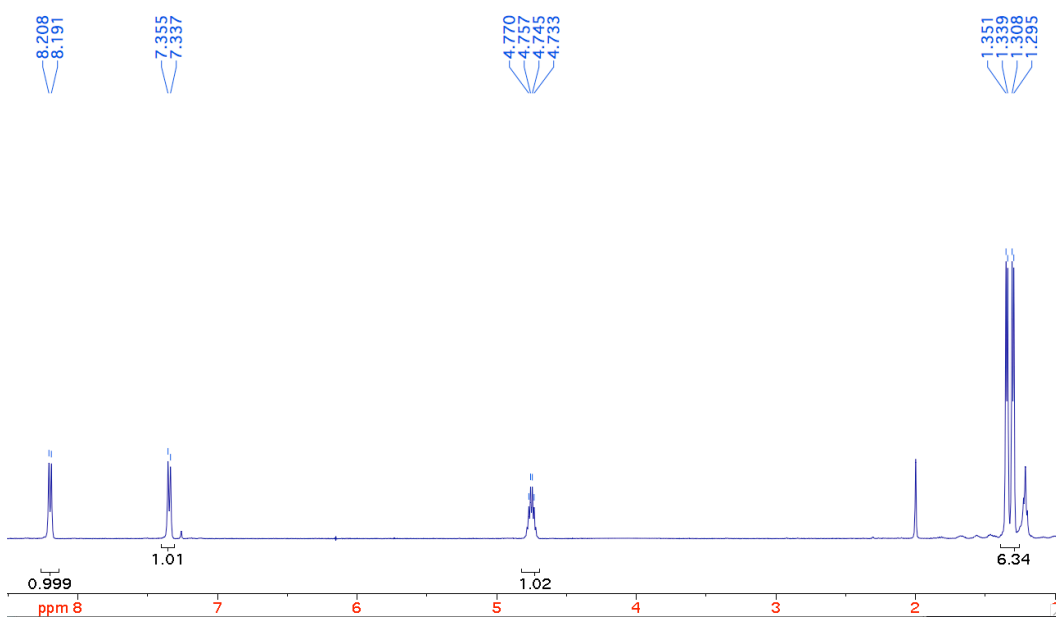
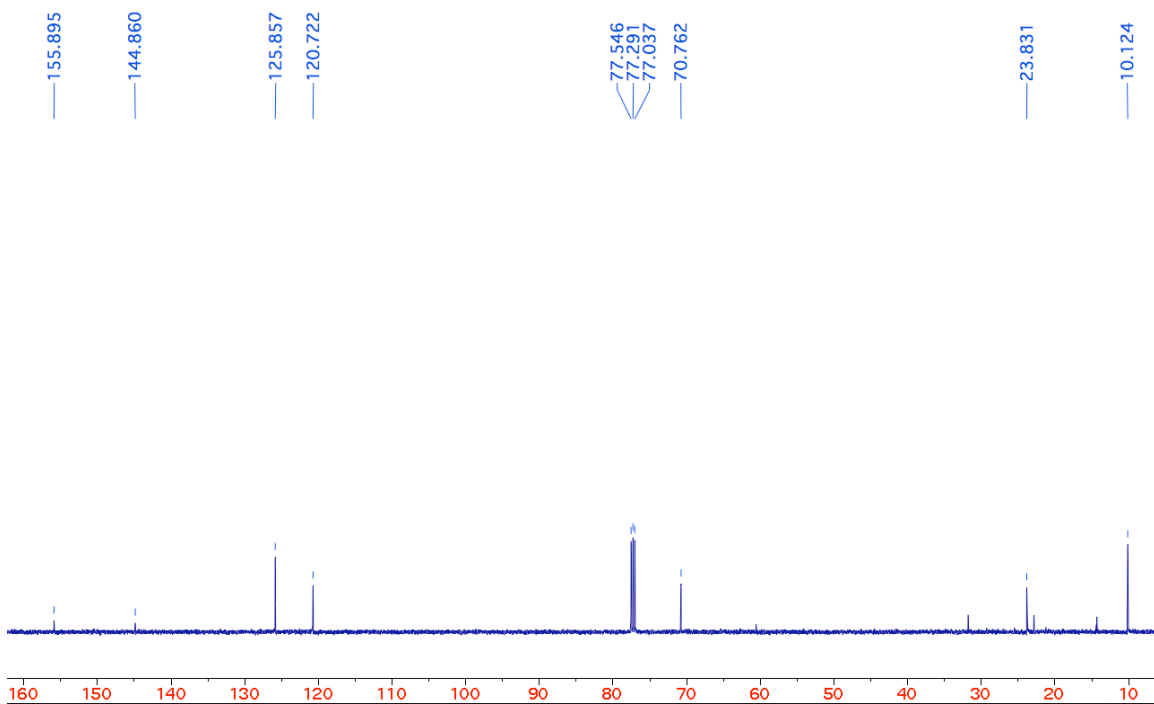
^{13}C NMR Spectrum



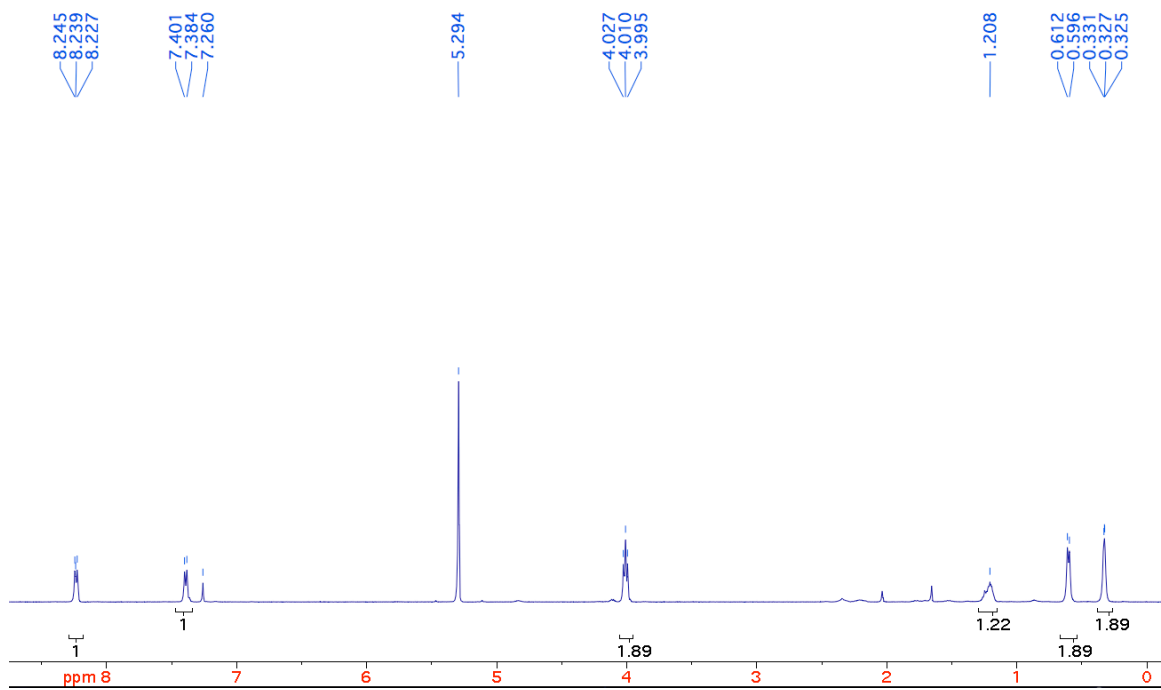
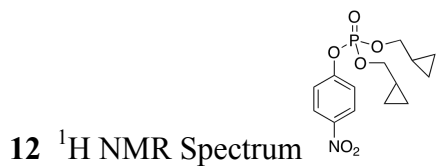
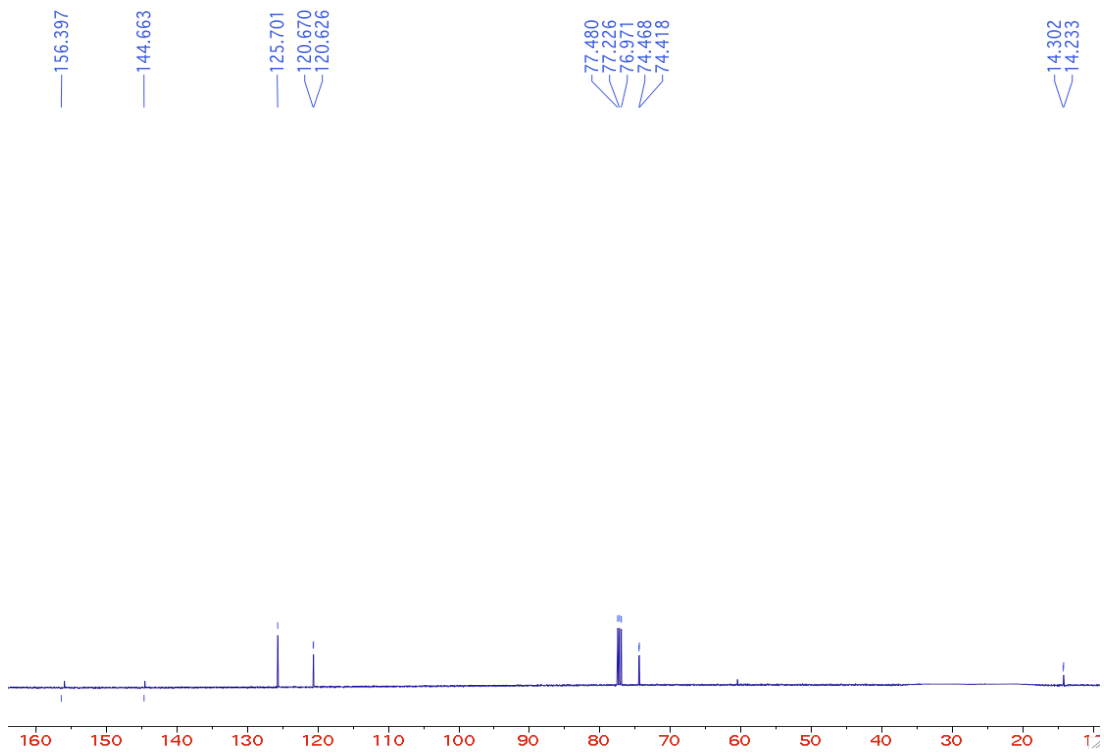
¹³C NMR Spectrum



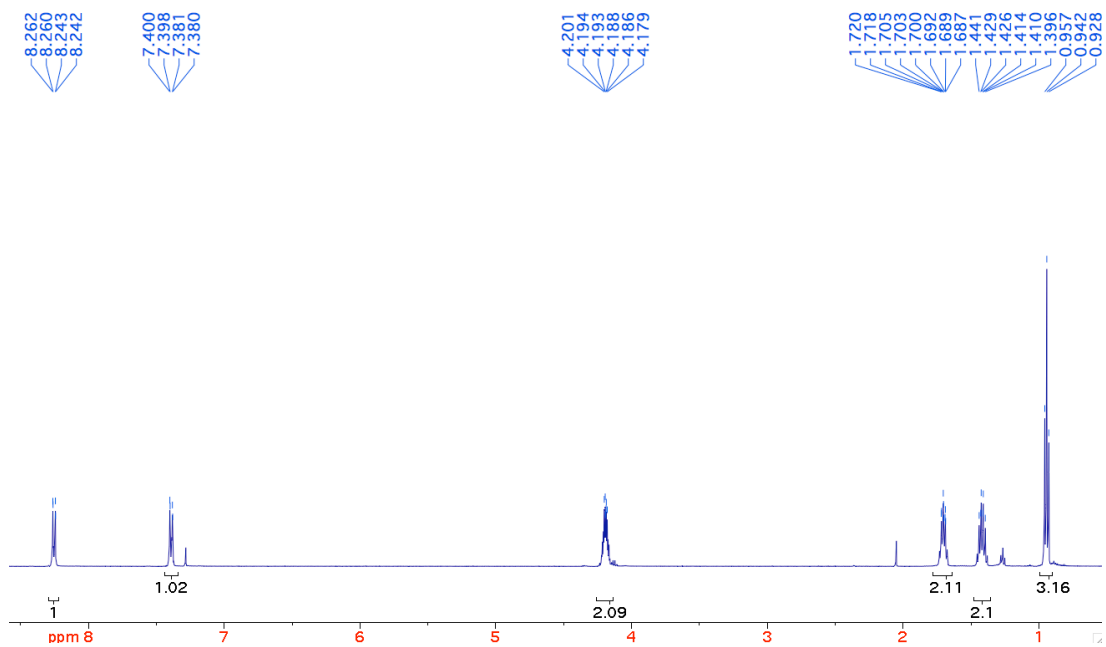
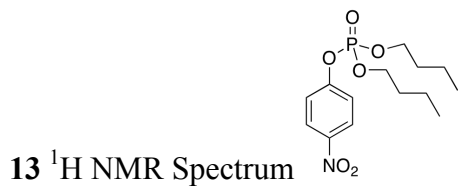
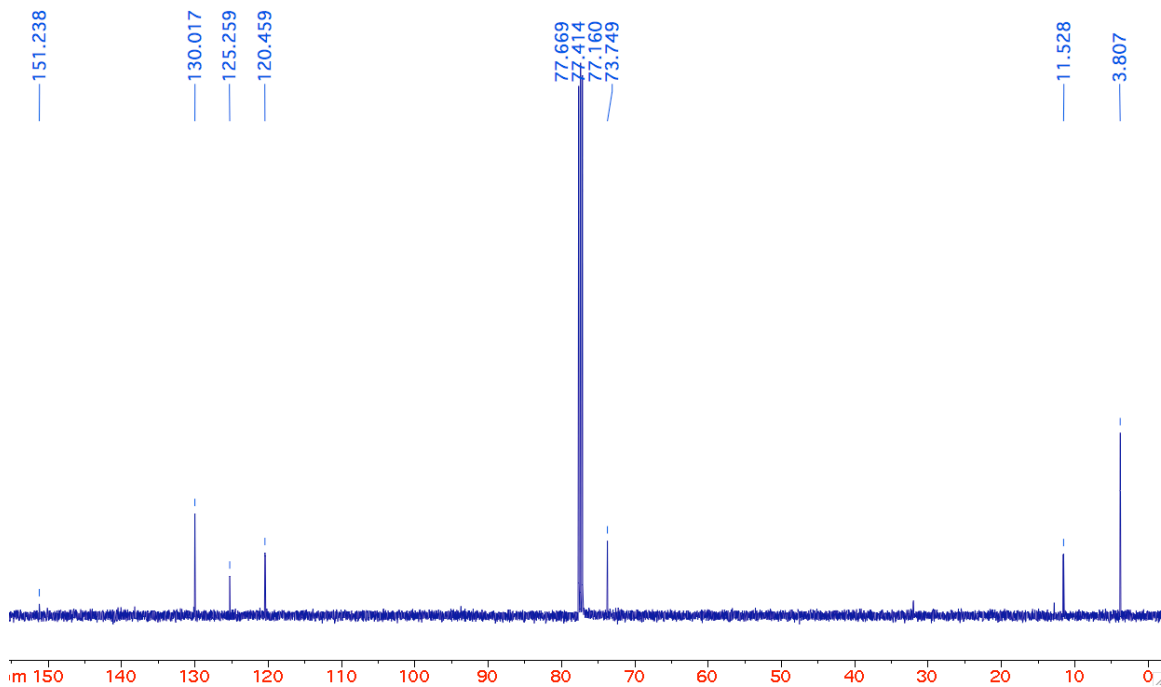
^{13}C NMR Spectrum



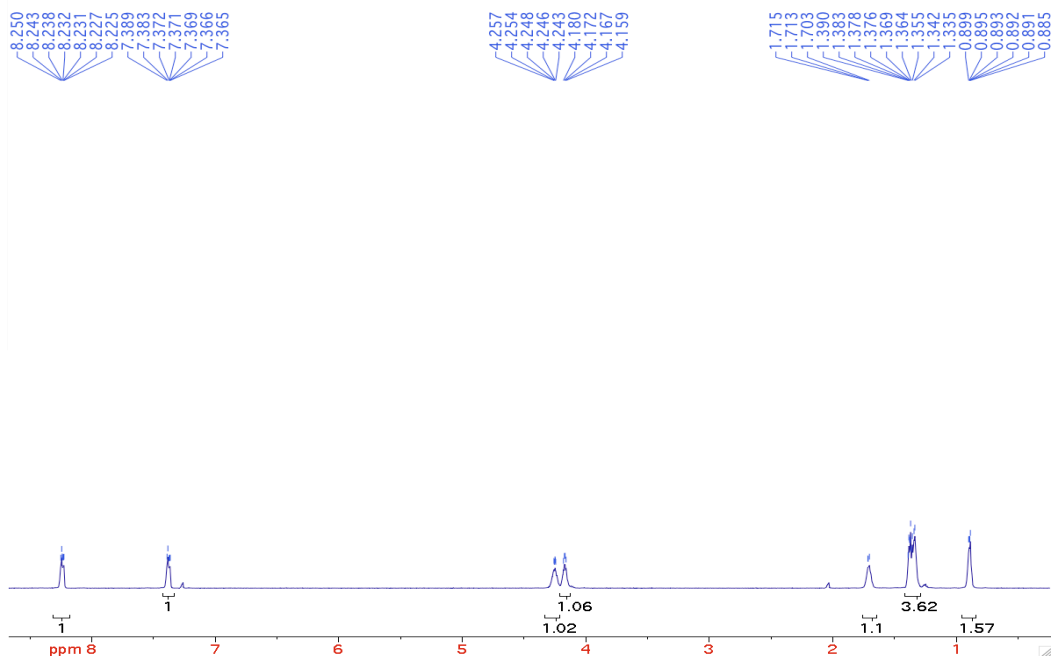
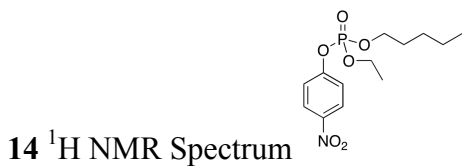
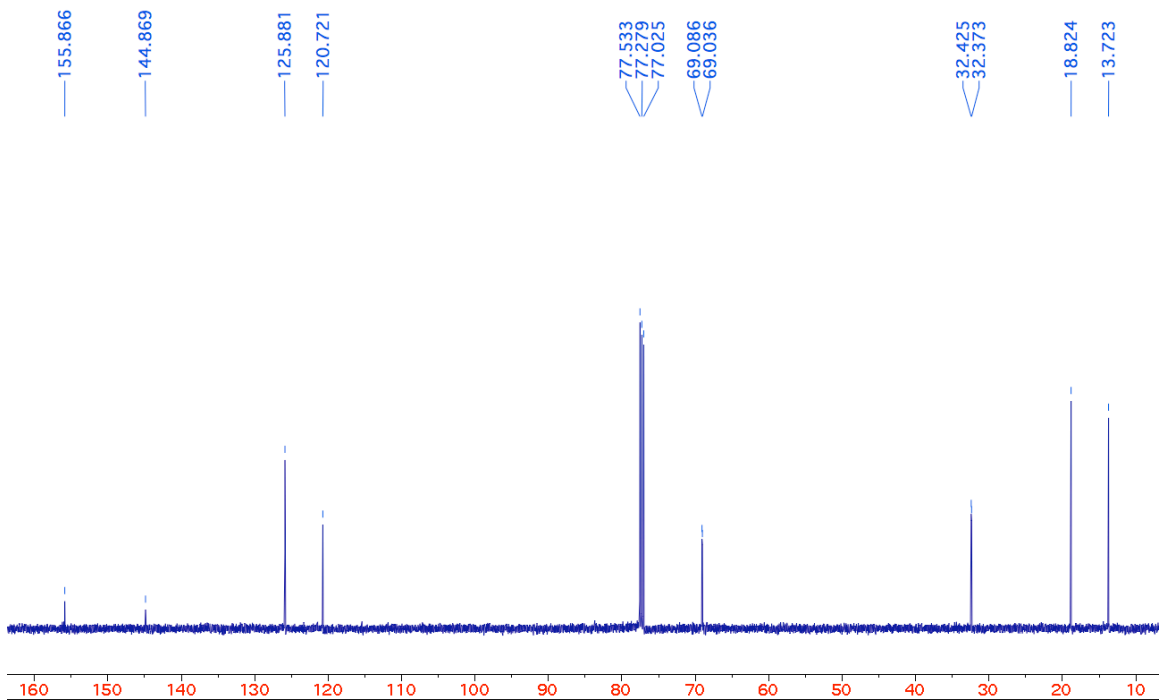
¹³C NMR Spectrum



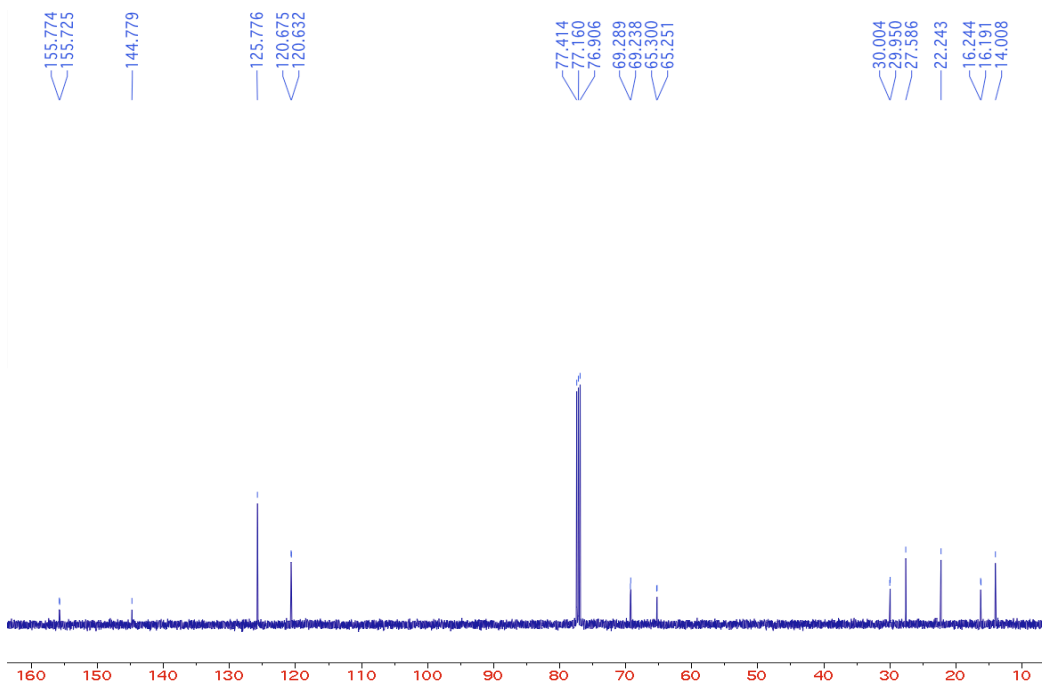
¹³C NMR Spectrum



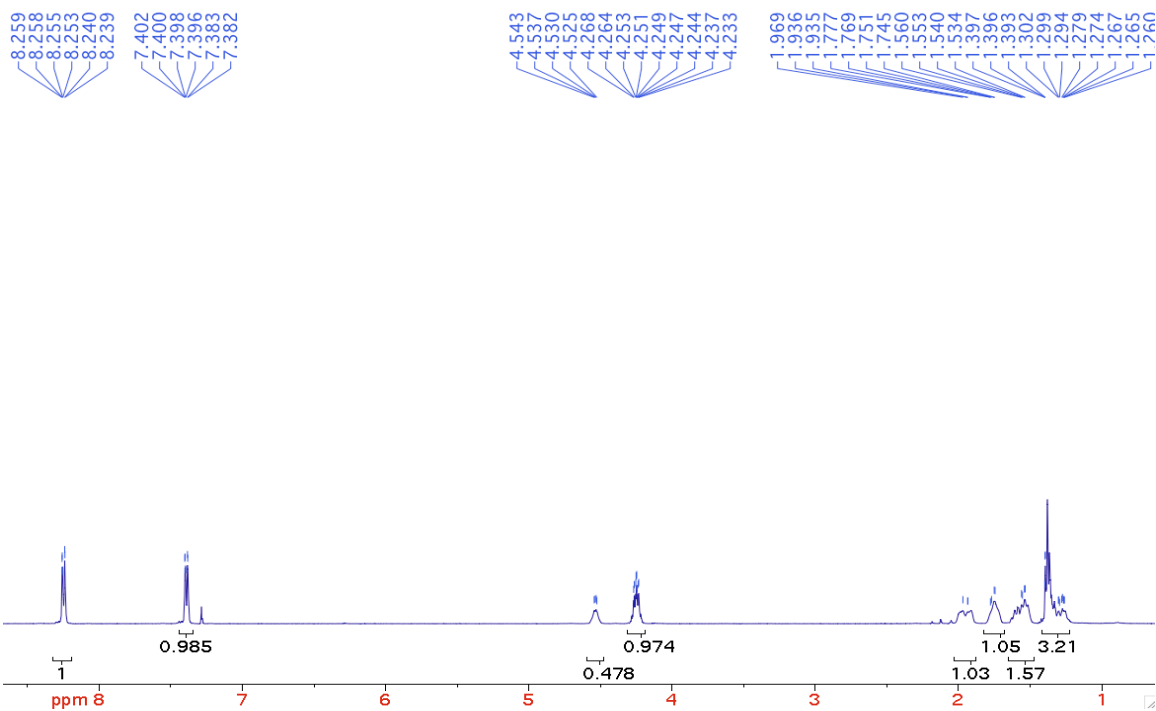
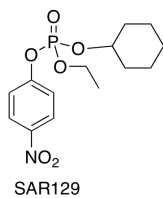
¹³C NMR Spectrum



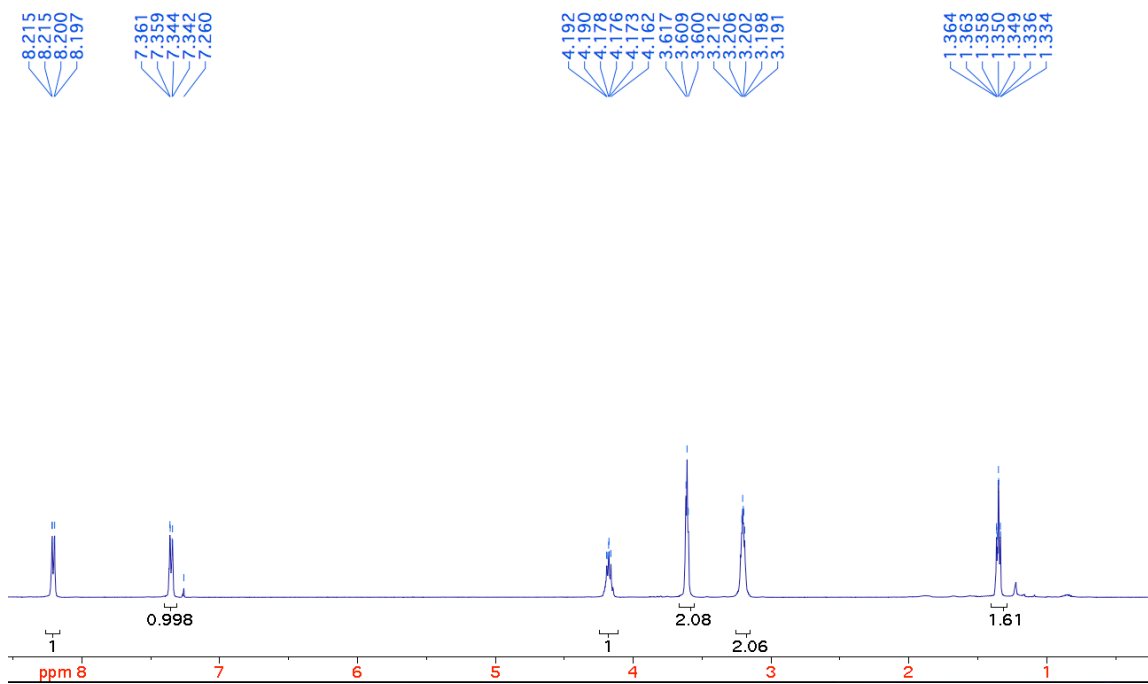
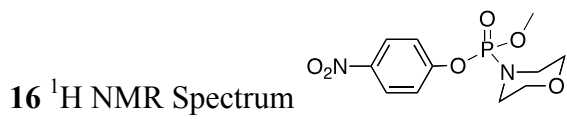
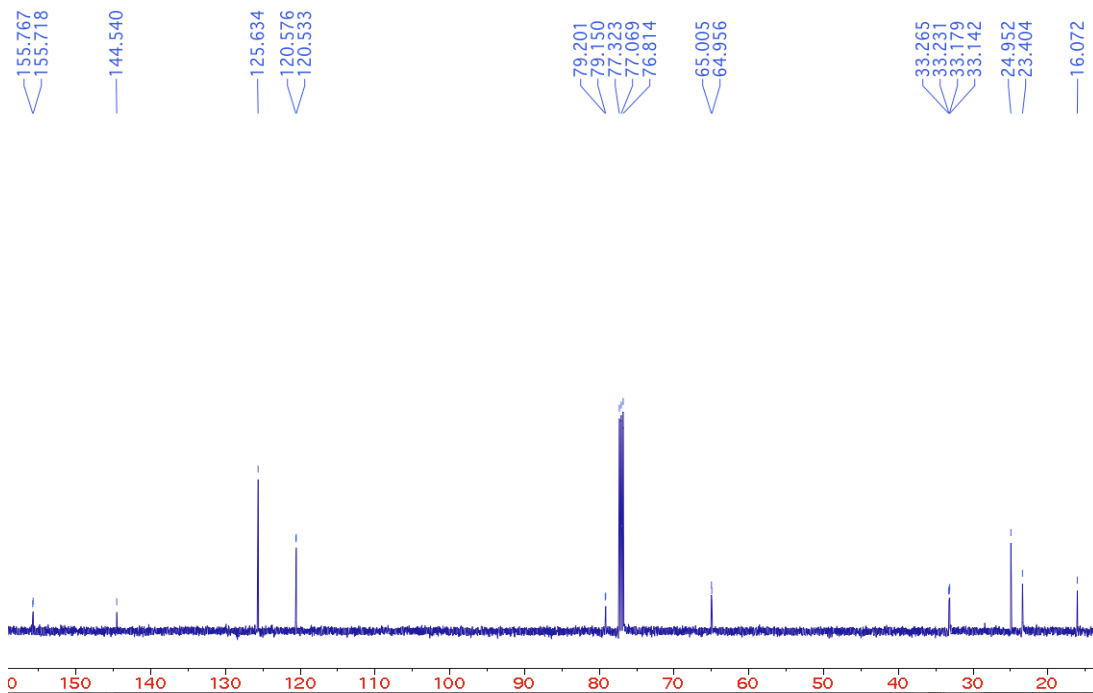
¹³C NMR Spectrum



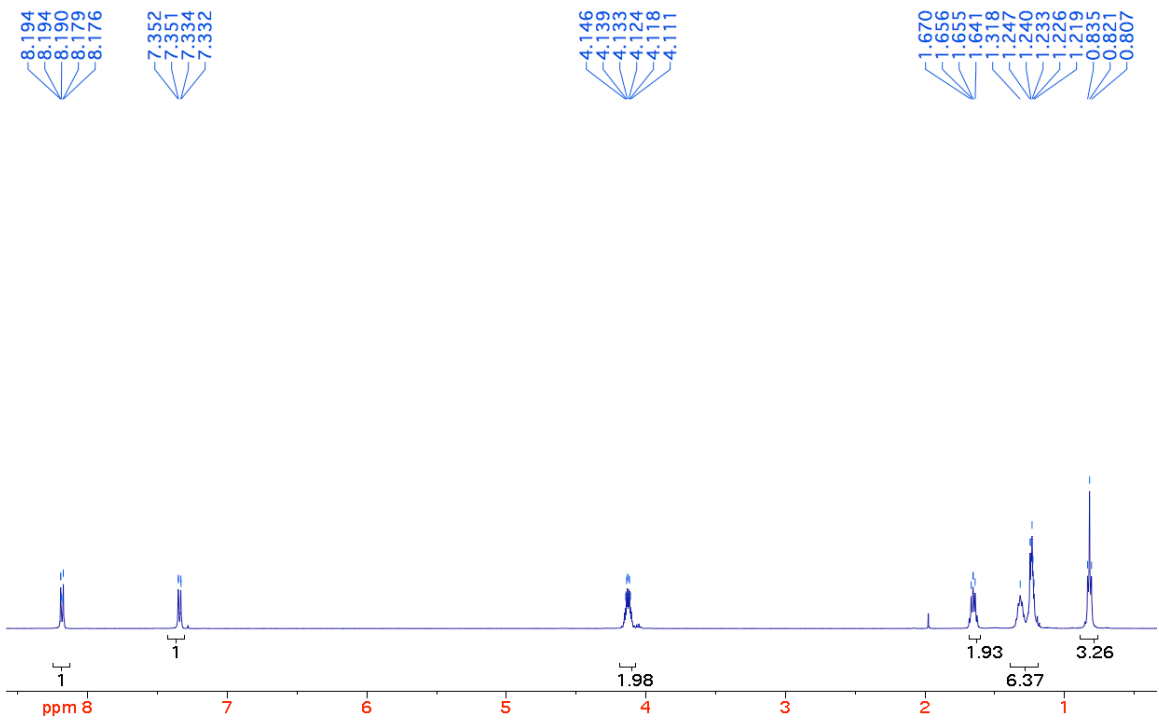
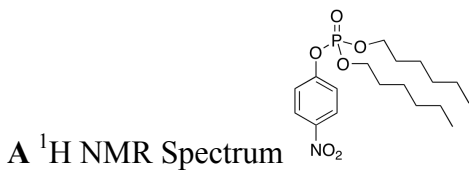
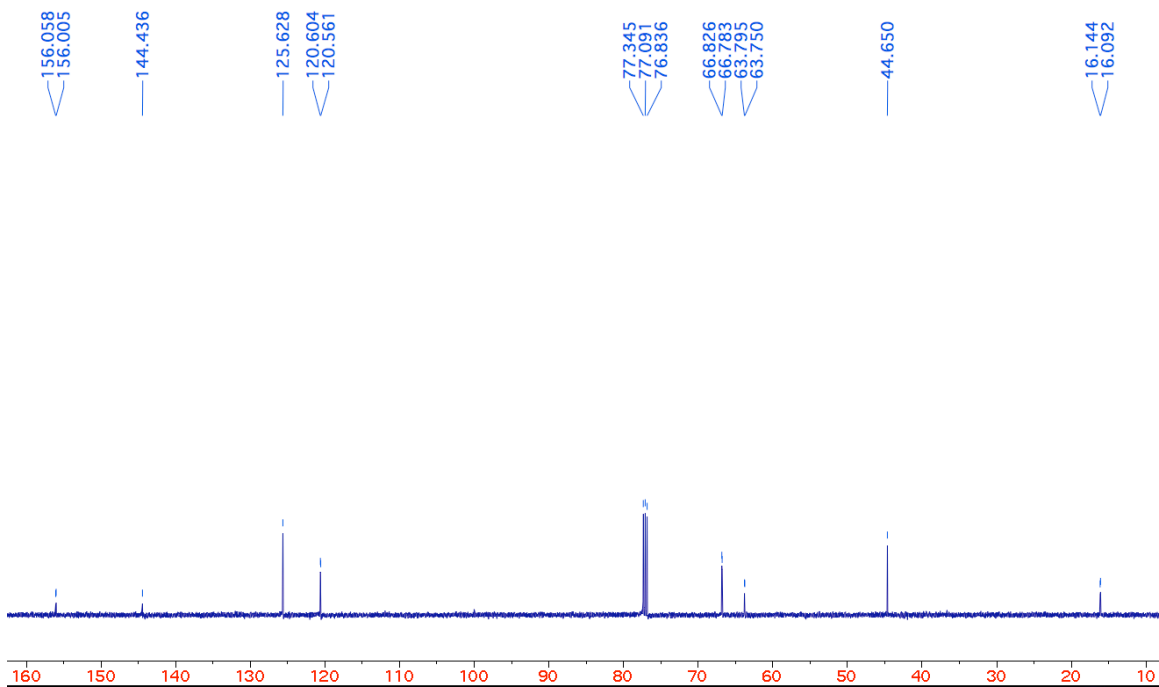
15 ¹H NMR Spectrum



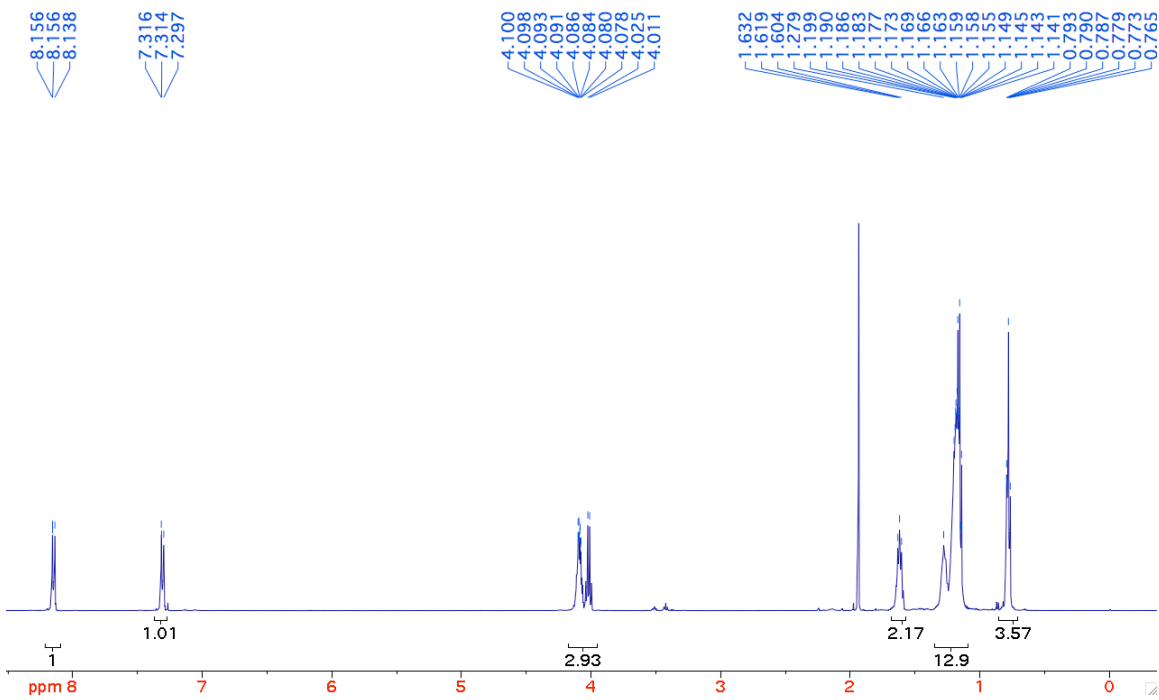
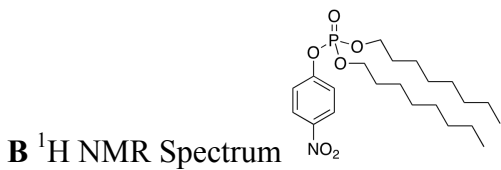
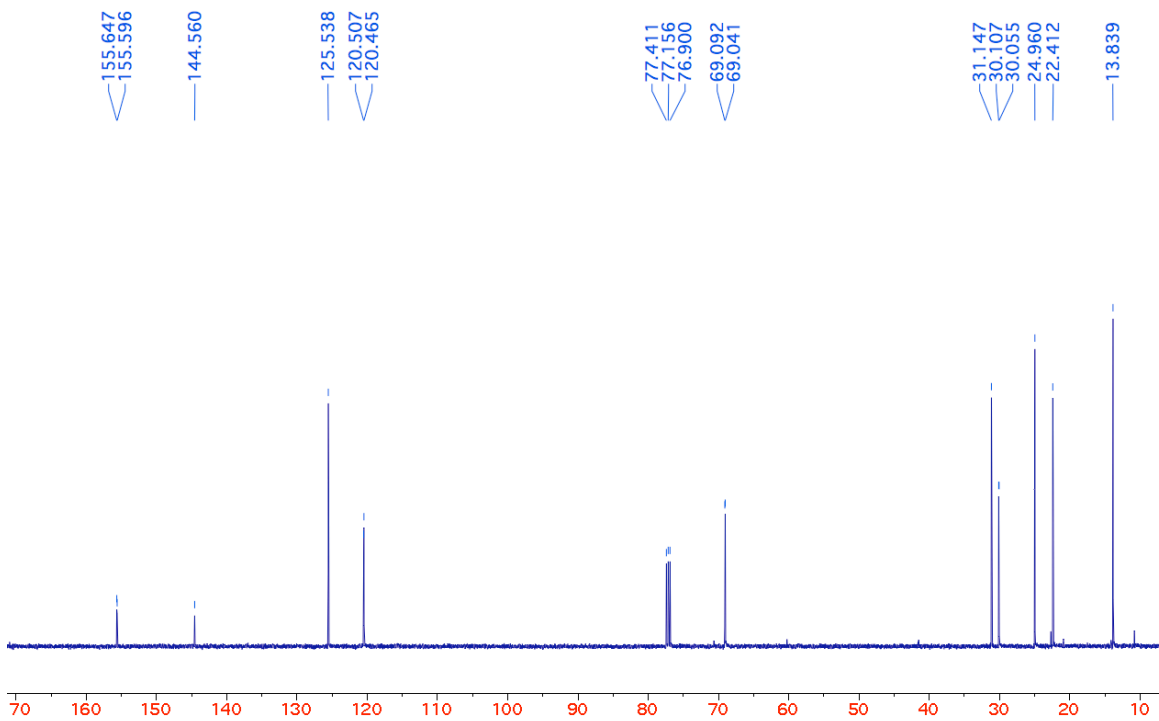
¹³C NMR Spectrum



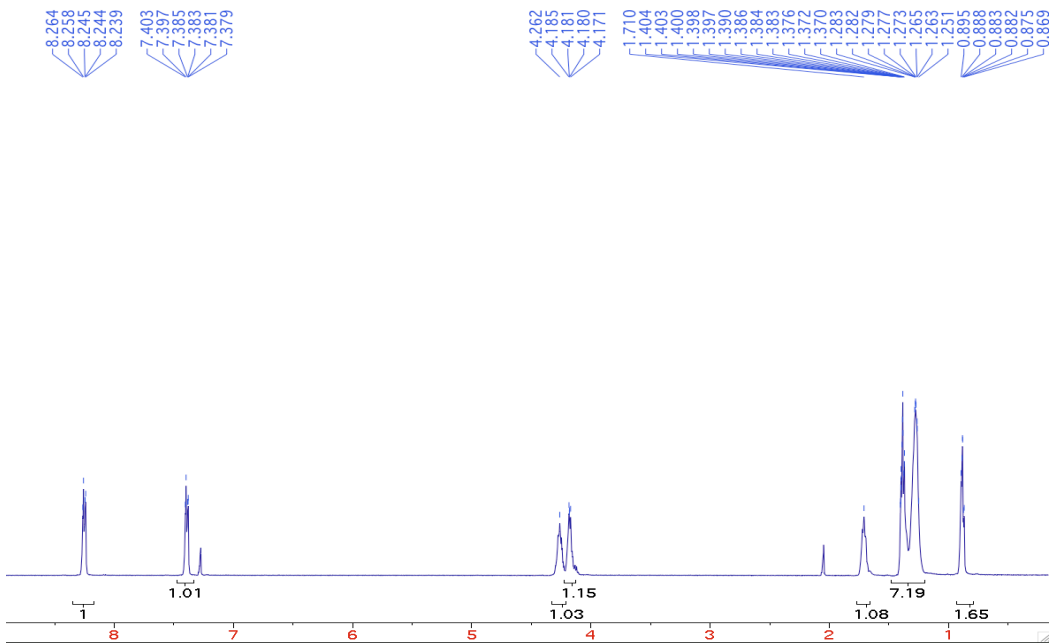
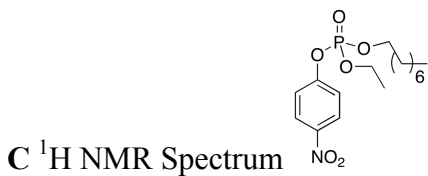
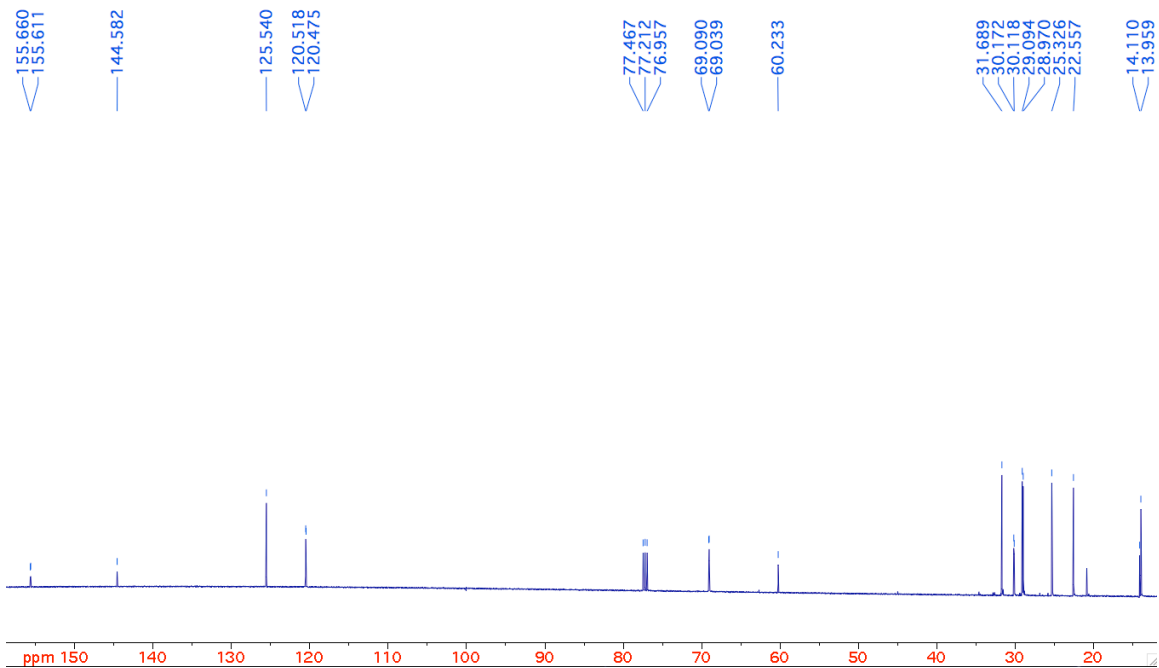
¹³C NMR Spectrum



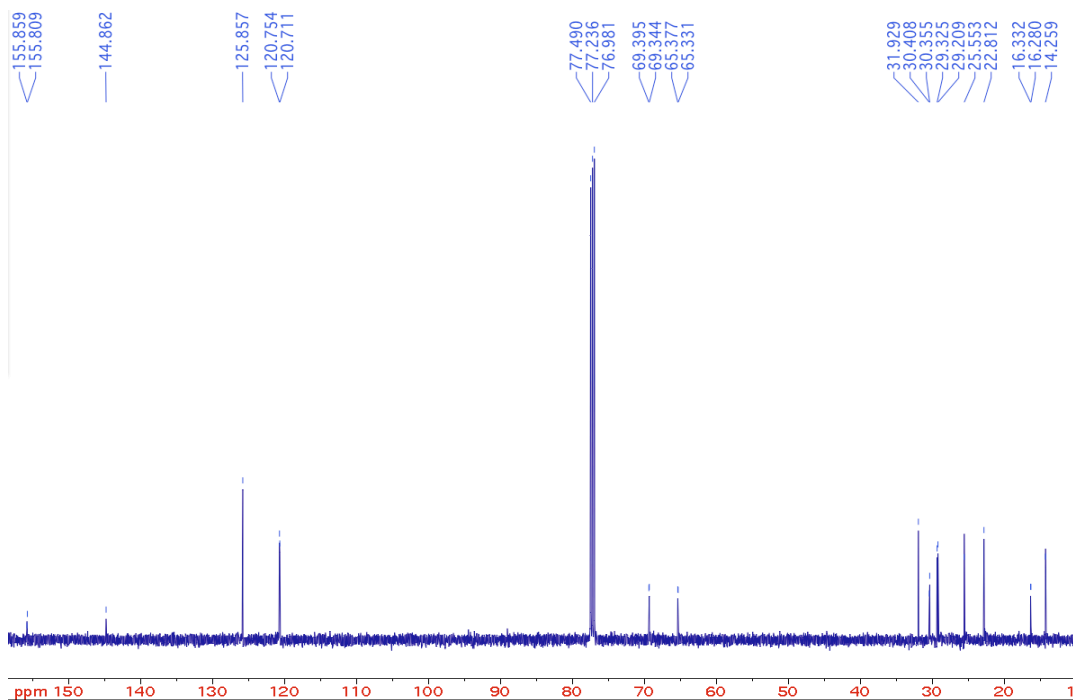
^{13}C NMR Spectrum



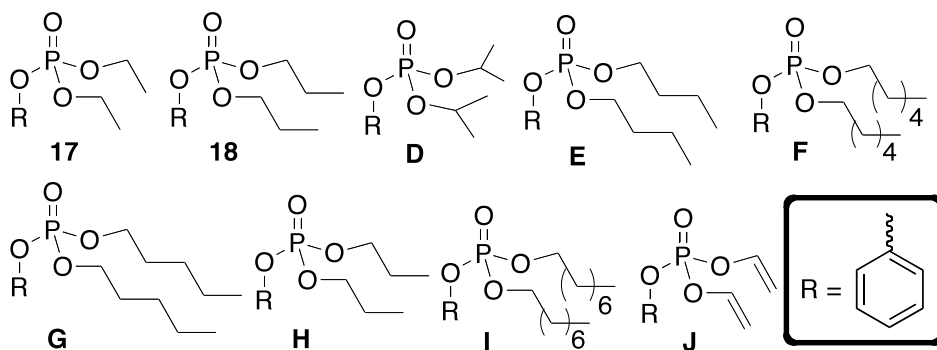
^{13}C NMR Spectrum



^{13}C NMR Spectrum



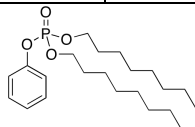
Group II



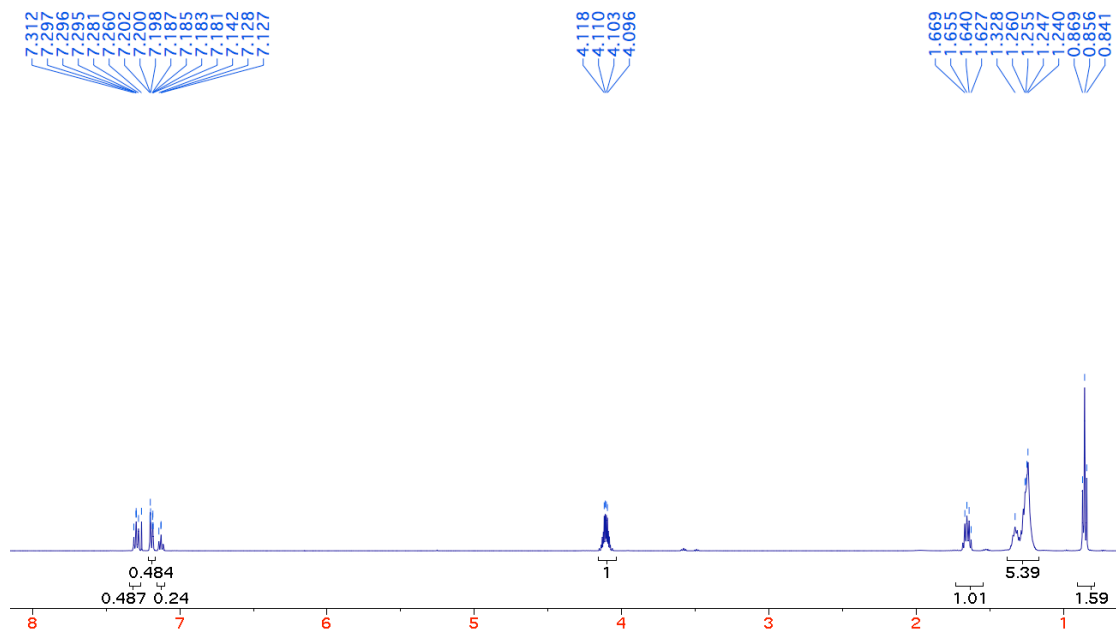
Molecules **17**, **18**, **D-H** are known and they were synthesized and characterized following reported procedure.¹

Molecule	¹ H NMR	¹³ C NMR	IR	MS
I	7.31-7.29 (2H, m), 7.20-7.18 (2H, m), 7.12-7.14 (1H, m), 4.09-4.11 (4H, m), 1.62-1.66 (4H, m), 1.26-1.24 (20H, m), 0.85 (6H, t, <i>J</i> 5Hz)	151.0, 129.8, 125.1, 120.2, 68.8, 31.9, 30.5, 29.3, 25.6, 22.8, 14.2	2927, 1491, 1213, 1024, 945	Calc (M+Na) ⁺ 398.2586 Expt 398.2582
J	7.33-7.30 (2H, m), 7.21-7.14 (3H, m),	150.7, 132.2, 129.7, 125.1,	3079, 2880, 1594, 1486,	Calc (M+Na) ⁺

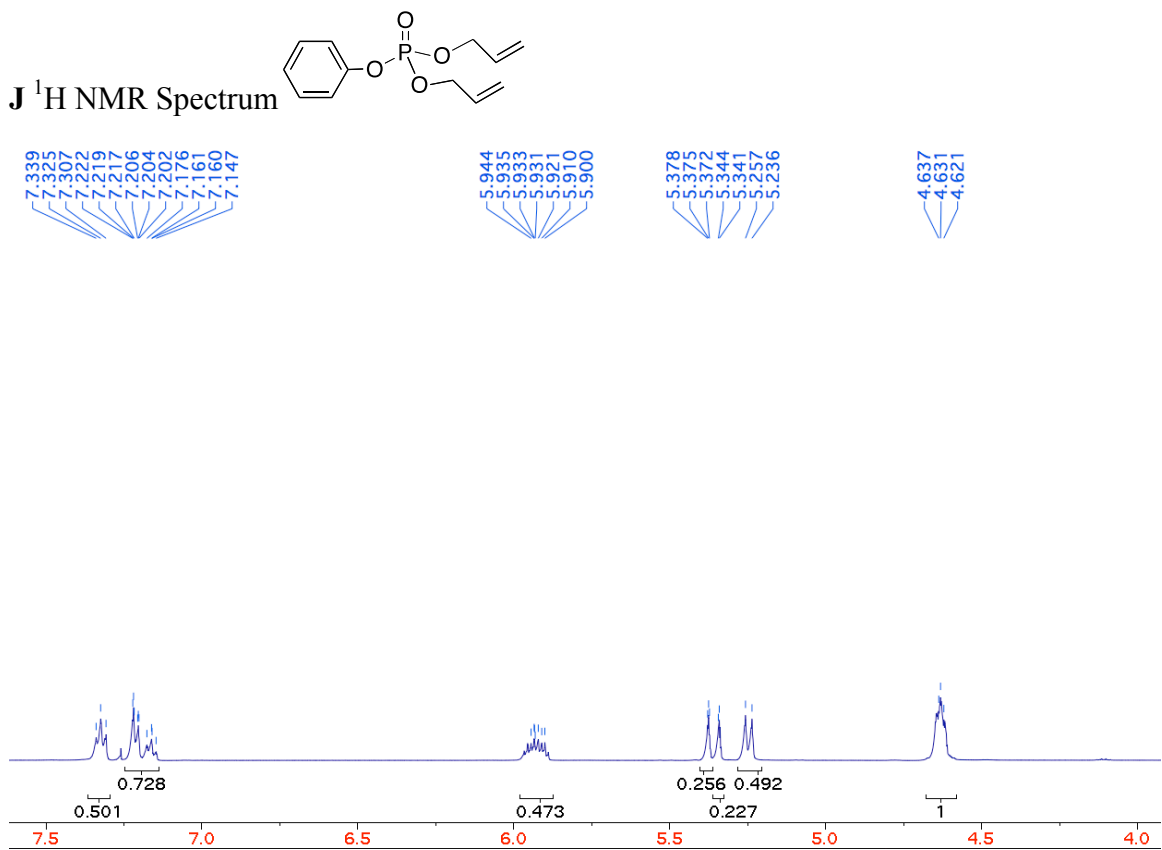
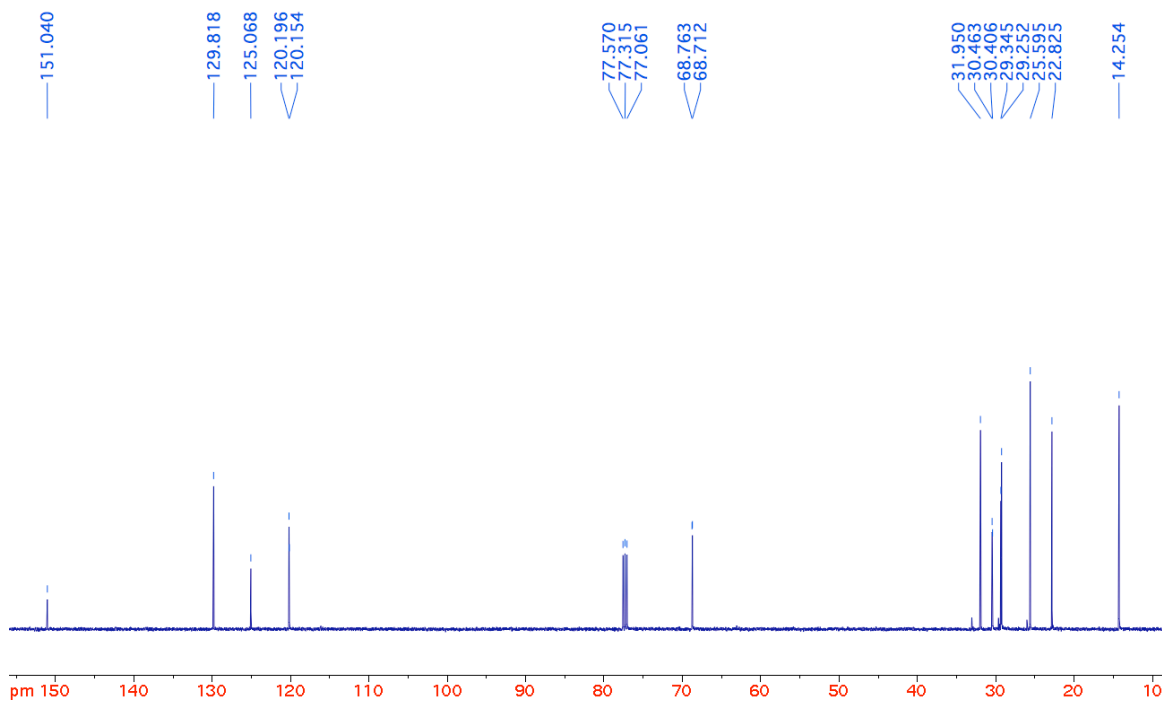
	5.94-5.90 (2H, m), 5.37-5.34 (2H, m), 5.25-5.23 (2H, m), 4.63-4.62 (4H, m)	120.1, 118.6, 68.8	1282, 1207, 1017	277.0606 Expt 277.0607
--	---	-----------------------	---------------------	---------------------------



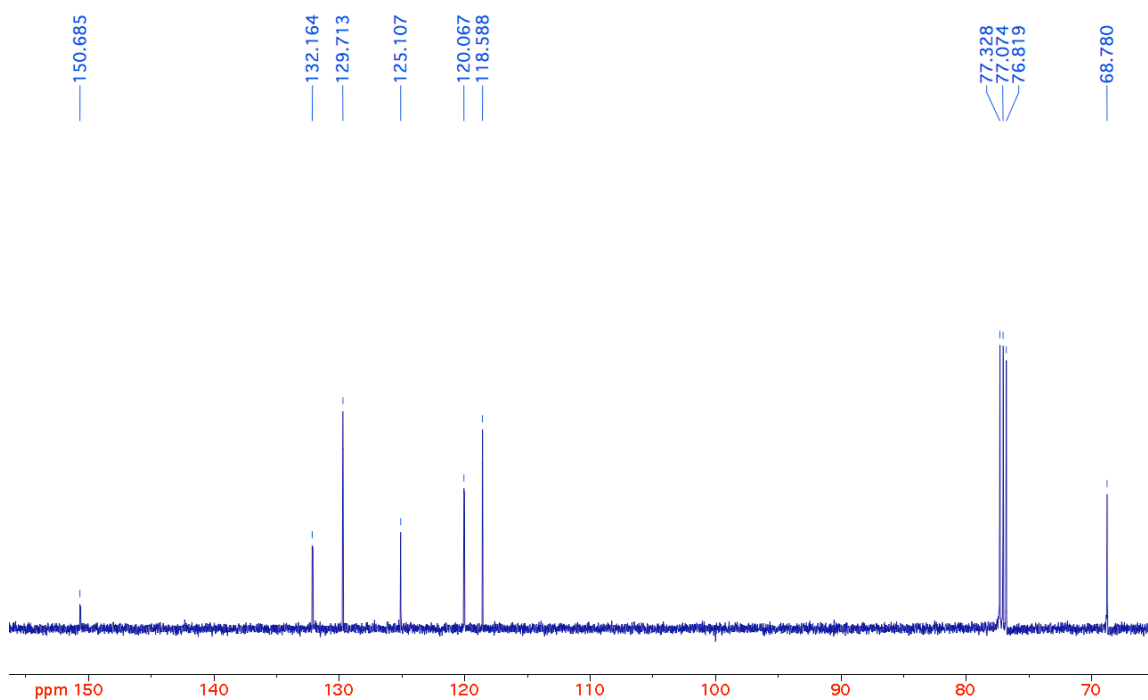
SAR70 ¹H NMR Spectrum



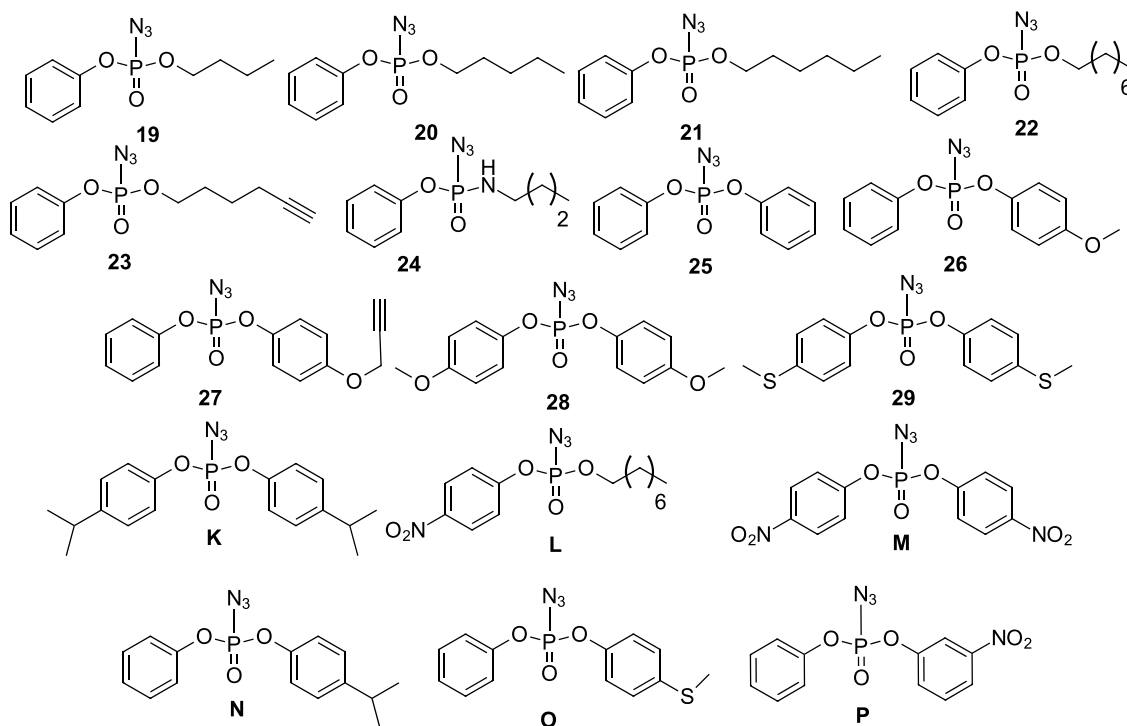
¹³C NMR Spectrum



^{13}C NMR Spectrum



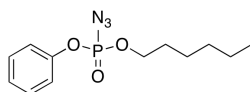
Group III



Molecules **M** and **25** are commercially available.

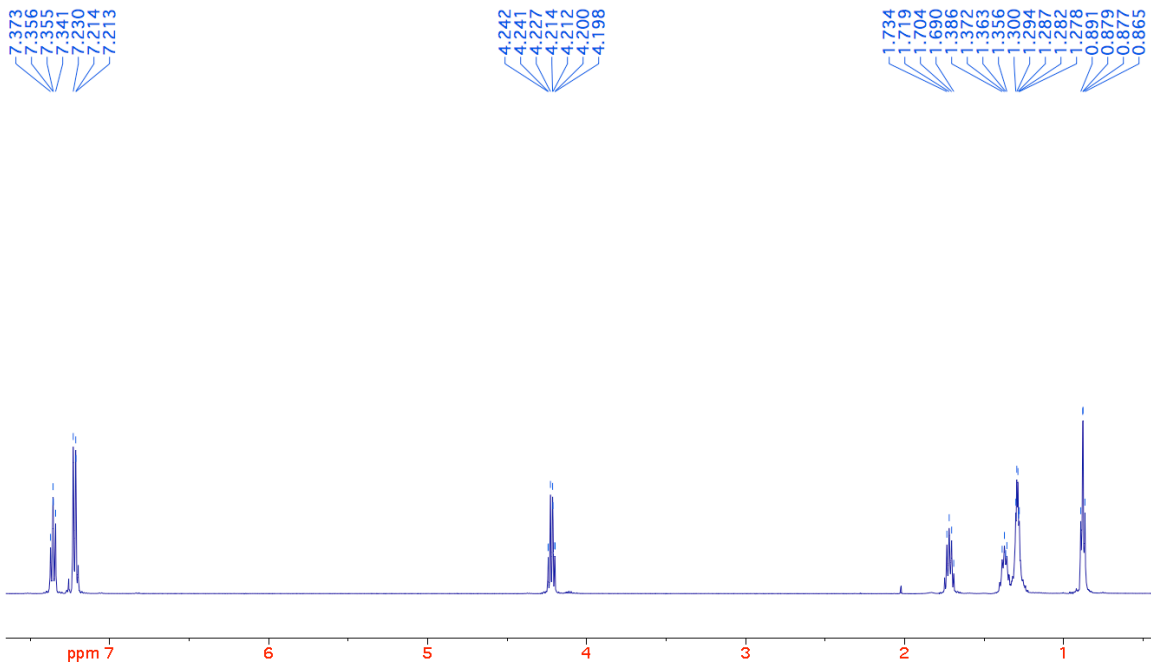
Molecule	¹H NMR	¹³C NMR	IR	MS
19	7.40-7.37 (2H, m), 7.28-7.24 (3H, m), 4.28-4.24 (2H, m), 1.77-1.71 (2H, m), 1.46-1.42 (4H, m), 0.96 (3H, t, J 5Hz)	150.2, 130.2, 126.1, 120.4, 69.7, 32.3, 18.8, 13.7	2970,2164, 1511, 1209	Calc (M+Na) ⁺ 278.0670 Expt 278.0673
20	7.41-7.38 (2H, m), 7.28-7.25 (3H, m), 4.28-4.23 (2H, m), 1.78-1.75 (2H, m), 1.39-1.35 (4H, m), 0.93 (3H, t, J 5Hz)	150.0, 130.0, 125.8, 120.2, 69.8, 31.2, 30.0, 24.9, 22.5, 14.0	2962, 2171, 1589, 1216	Calc (M+Na) ⁺ 292.0827 Expt 292.0829
21	7.37-7.34 (2H, m), 7.23-7.21 (3H, m), 4.24-4.19 (2H, m), 1.73-1.69 (2H, m), 1.38-1.27 (6H, m), 0.87 (3H, t, J 5Hz)	150.2, 130.2, 126.0, 120.4, 69.9, 31.4, 30.2, 25.2, 22.7, 14.2	2929, 2171, 1593, 1217	Calc (M+Na) ⁺ 306.2532 Expt 306.2530
22	7.37-7.34 (2H, m), 7.23-7.21 (3H, m), 4.24-4.19 (2H, m), 1.73-1.70 (2H, m), 1.38-1.25 (10H, m), 0.87 (3H, t, J 5Hz)	150.0, 129.5, 125.8, 120.2, 69.8, 31.7, 30.1, 30.0, 29.1, 25.3, 22.6, 14.1	2969, 2156, 1588, 1291	Calc (M+Na) ⁺ 334.1296 Expt 334.1291
23	7.38-7.35 (2H, m), 7.24-7.21 (3H, m), 4.28-4.24 (2H, m), 2.24-2.22 (2H, m), 1.98 (1H, s), 1.88-1.85 (2H, m), 1.65-1.60 (2H, m),	149.9, 130.0, 125.9, 120.2, 83.4, 69.1, 60.4, 29.1, 24.2, 21.0, 17.9	3303, 3252, 2949, 2167, 1490, 1271	Calc (M+H) ⁺ 280.0846 Expt 280.0842
24	7.37-7.34 (2H, m), 7.24-7.19 (2H, m), 3.14 (1H, bs), 3.07-3.03 (2H, m), 1.52-1.49(2H, m), 1.37-1.33 (2H, m), 0.92 (3H, t, J 5Hz)	150.4, 130.2, 125.8, 120.6, 41.7, 33.7, 19.9, 13.9	3219, 2962, 2143, 1595, 1256	Calc (M+Na) ⁺ 277.0830 Expt 277.0825
26	7.39-7.38 (3H, m), 7.19-7.17 (4H, m), 6.89-6.88 (2H, m), 3.80 (3H, s)	157.6, 150.0, 143.5, 130.2, 126.2, 121.2, 120.4, 115.0, 55.8	3111, 2947, 1589, 1339, 1216	Calc (M+H) ⁺ 306.0644 Expt 306.0647
27	7.41-7.38 (2H, m), 7.26-7.22 (3H, m), 6.98	155.6, 150.0, 144.2, 130.2,	3294, 3024, 2919, 2171,	Calc (M+H) ⁺ 330.0644

	(2H, d, J 10Hz), 4.69 (2H, s), 2.54 (4H, s)	126.3, 121.4, 120.4, 116.3, 116.3, 78.3, 76.1, 54.5	1508, 1297, 1161	Expt 330.0641
28	7.18(4H, d, J 10 Hz), 6.88(4H, d, J 10Hz), 3.77(6H, s)	157.0, 144.2, 121.1, 114.7, 55.6	3073, 2837, 2157, 1501, 1300, 958	Calc (M+Na) ⁺ 358.0569 Expt 358.0565
29	7.26(2H, d, J 10Hz), 7.16(2H, d, J 10Hz), 2.42(6H, s)	157.0, 144.2, 121.1, 114.7, 55.6	2170, 1487, 1191, 967	Calc (M+Na) ⁺ 390.0079 Expt 390.0078
K	7.24-7.20 (4H, m), 2.92 (2H, m), 3.77(6H, d, J 5Hz)	147.9, 146.7, 127.9, 120.0, 33.6, 23.9	2962, 2100, 1506, 974	Calc (M+Na) ⁺ 382.1296 Expt 382.1283
L	8.27 (2H, d, J 10Hz), 7.40 (2H, d, J 10Hz), 4.30-4.25 (2H, m), 1.77-1.72 (2H, m), 1.28-1.26(10H, m), 0.88 (3H, t, J 5Hz)	154.5, 145.3, 125.8, 120.9, 70.4, 31.7, 30.0, 29.1, 28.9, 25.2, 22.6, 14.0	2929, 2170, 1526, 1348, 1025	Calc (M+Na) ⁺ 379.1147 Expt 379.1149
N	7.42-7.19 (9H, m), 2.93-2.92 (1H, m), 1.27 (6H, d, J 5Hz)	146.8, 130.0, 127.9, 126.1, 120.3, 120.0, 33.6, 24.0	3097, 2917, 2158, 1589, 1190	Calc (M+Na) ⁺ 340.0827 Expt 340.0824
O	7.42-7.19 (5H, m), 7.22-7.21 (4H, m), 2.50 (3H, s)	149.9, 147.5, 136.4, 130.1, 128.4, 126.1, 120.8, 16.4	3014, 2962, 2171, 16112, 1112	Calc (M+H) ⁺ 322.0415 Expt 322.0416
P	8.28-8.26 (3H, m), 7.43-7.39 (3H, m), 7.25-7.24 (3H, m)	154.5, 149.8, 145.5, 130.3, 126.0, 120.8, 119.9, 115.6	3067, 2955, 2156, 1589, 1196	Calc 329.0389 Expt 329.0385

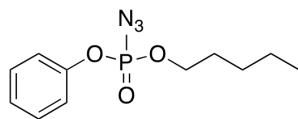
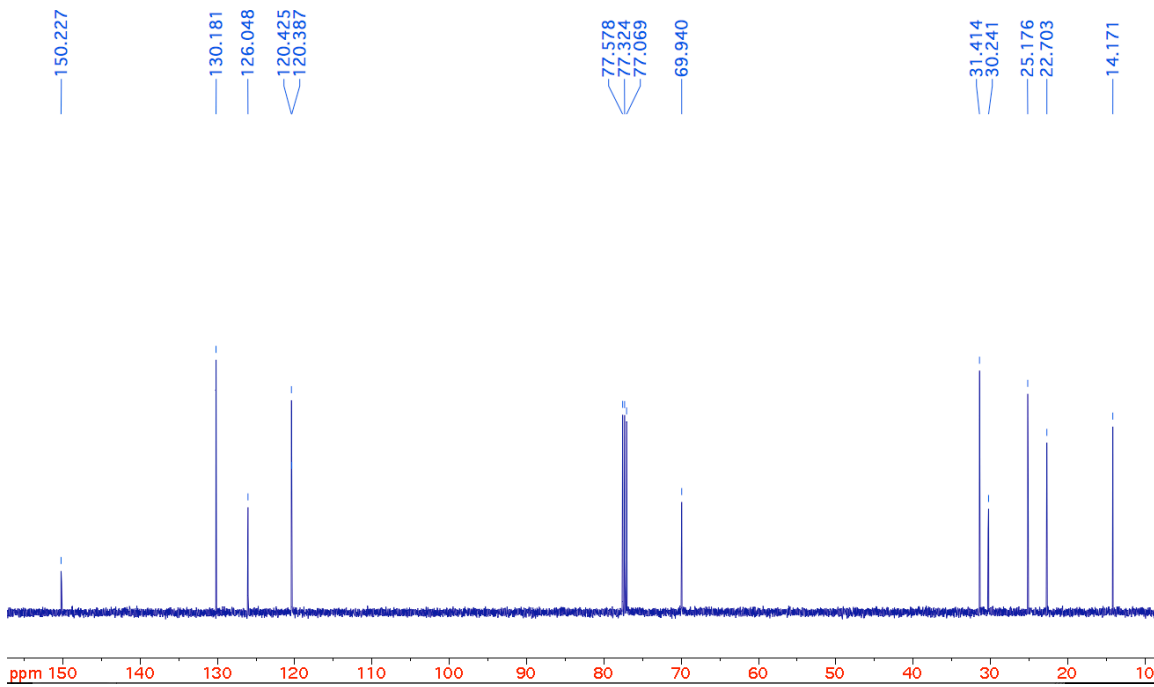


19 ¹H NMR Spectrum

SAR132

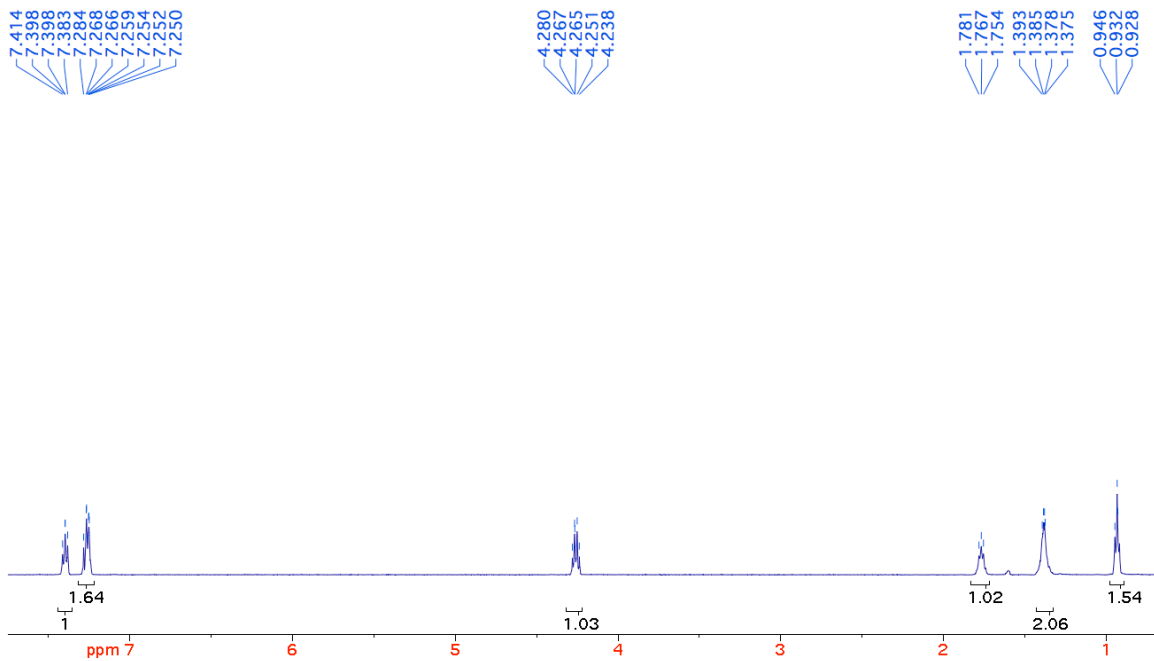


¹³C NMR Spectrum

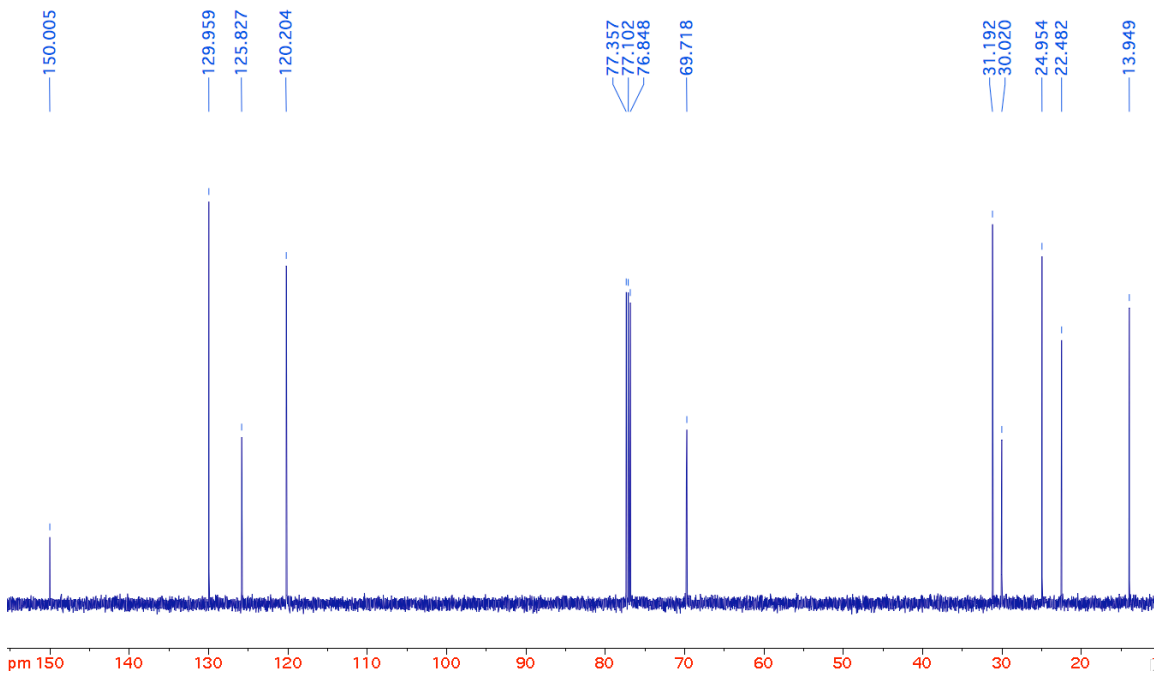


¹H NMR Spectrum

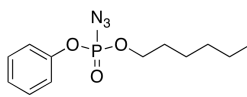
SAR134



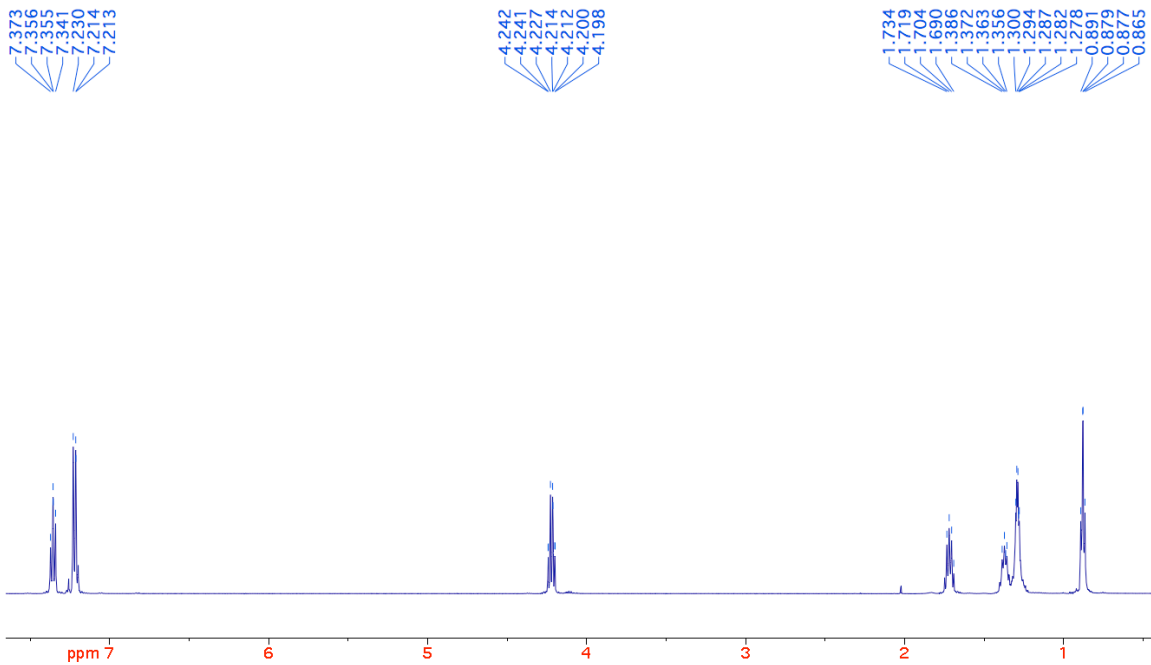
¹³C NMR Spectrum



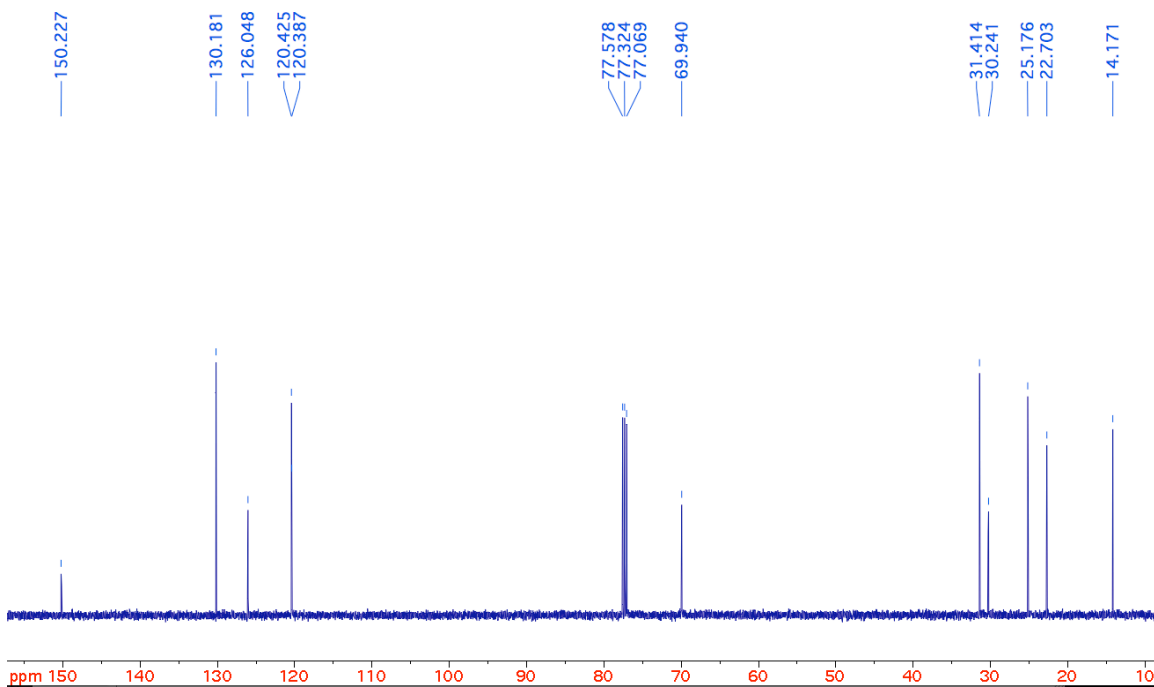
21 ¹H NMR Spectrum



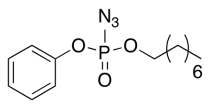
SAR132



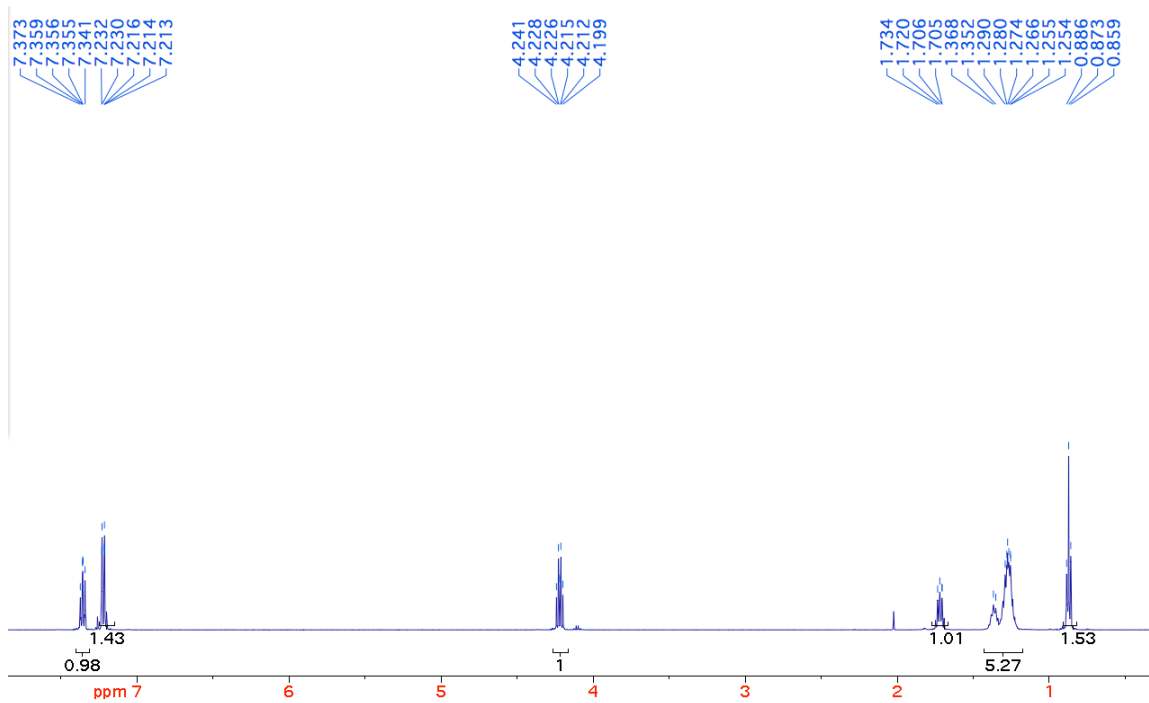
¹³C NMR Spectrum



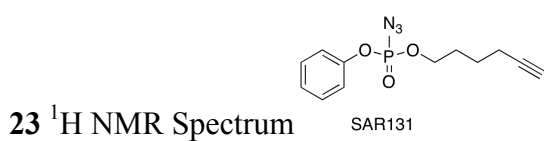
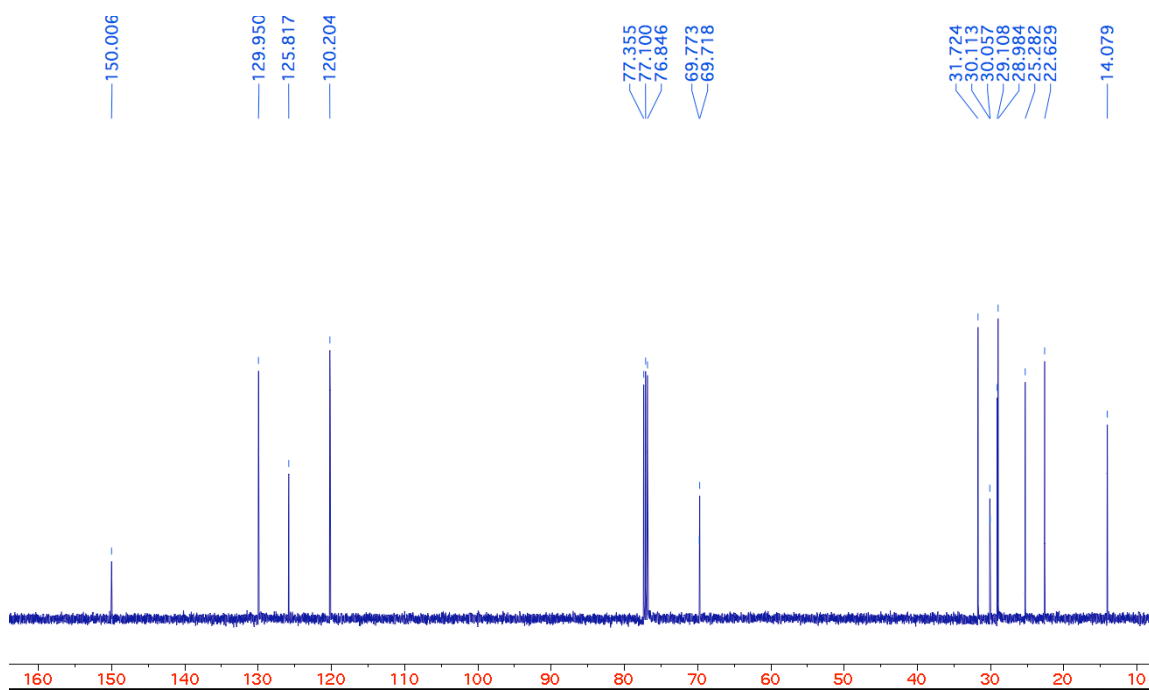
22 ¹H NMR Spectrum

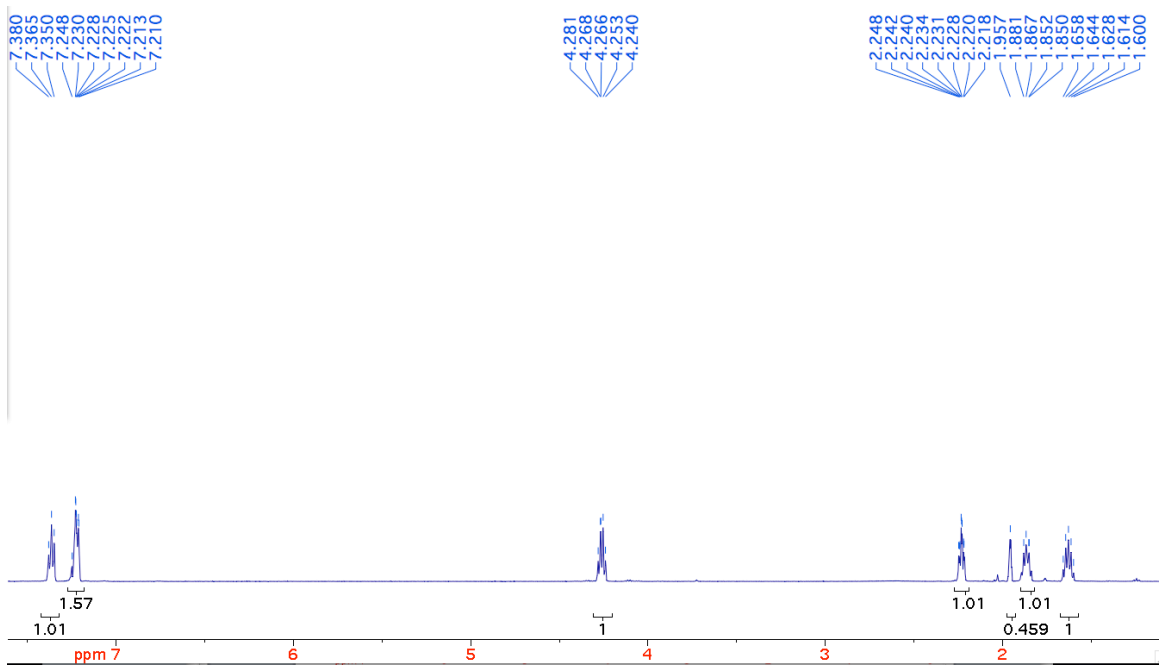


SAR133

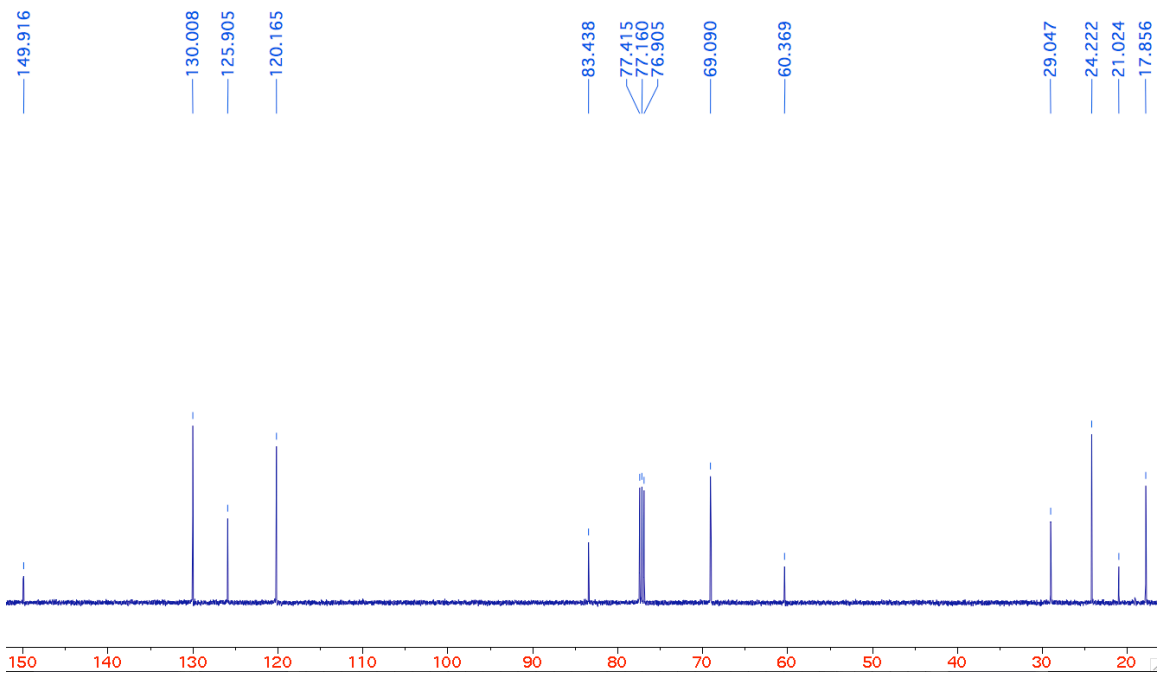


¹³C NMR Spectrum

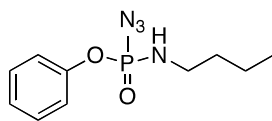


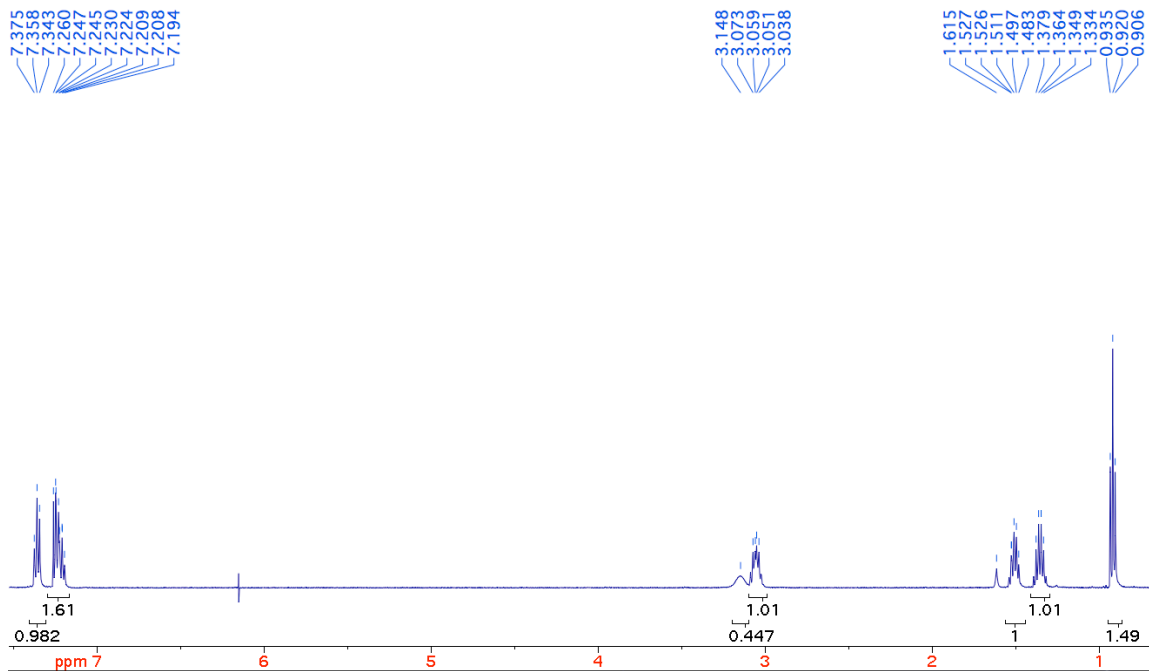


^{13}C NMR Spectrum

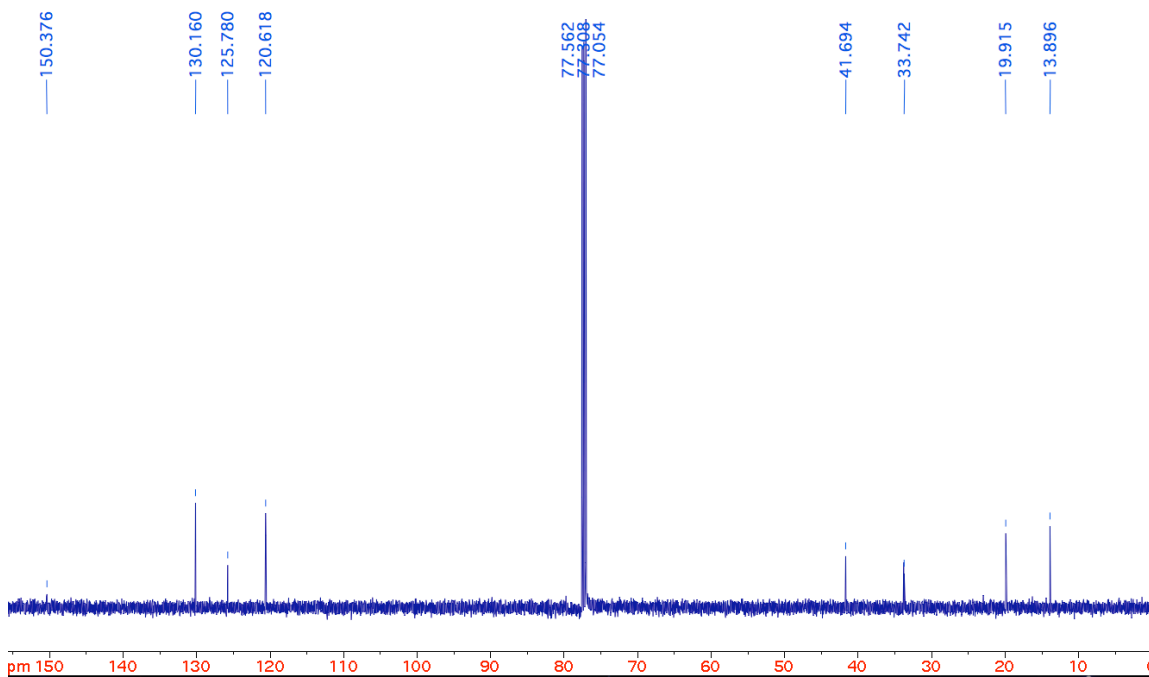


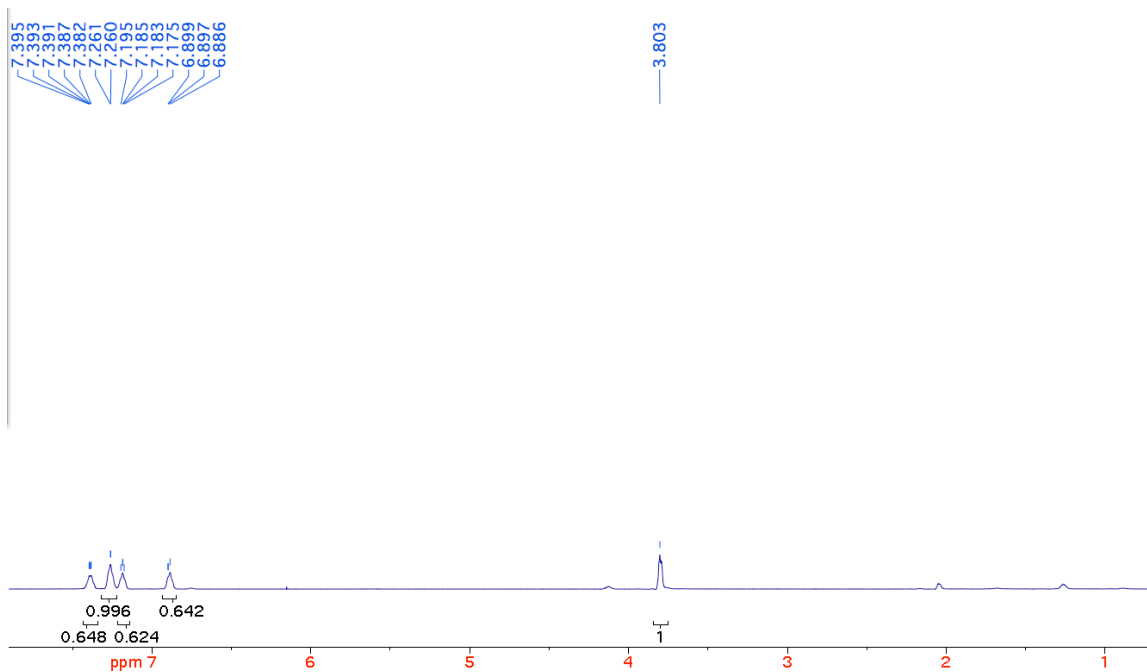
^1H NMR Spectrum



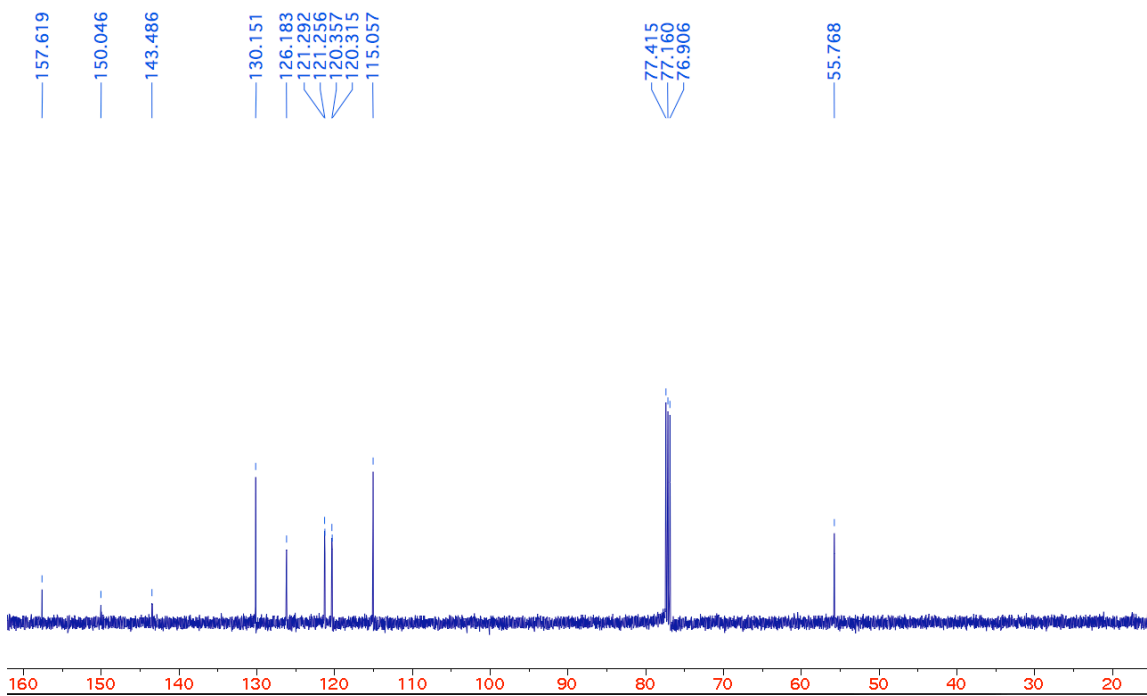


¹³C NMR Spectrum

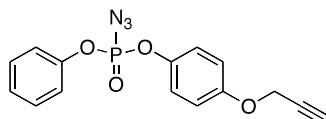


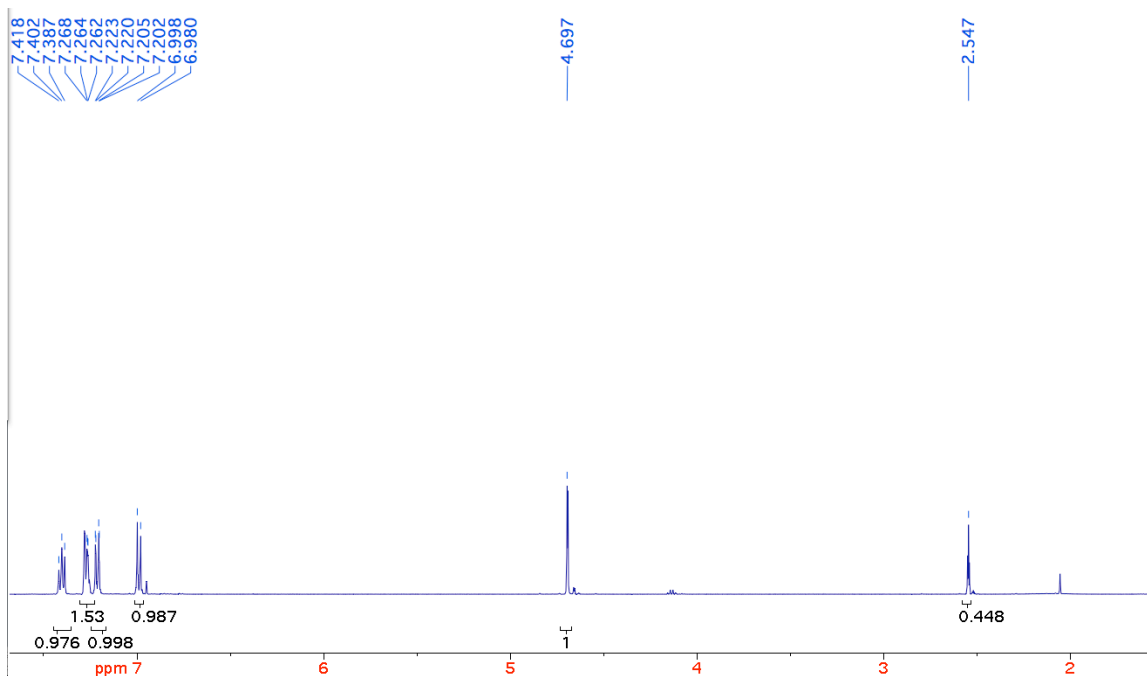


¹³C NMR Spectrum

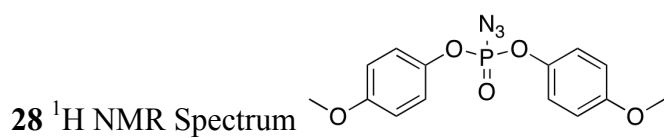
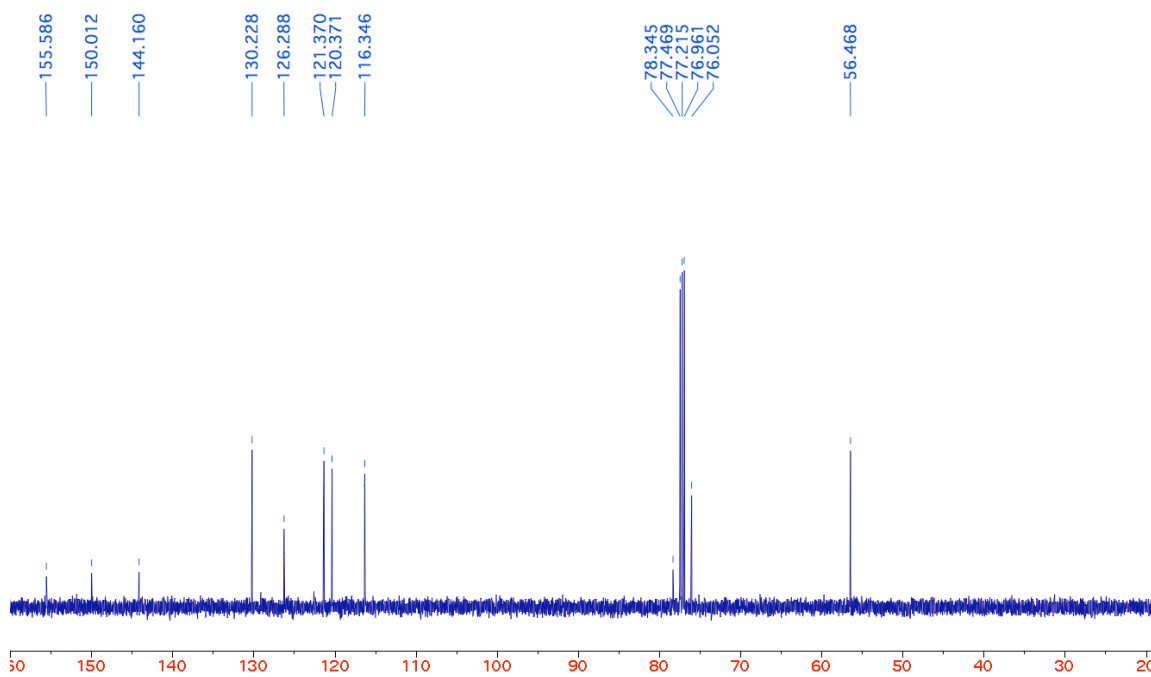


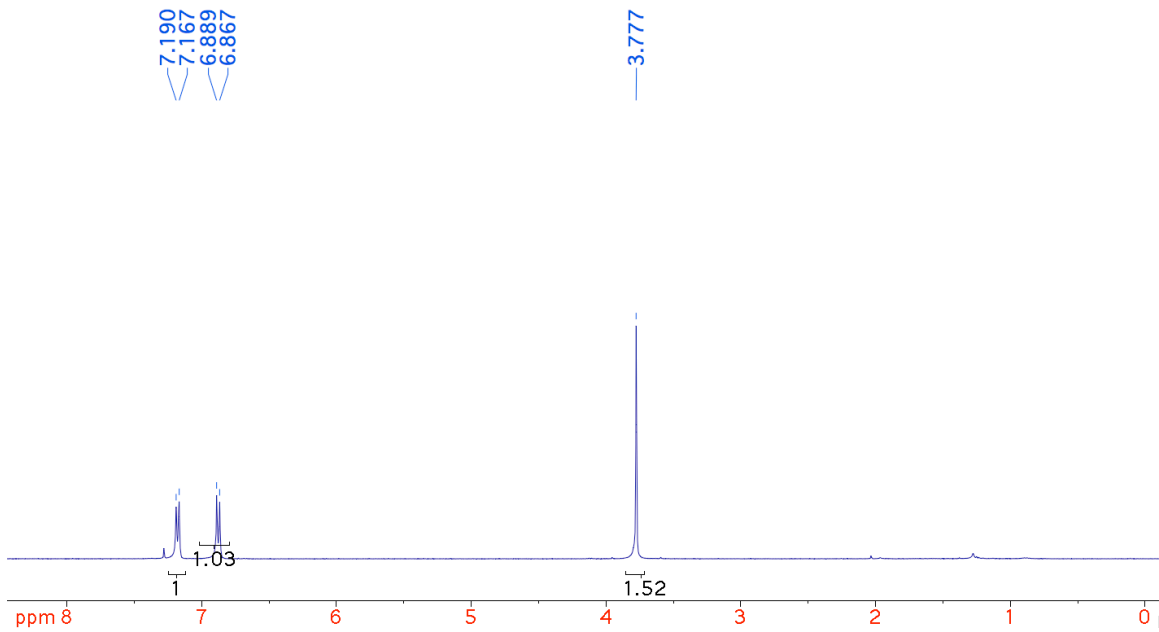
²⁷H NMR Spectrum



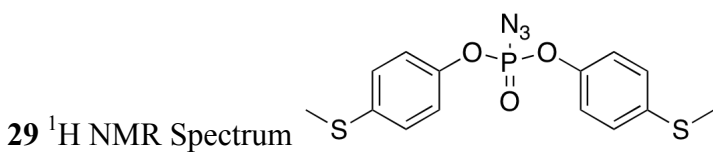
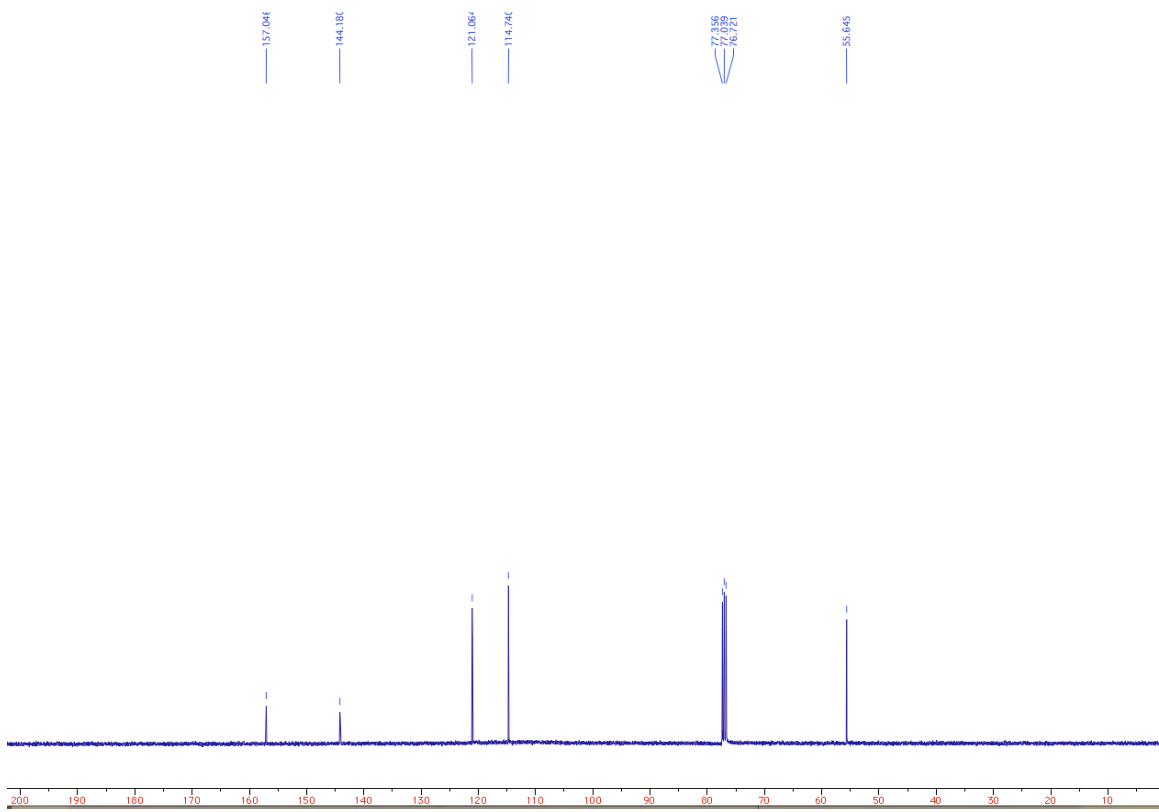


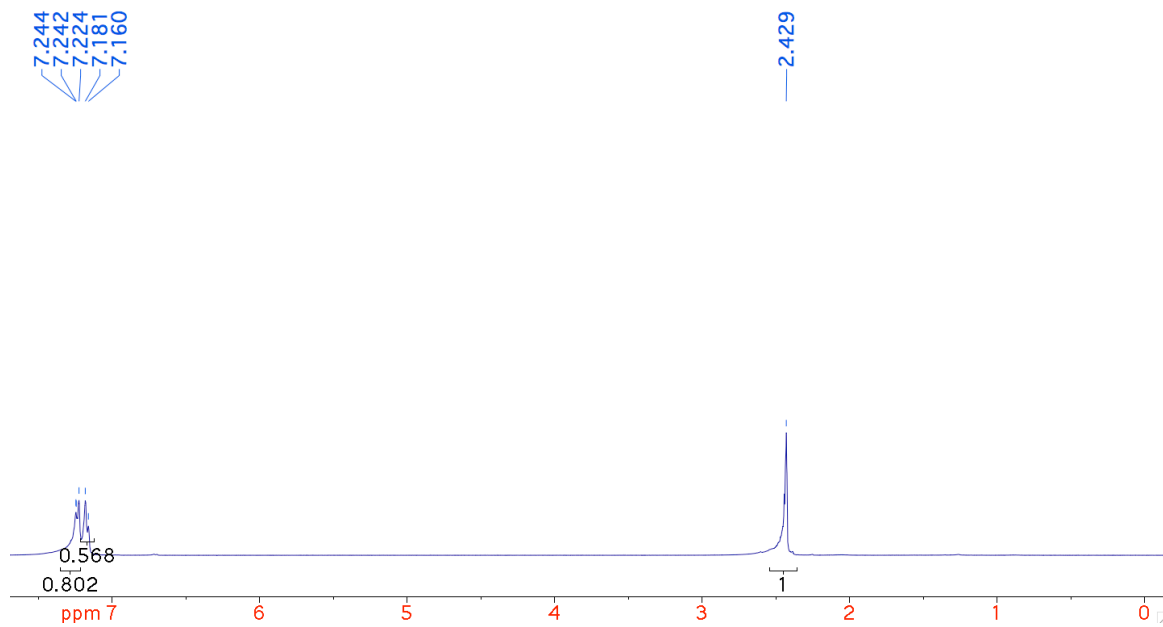
¹³C NMR Spectrum



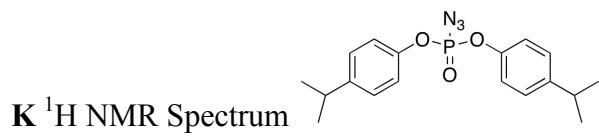
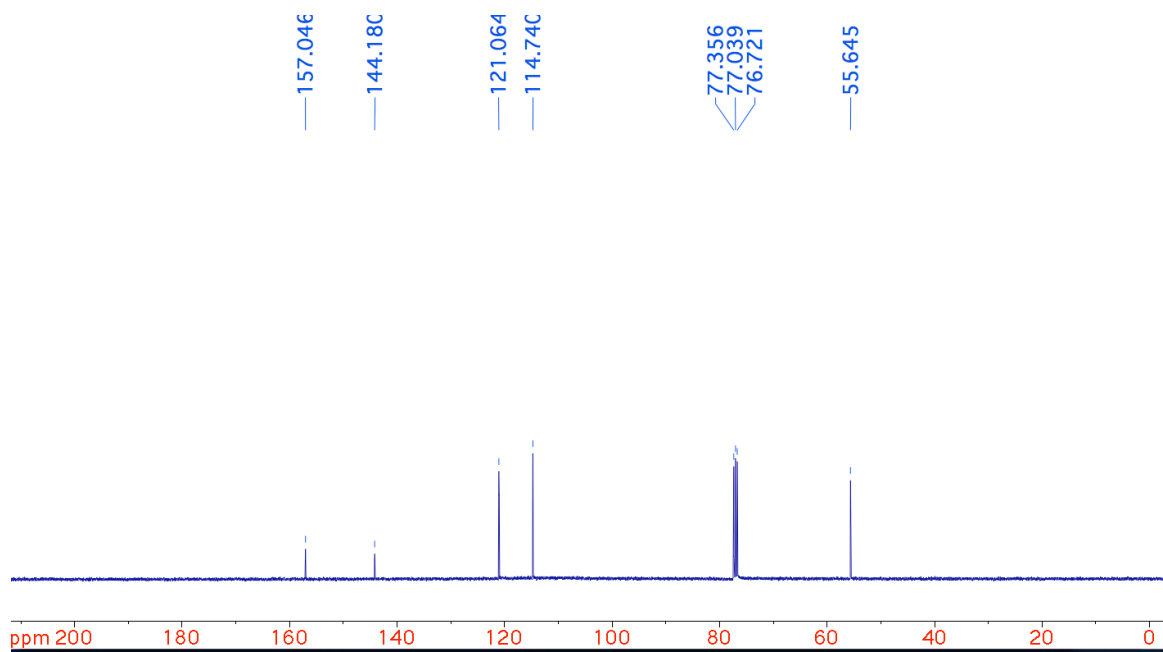


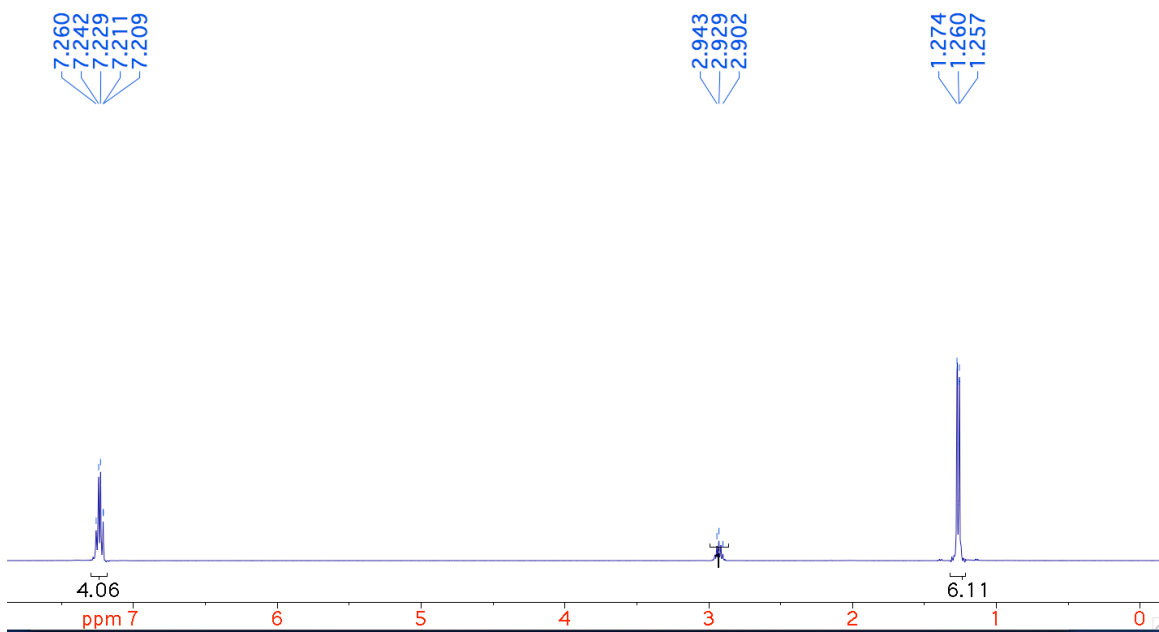
^{13}C NMR Spectrum



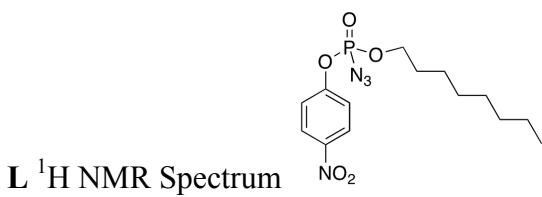
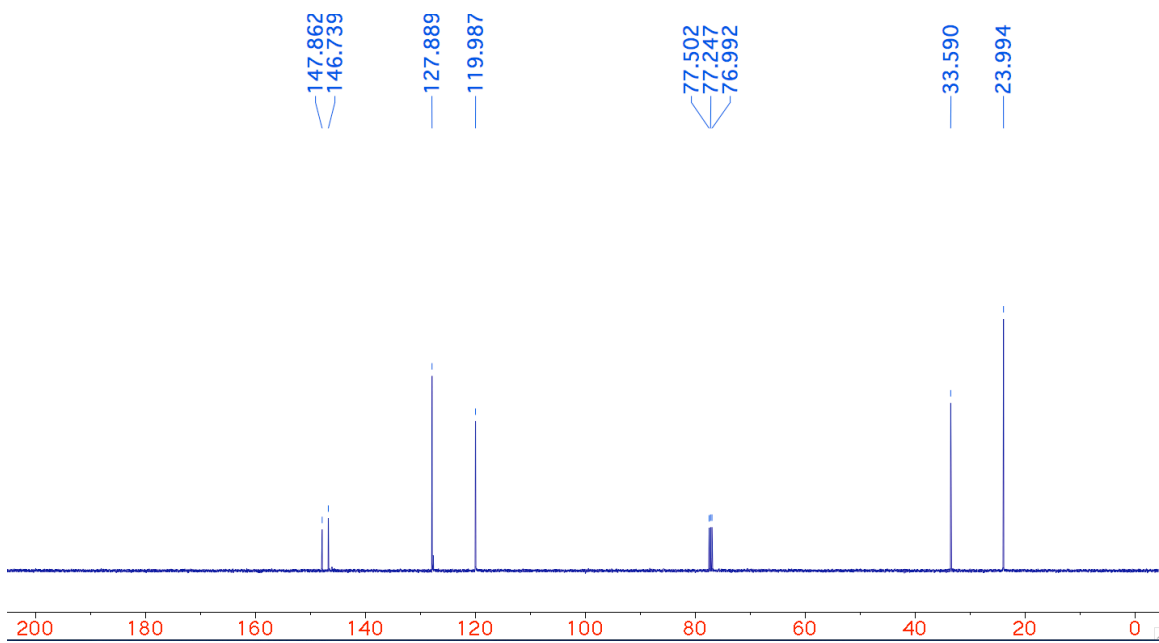


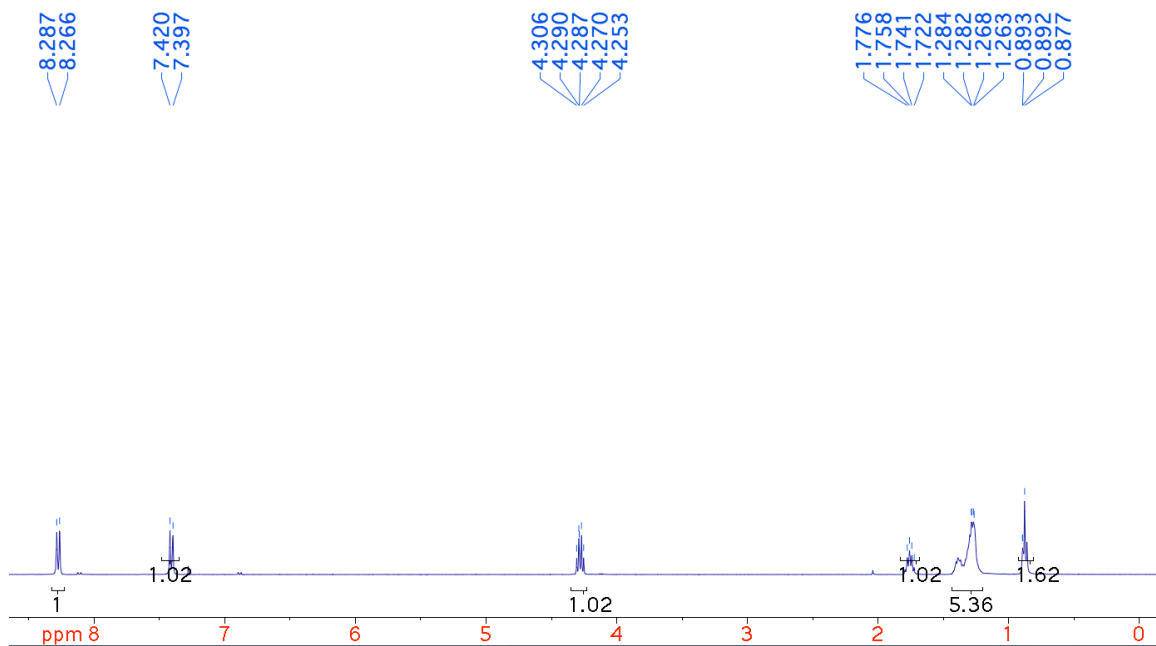
^{13}C NMR Spectrum



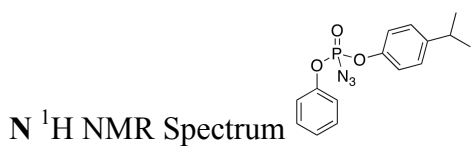
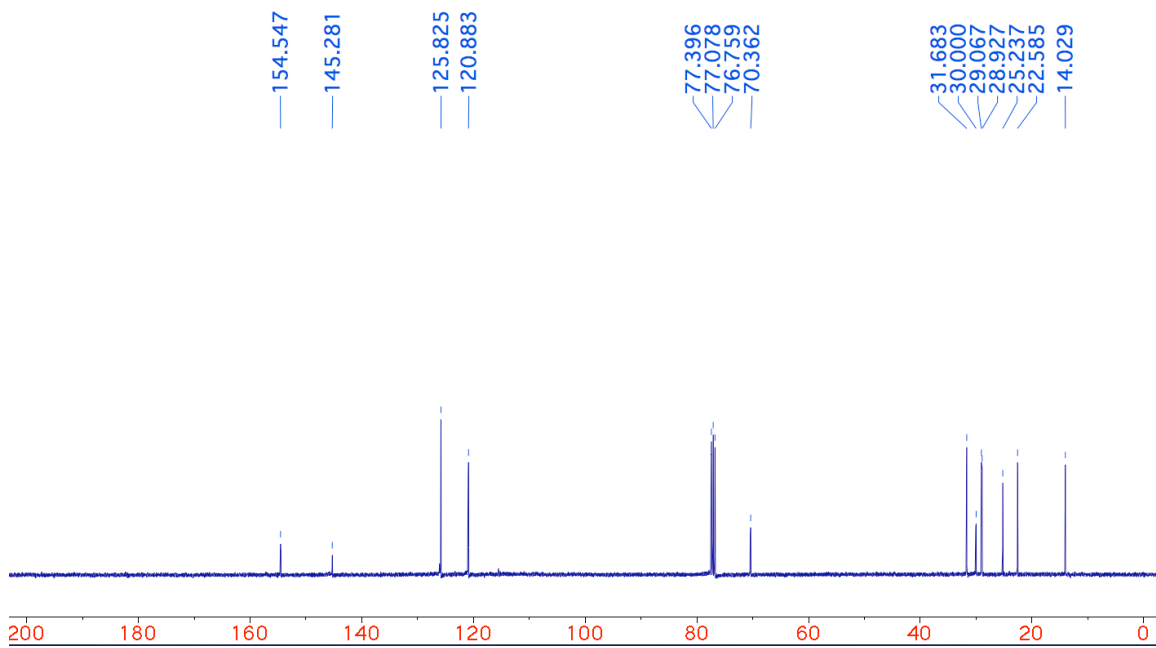


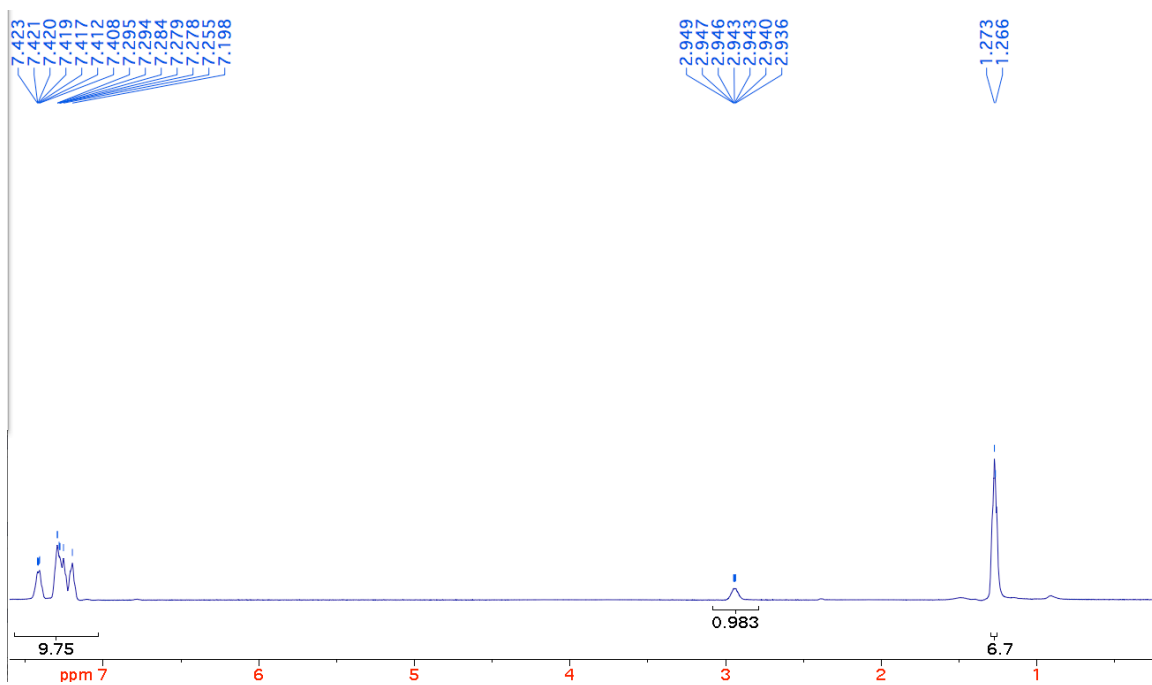
¹³C NMR Spectrum



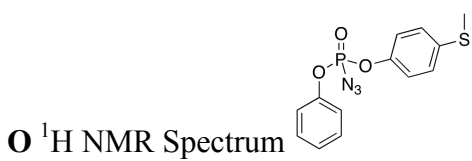
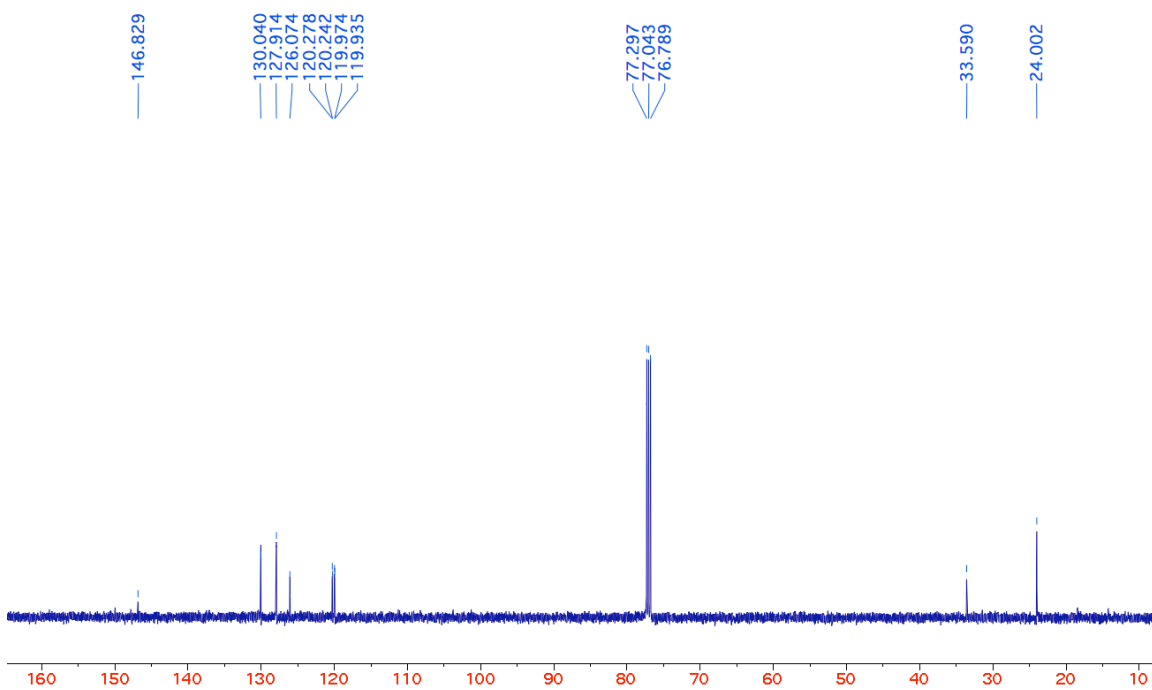


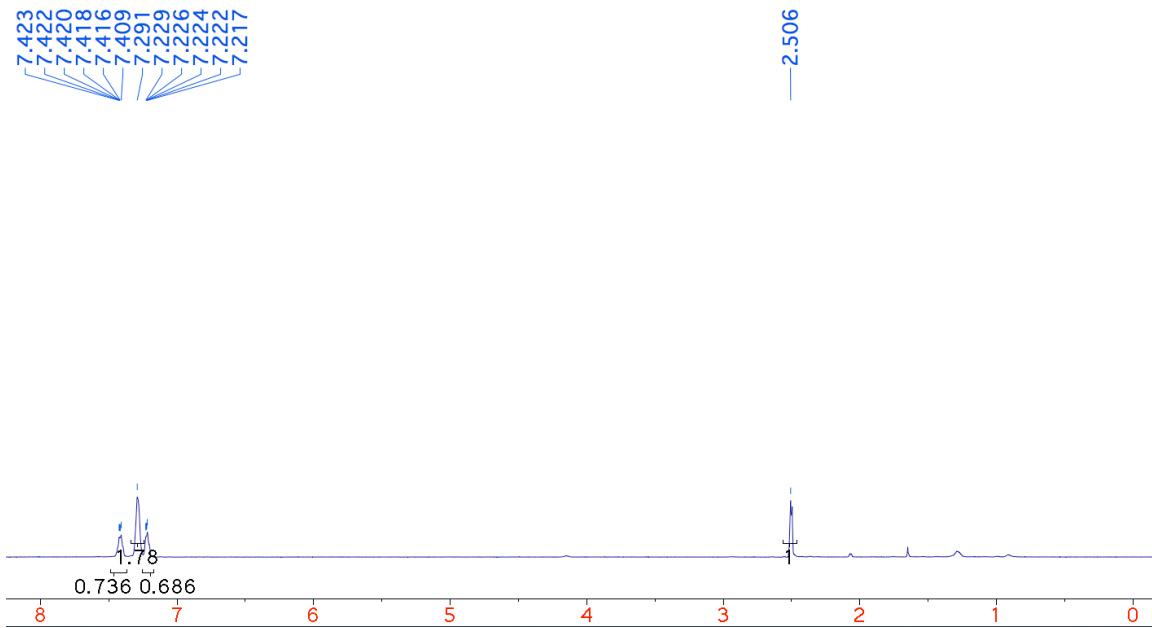
^{13}C NMR Spectrum



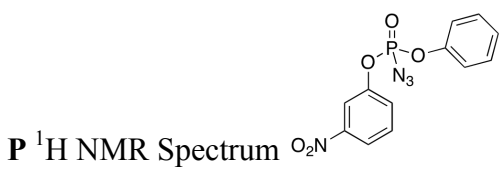
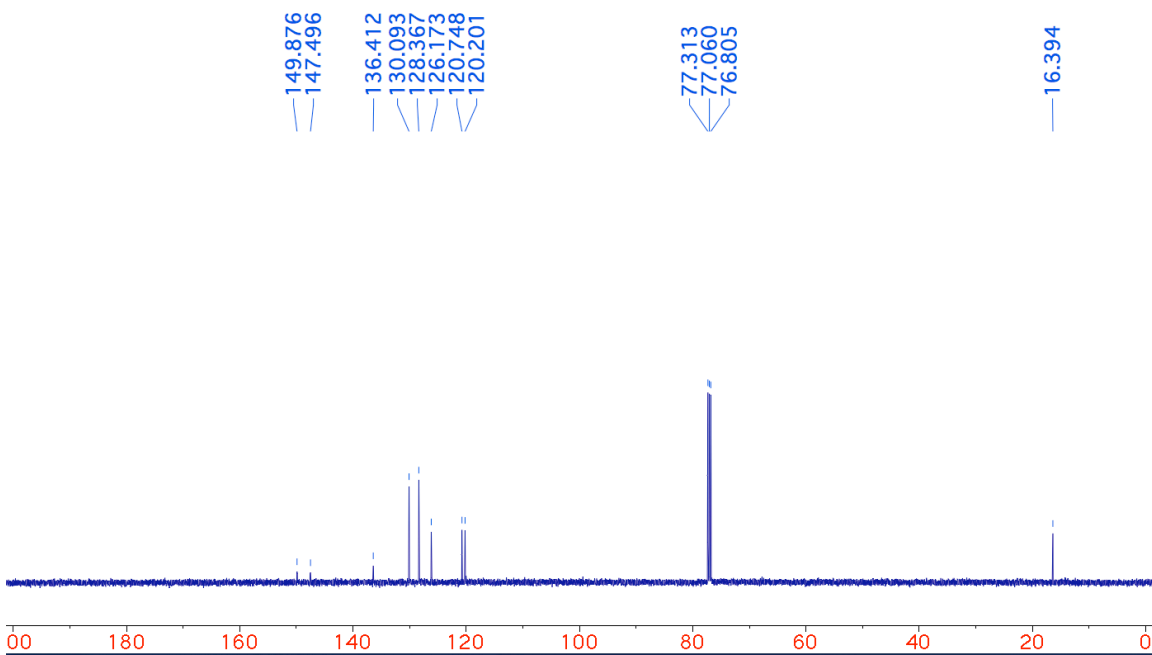


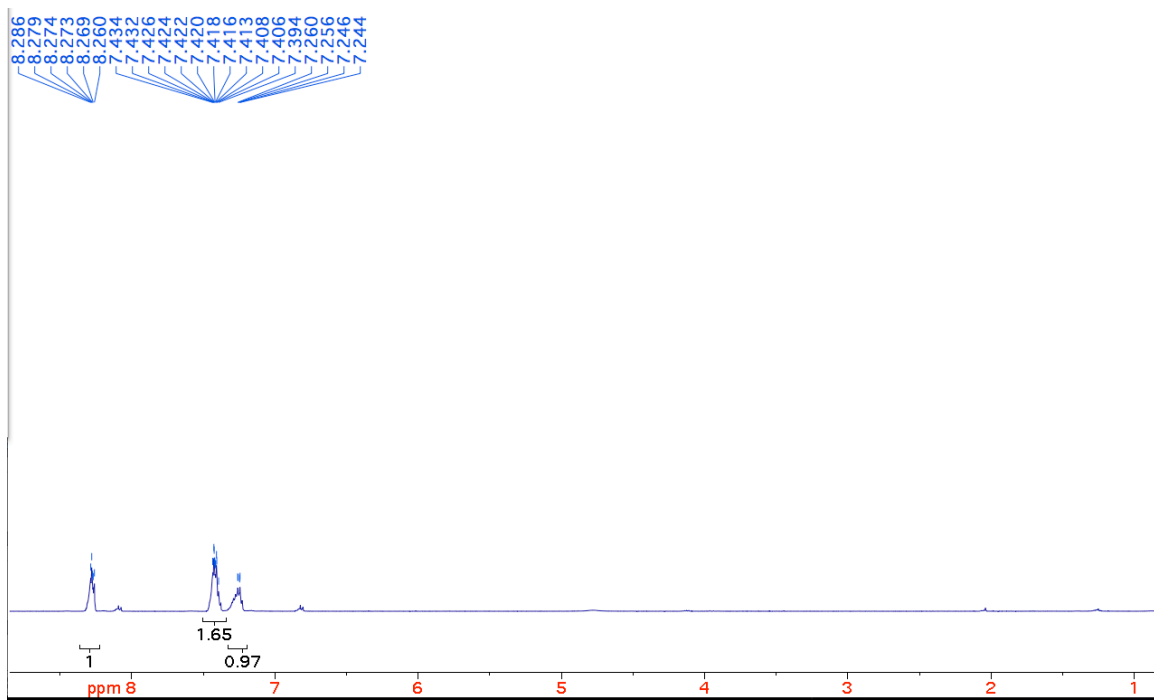
¹³C NMR Spectrum



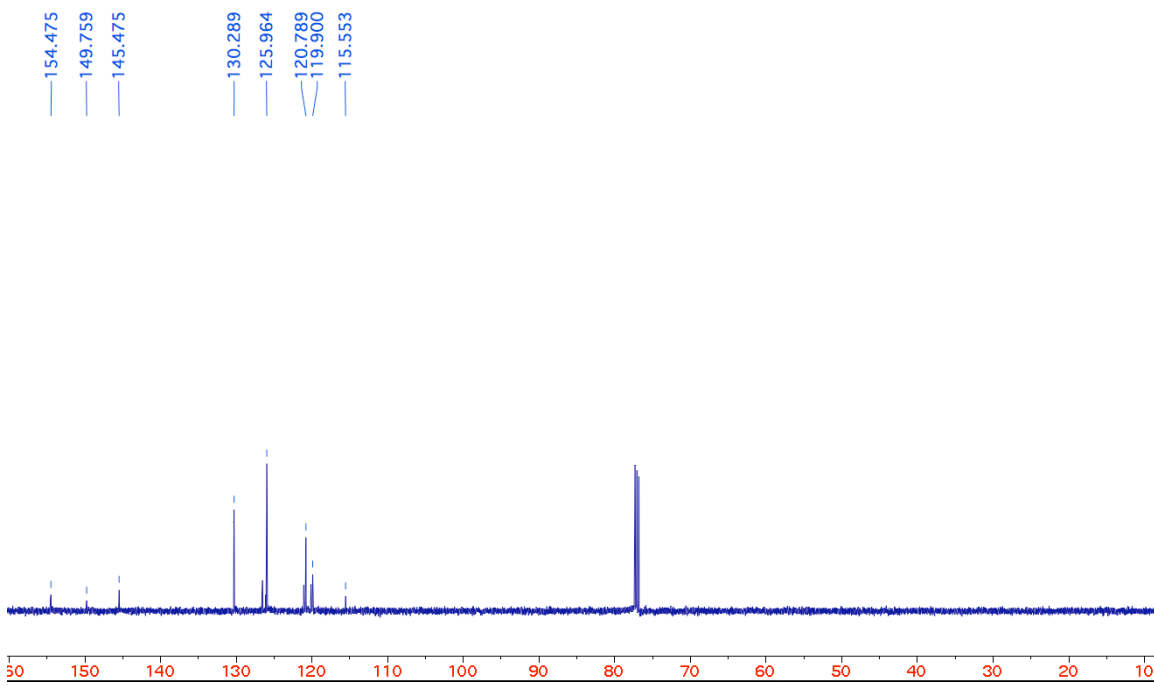


¹³C NMR Spectrum

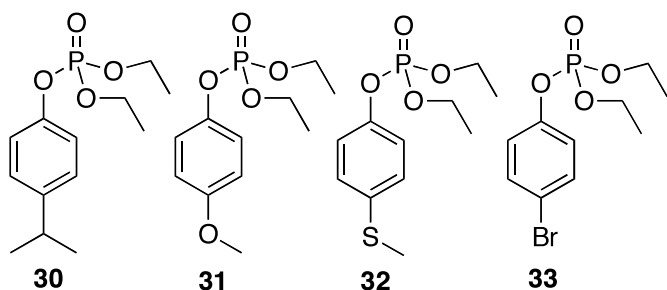




^{13}C NMR Spectrum



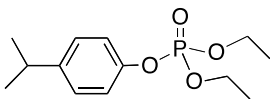
Group IV

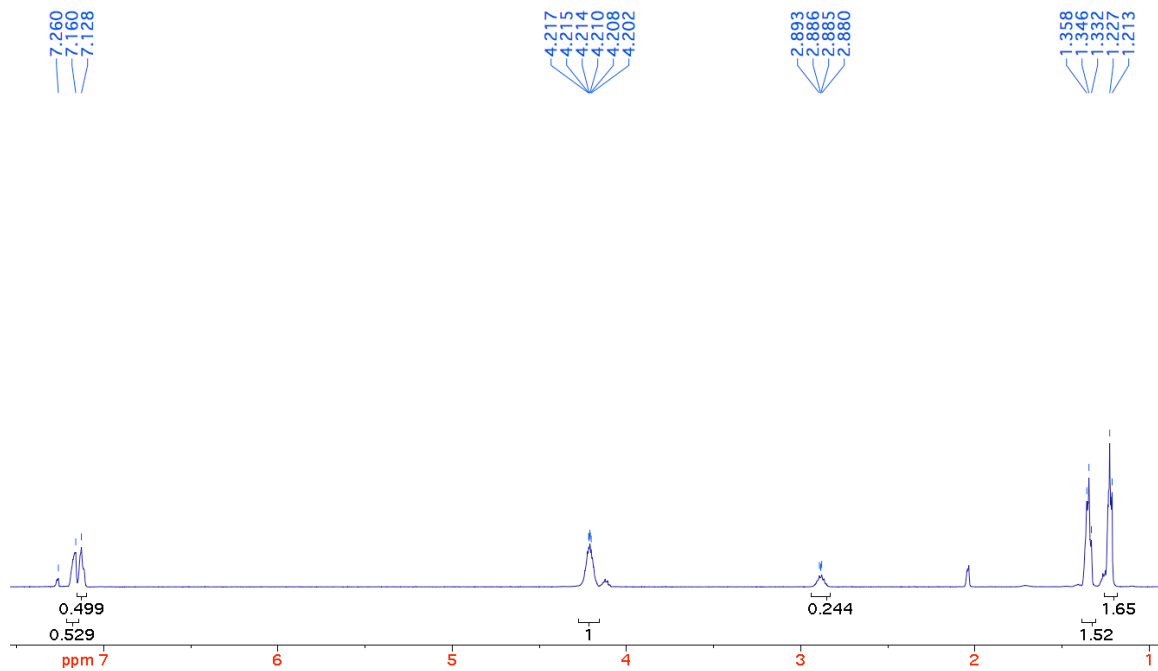


Group IV

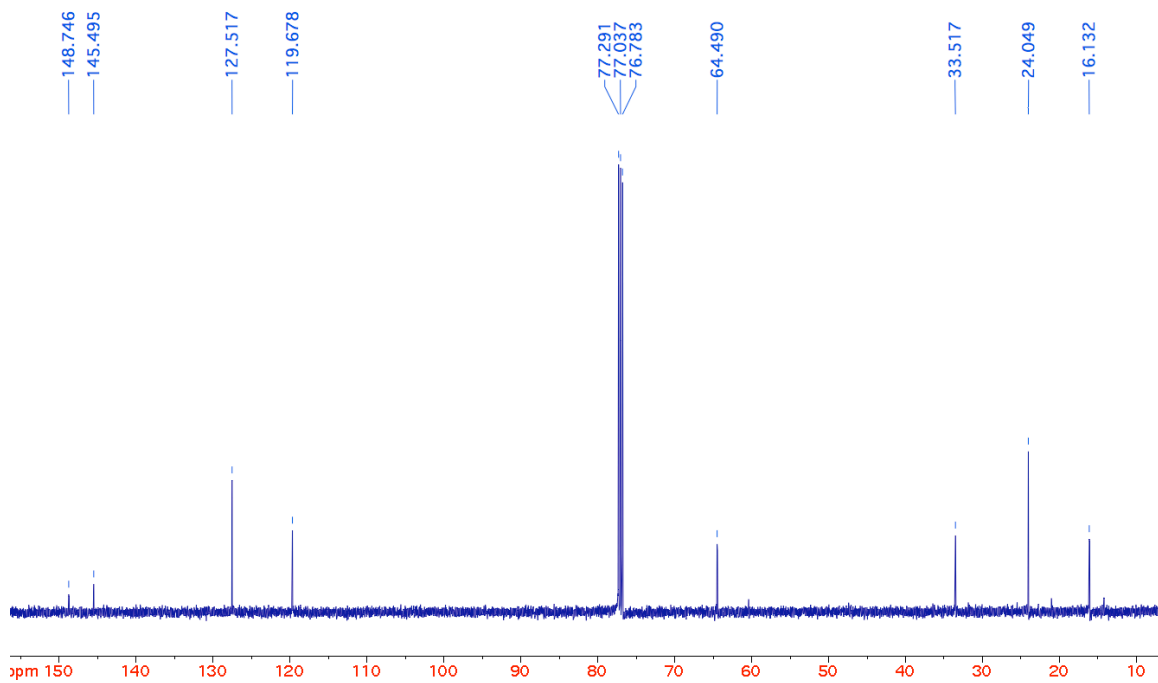
Molecule	¹ H NMR	¹³ C NMR	IR	MS
30	7.16 (2H, d, <i>J</i> 10Hz), 7.12 (2H, q, <i>J</i> 10Hz), 4.21-4.20 (4H, m), 2.89-2.88 (1H, m), 1.35 (6H, t, <i>J</i> 5Hz), 1.22 (6H, d, <i>J</i> 5Hz)	148.7, 145.5, 127.5, 119.7, 64.5, 33.5, 24.1, 16.1	2956, 1602, 1507, 1282, 1216	Calc (M+Na) ⁺ 256.1075 Expt 256.1071
31	7.20 (2H, d, <i>J</i> 10Hz), 7.11 (2H, d, <i>J</i> 10Hz), 4.16-4.14 (4H, m), 2.41 (3H, s), 1.32-1.29 (6H, m)	148.6, 134.7, 128.5, 120.5, 64.6, 16.6, 16.1	2981, 1490, 1218, 1030, 958, 772	Calc (M+Na) ⁺ 283.0711 Expt 283.0715
32	7.16 (2H, d, <i>J</i> 10Hz), 7.07 (2H, q, <i>J</i> 10Hz), 4.12 (4H, q, <i>J</i> 5Hz), 2.36 (3H, s), 1.28 (6H, t, <i>J</i> 5Hz)	148.5, 134.6, 128.3, 120.4, 64.5, 16.5, 16.0	2984, 1491, 1279, 1031, 883, 550	Calc (M+Na) ⁺ 299.0483 Expt 299.0488
33	7.43 (2H, d, <i>J</i> 10Hz), 7.10 (2H, q, <i>J</i> 10Hz), 4.21-4.17 (4H, m), 1.33 (6H, t, <i>J</i> 5Hz)	150.1, 132.9, 122.0, 118.0, 64.9, 16.3	2988, 1485, 1218, 1030, 958, 834	Calc (M+Na) ⁺ 330.9711 Expt 330.9705

30 ¹H NMR Spectrum

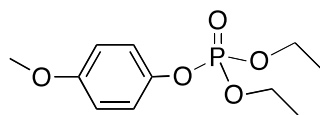


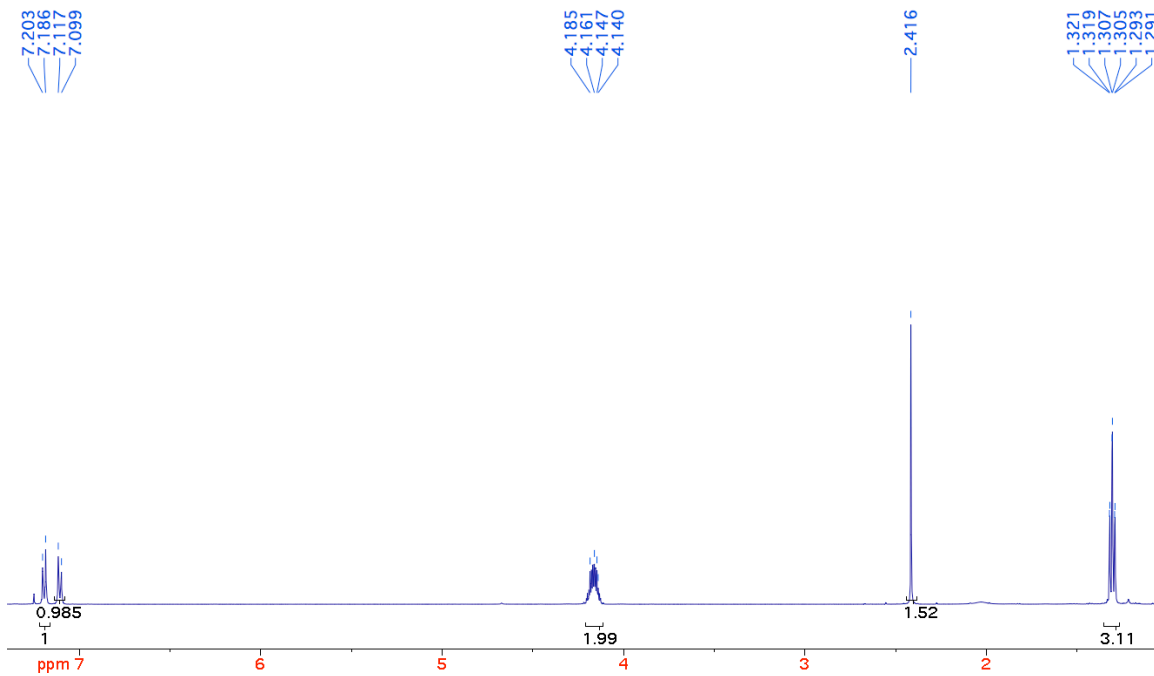


¹³C NMR Spectrum

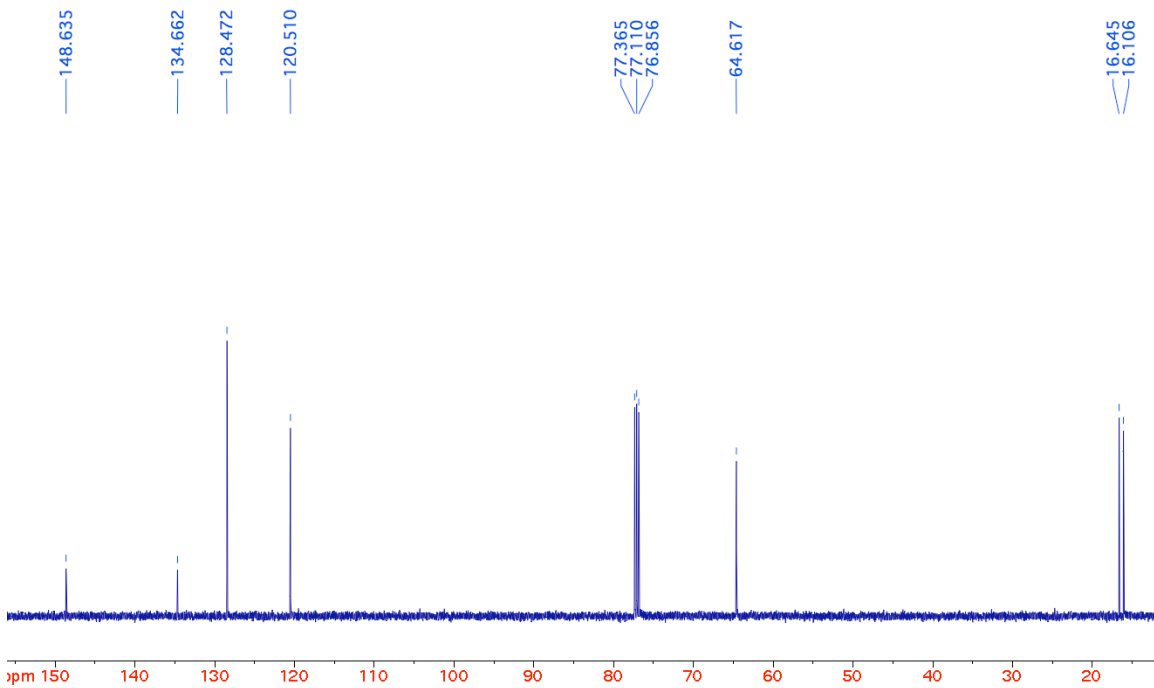


³¹P NMR Spectrum

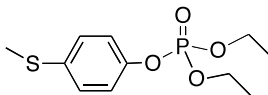


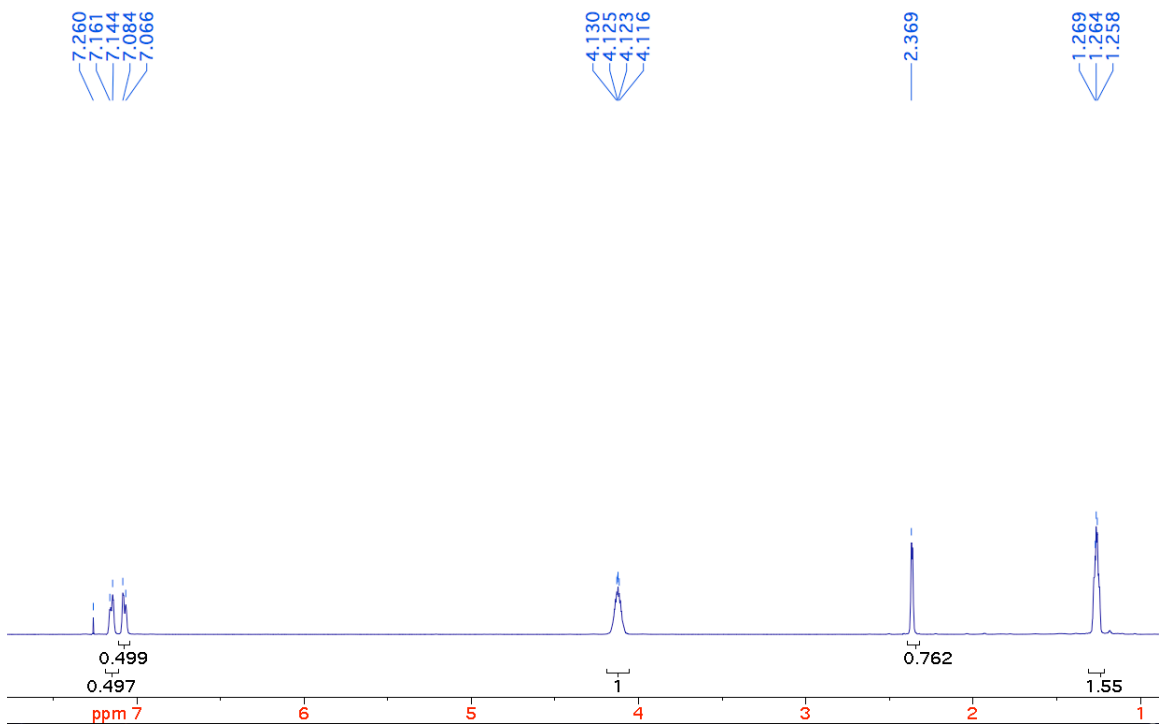


^{13}C NMR Spectrum

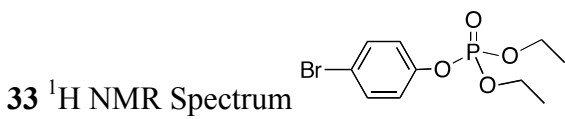
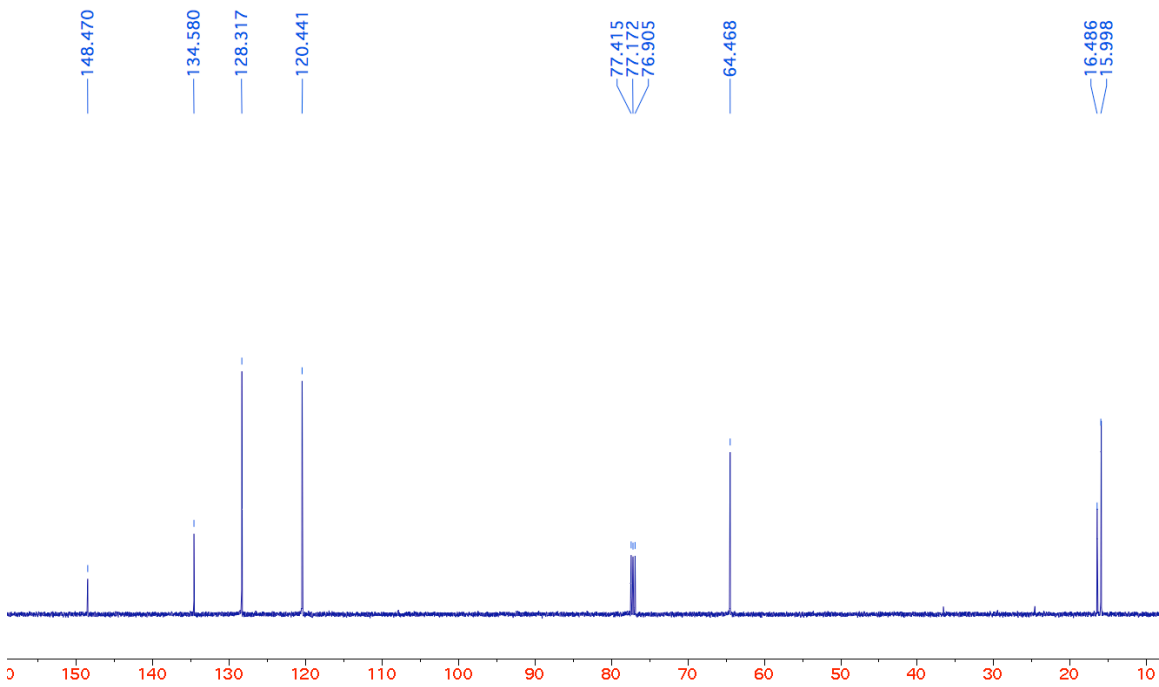


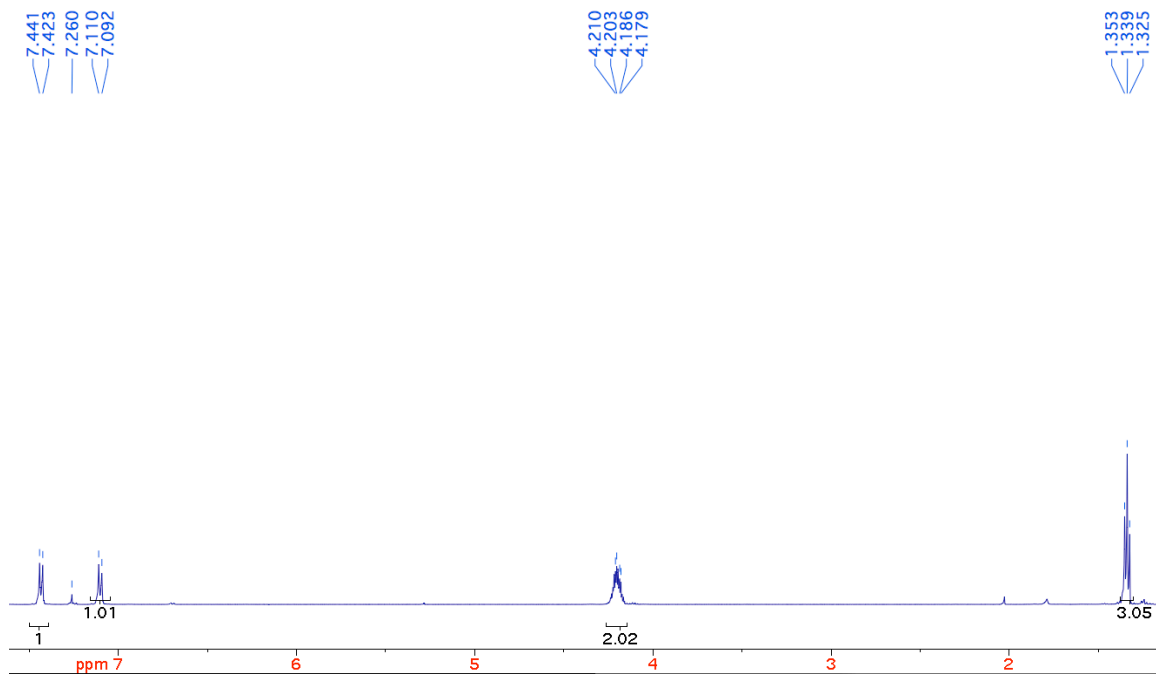
^1H NMR Spectrum



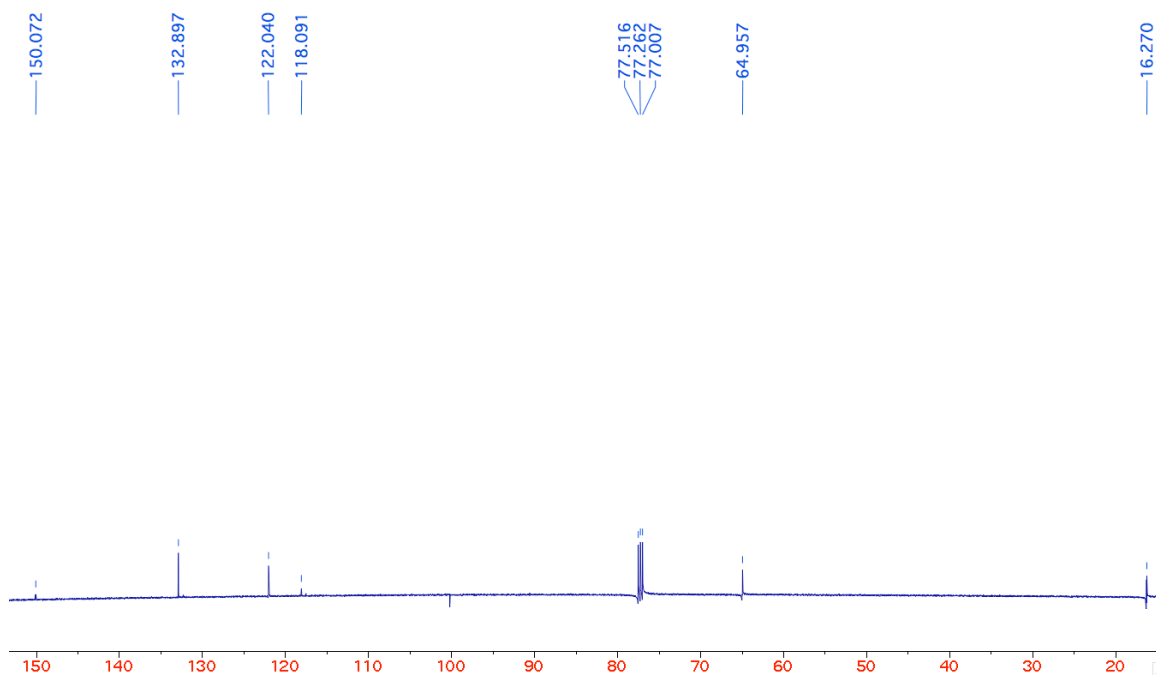


^{13}C NMR Spectrum

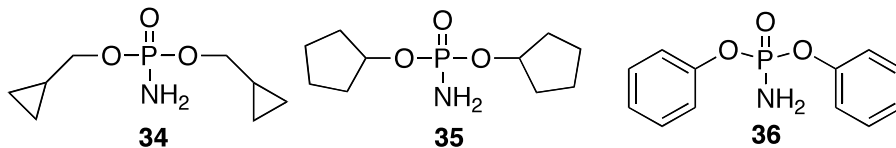




¹³C NMR Spectrum

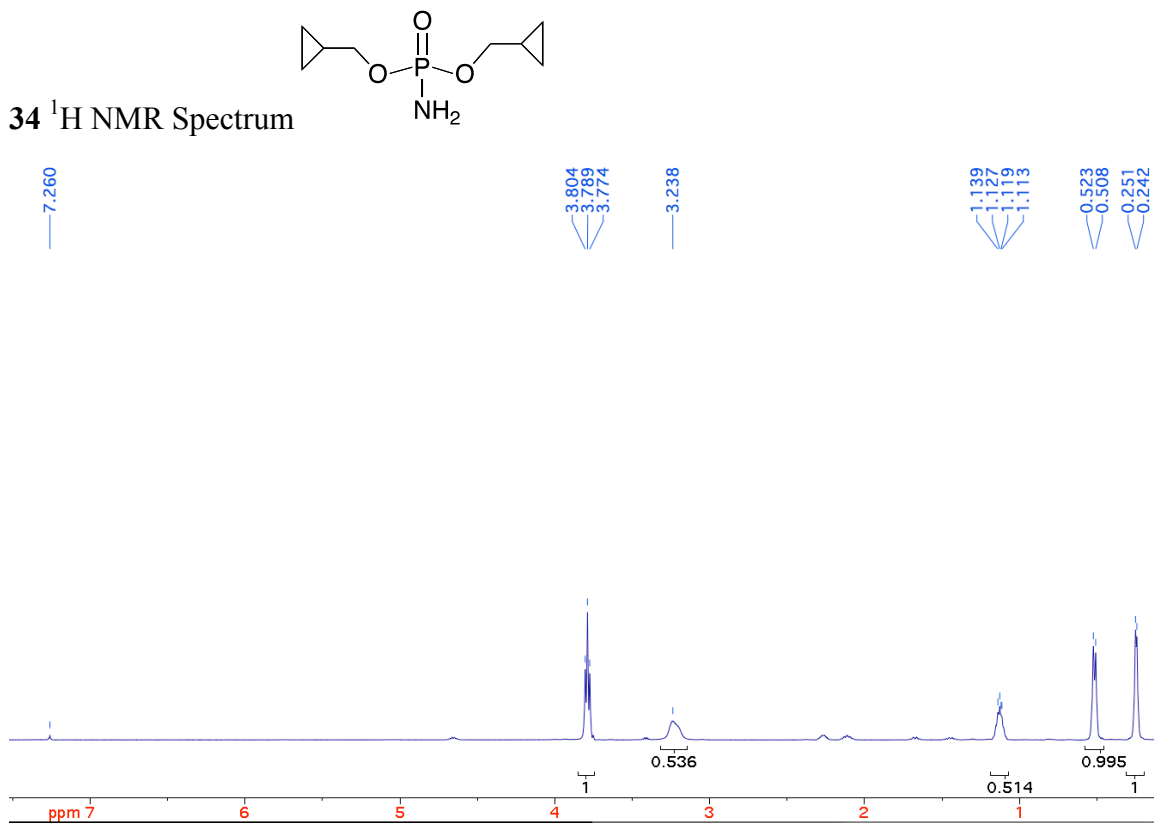


Group V

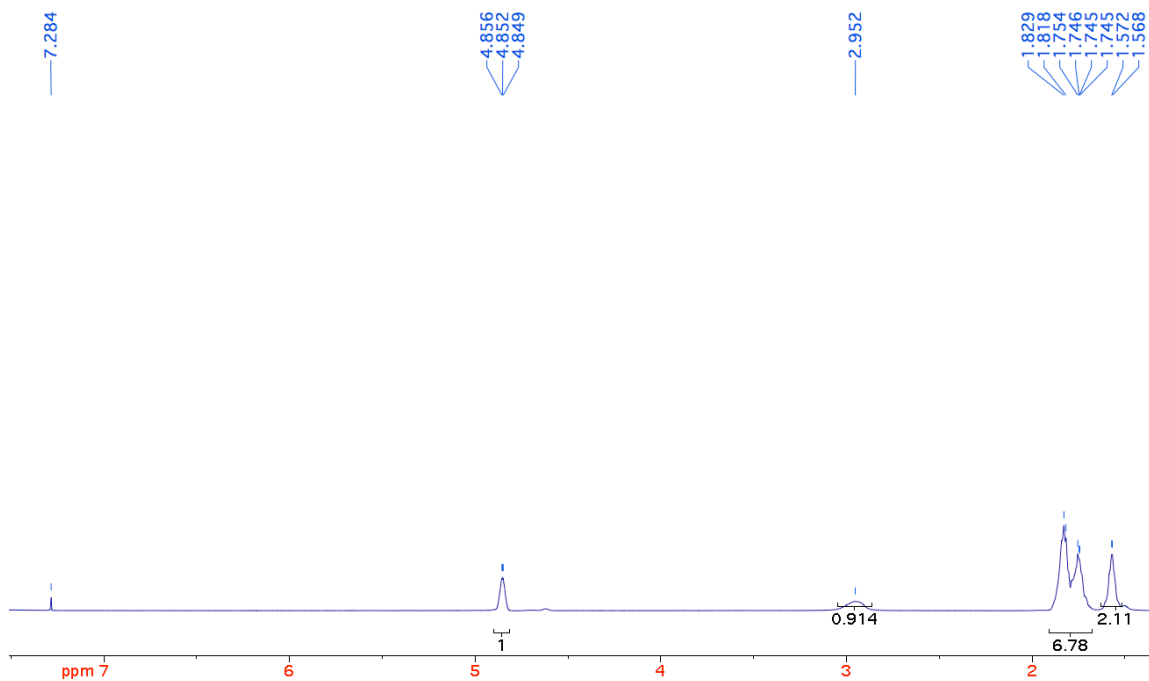
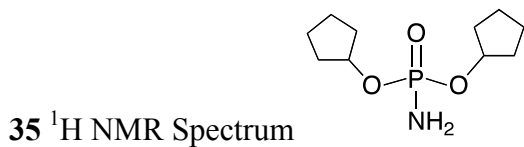
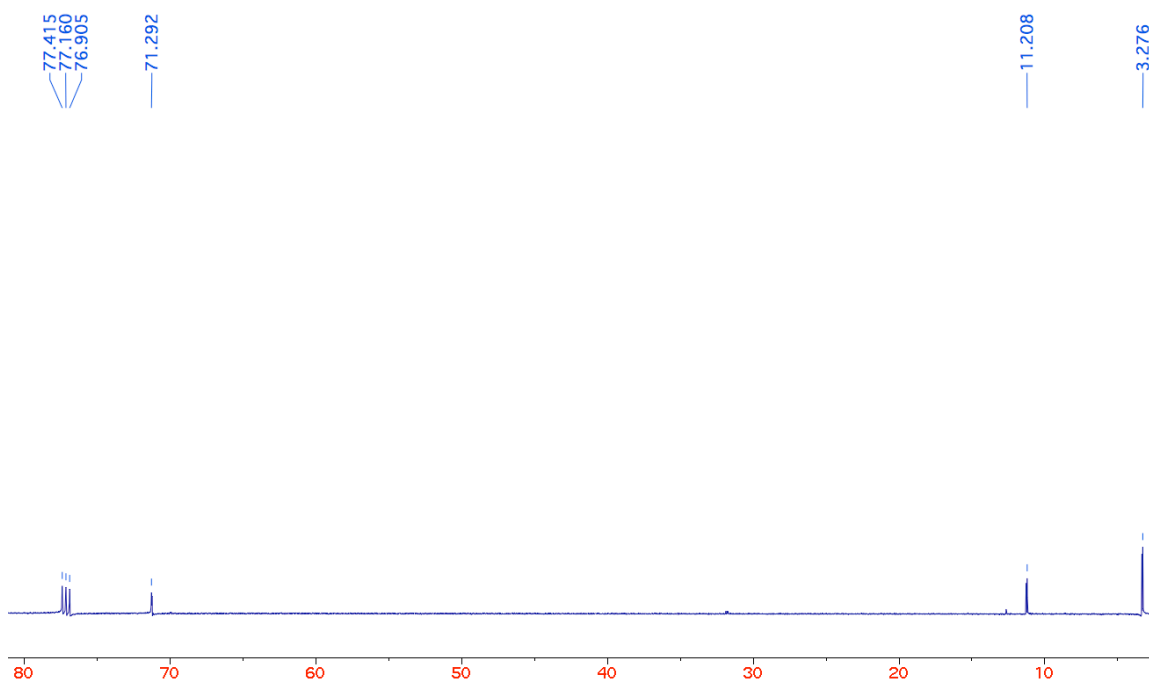


34 and **35** were synthesized following a reported procedure and the two molecules are known DFPase inhibitors.³ **36** is commercially available

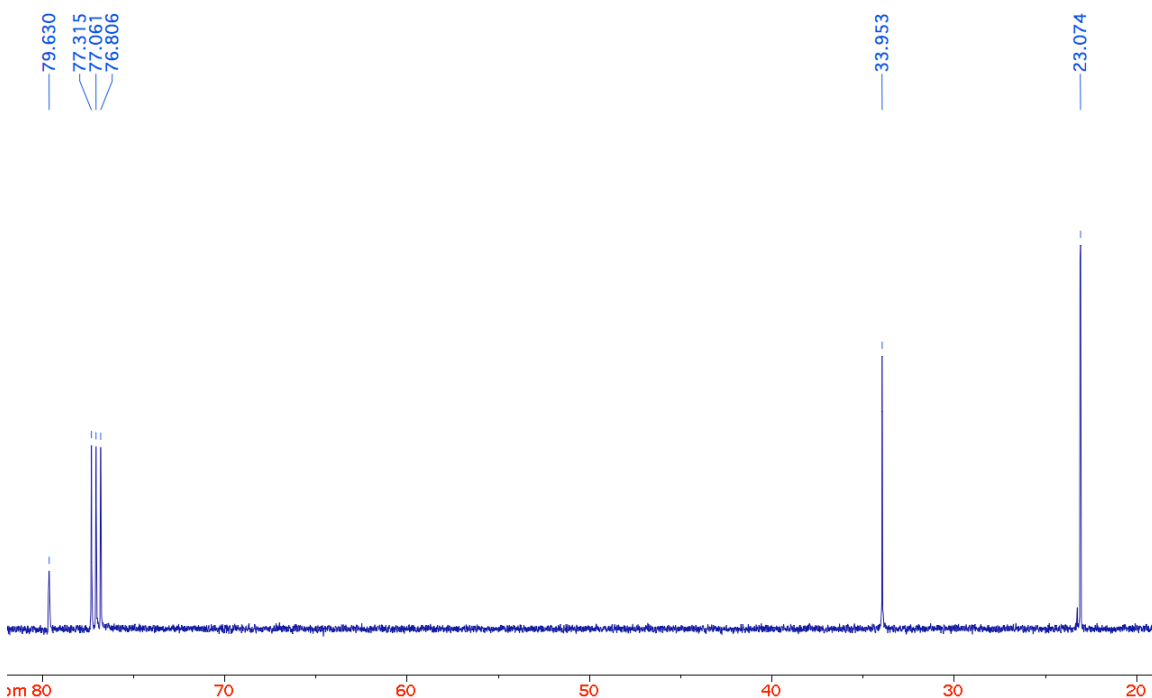
Molecule	¹ H NMR	¹³ C NMR	IR	MS
34	3.78 (3H, d, <i>J</i> 10Hz), 3.23(2H, s), 1.13-1.11 (2H, m), 0.52-0.50 (4H, d, <i>J</i> 5Hz), 0.25 (4H, d, <i>J</i> 5Hz)	71.3, 11.2, 3.3	3343, 1567, 1226, 1039, 730	Calc (M+Na) ⁺ 228.0766 Expt 228.0767
35	4.85-4.84(2H, m), 2.95(2H, bs), 1.82-1.74 (10H, m), 1.57-1.56 (4H, m)	79.6, 33.9, 23.1	3328, 2955, 1570, 1446, 990	Calc (M+Na) ⁺ 256.1078 Expt 256.1077



¹³C NMR Spectrum



¹³C NMR Spectrum

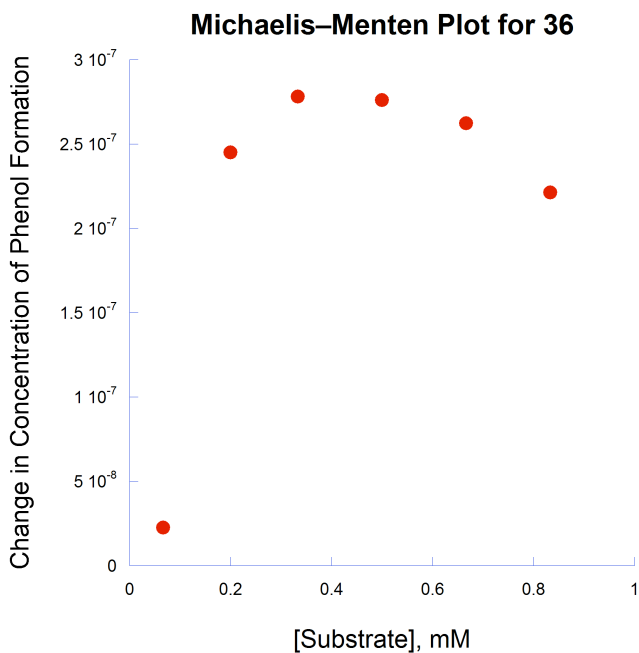
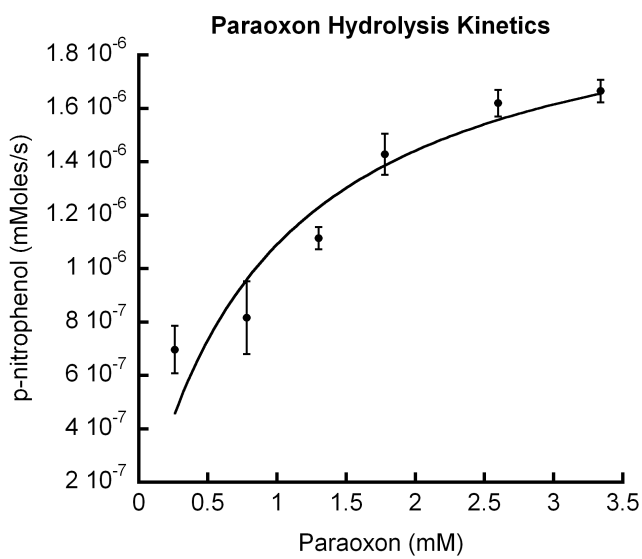


4. Details on Enzyme Preparation and determination of Enzyme Kinetics

Expression and Purification of G2E6: Briefly, plasmid encoding Trx-G2E6 fusion gene was expressed in Origami B(DE3) cells (Novagen, Madison, WI). The expression was carried out in 2YT culture media. The culture was grown at 37°C until OD₆₀₀ was reached at 0.8 when it was induced with 0.1 mM IPTG and expressed further for 3 hours at 30°C. The cells were then harvested by centrifugation and stored at -80°C until further use. The harvested cells were resuspended in lysis buffer [50 mM Tris-HCl pH 8.0, 50 mM NaCl, 1 mM CaCl₂, 0.1 mM DTT, and 10% glycerol] and were passed through a syringe needle. The crude lysate was then sonicated and recovered further by incubation with 0.1% tergitol NP-10 (Sigma-Aldrich, St. Louis, MO) with shaking at 4°C for 2.5 hours. After centrifugation, Ni-NTA resin (Qiagen, Valencia, CA), pre-equilibrated with lysis buffer containing 0.1% tergitol NP-10, was added to the supernatant, and the mixture was shaken for 3 hours. The resin was then washed with activity buffer [50 mM Tris-HCl pH 8.0, 50 mM NaCl, 1 mM CaCl₂, 0.1% tergitol NP-10, 10% glycerol] containing increasing concentrations of imidazole (5 mM, 10 mM, and 25 mM, respectively). The fusion protein was eluted with activity buffer containing 125 mM imidazole. The final elution was then dialyzed (10000 MW cutoff; slide-a-lyzer, Pierce, Rockford, IL) in activity buffer to remove imidazole and monitored on SDS-PAGE gel for homogeneity. The protein concentration was determined using a Bradford assay (Bio-Rad Laboratories, Hercules, CA).

Determination of kinetic parameters: The kinetic parameters (k_{cat} , K_M) were determined using a Michaelis-Menten plot as demonstrated for a reference substrate. Briefly, to

assay buffer [50 mM Tris-HCl pH 7.4, 1mM CaCl₂], varying concentrations of substrates (paraoxon, 0.26 mM to 2.6 mM) and known concentration of enzyme (rePON1 G2E6) were added, and hydrolysis was monitored by UV-vis spectroscopy at 405 nm for 10 minutes. The rate of product (*p*-nitrophenol) formation was then plotted against substrate concentration and fitted to the Michaelis–Menten equation using KaleidaGraph. A typical curve is shown below.



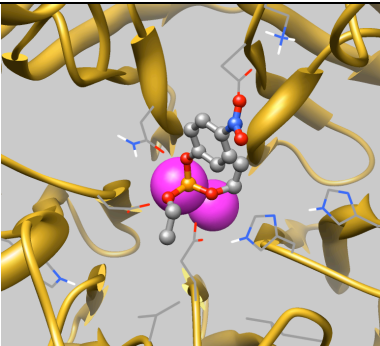
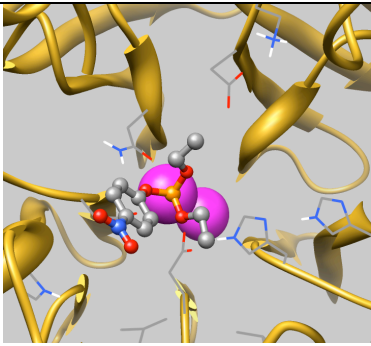
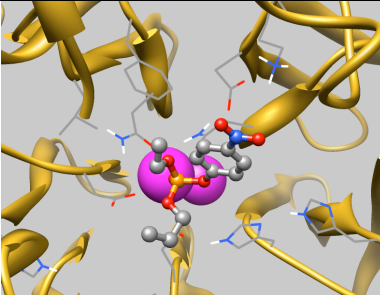
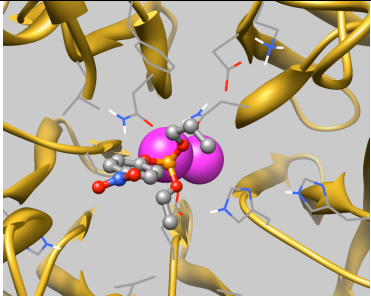
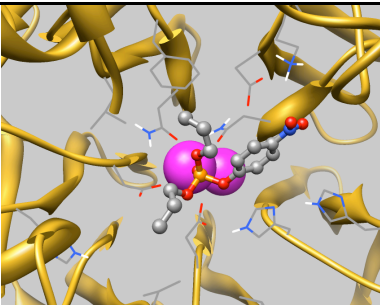
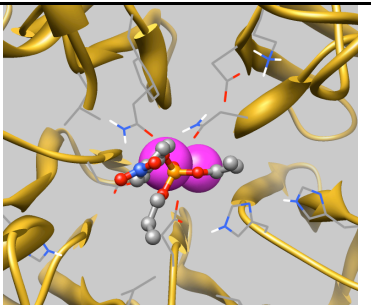
5. Selected Poses from docking of ligands in G2E6

In general, the docking poses obtained from Autodock revealed an adequate job of sampling ligand orientations in the active site. Both the leaving groups as well as the

other phosphoryl substituents were found to orient themselves into the various pockets comprising the active site region. However, a significant percentage of poses were found to result in the substrate not coordinating to the calcium ion owing to the vertical extension of the active site box. These were discarded from further refinement due to the lack of catalytic relevance, based on the assumption that calcium coordination to the phosphoryl oxygen is critical for catalytic activity.

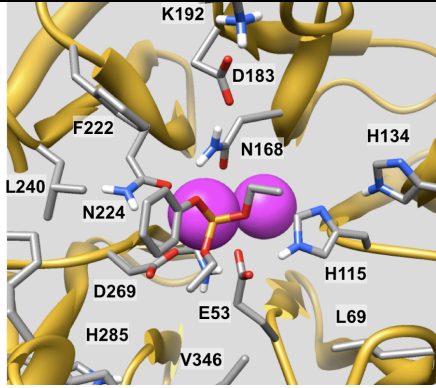
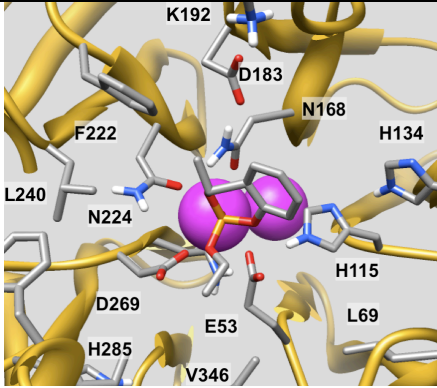
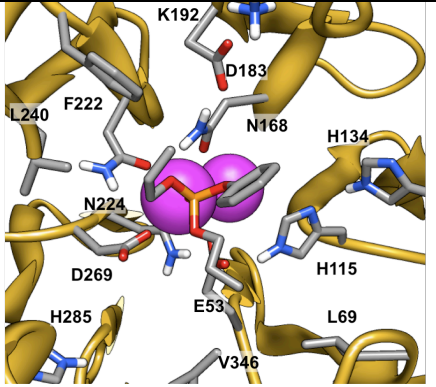
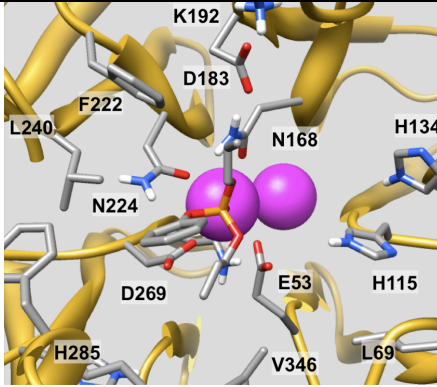
The energy scores from the docking simulations were not a useful metric for determining the quality of the pose. Similar energy scores were obtained for poses that placed the phosphoryl oxygen in proximity to calcium and those that placed the ligand into the HDL binding domain of the protein. Moreover, treatment of electrostatic interactions, particularly on the leaving group, was not very reliable. In many cases, the nitro group was placed in highly nonpolar pockets without a significant energetic penalty relative to those that provided suitable hydrogen bond donors, for instance. The principal utility of the docking simulations, then, was on giving a series of poses for subsequent MD simulations. Representative poses from docking are shown below:

Representative Docking Poses from Group I Molecules. All scores are in kcal/mol

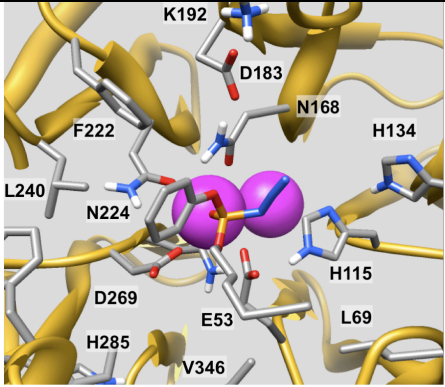
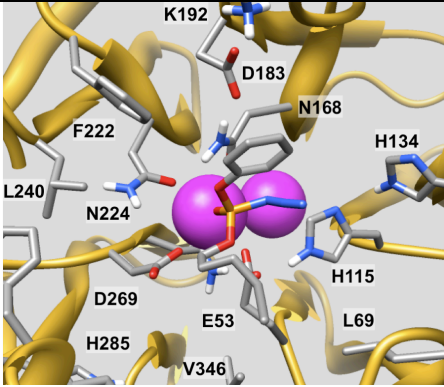
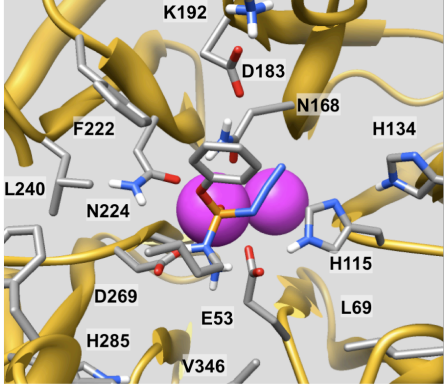
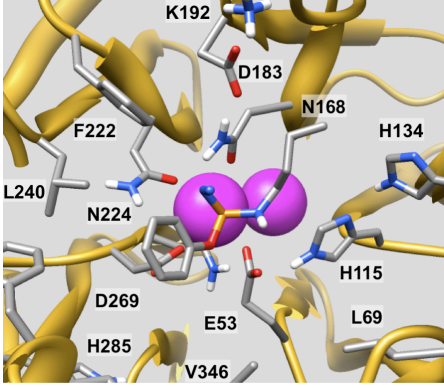
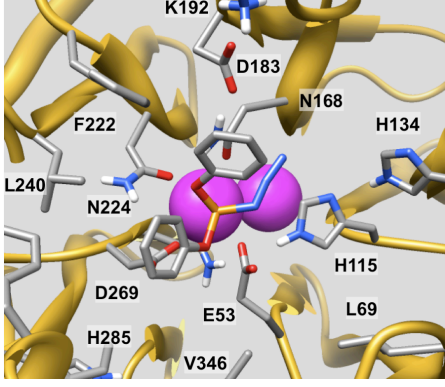
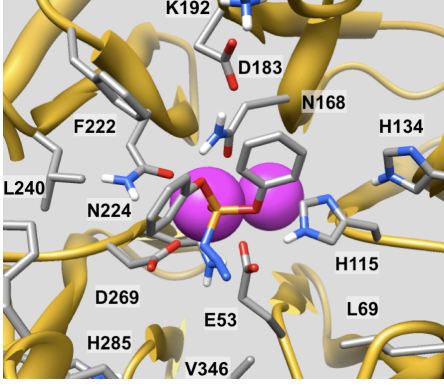
Molecule	Pose 1	Pose 2
Paraoxon (1)	 <p data-bbox="537 1289 753 1318">Docking Score: -9.1</p>	 <p data-bbox="948 1289 1164 1318">Docking Score: -8.8</p>
8	 <p data-bbox="537 1646 753 1675">Docking Score: -8.6</p>	 <p data-bbox="948 1646 1164 1675">Docking Score: -7.5</p>
10		

	Docking Score: -9.2	Docking Score: -8.4
--	---------------------	---------------------

Representative Docking Poses from Group II Molecules

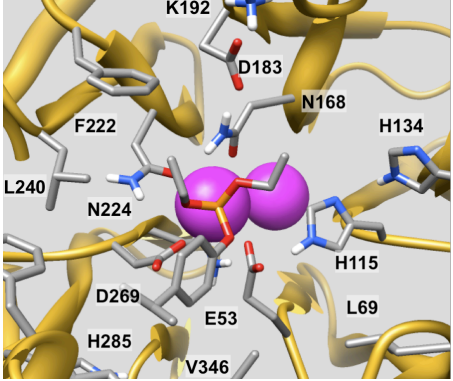
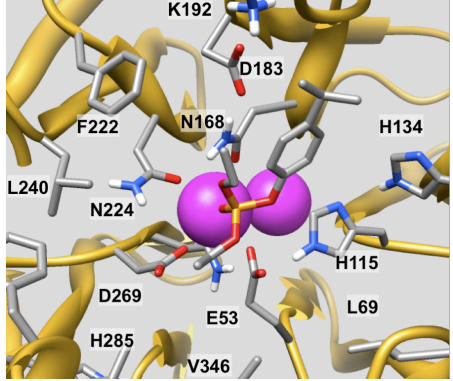
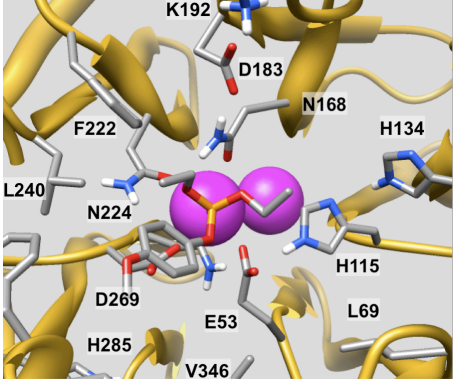
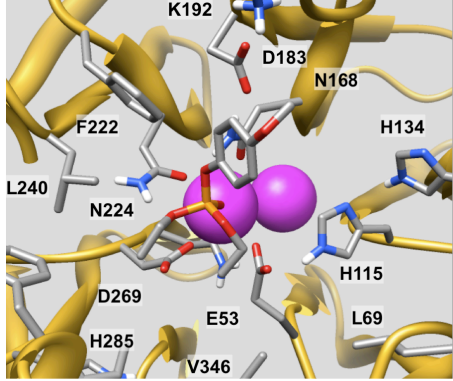
Molecule	Pose 1	Pose 2
17 (65)	 <p>Docking Score: -9.7</p>	 <p>Docking Score: -9.4</p>
18 (120)	 <p>Docking Score: -9.1</p>	 <p>Docking Score: -7.5</p>

Representative Docking Poses from Group III Molecules

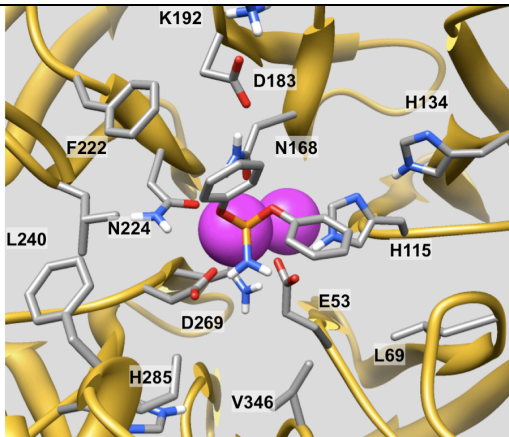
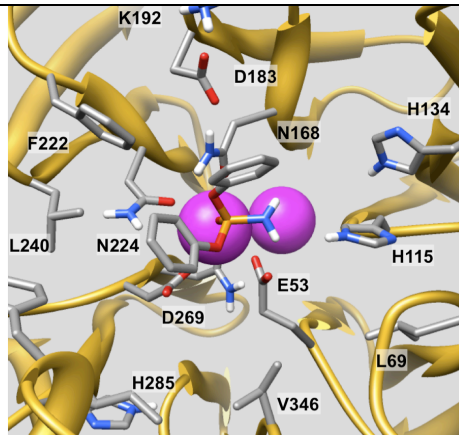
Molecule	Pose 1	Pose 2
23 (131)	 <p>Docking Score: -8.5</p>	 <p>Docking Score: -8.0</p>
24 (118)	 <p>Docking Score: -9.6</p>	 <p>Docking Score: -9.5</p>
25 (71)	 <p>Docking Score: -10.0</p>	 <p>Docking Score: -9.1</p>

Representative Docking Poses from Group IV Molecules

Molecule	Pose 1	Pose 2
----------	--------	--------

<p>30 (79)</p>	 <p>Docking Score: -10.5</p>	 <p>Docking Score: -9.4</p>
<p>31 (75)</p>	 <p>Docking Score: -9.2</p>	 <p>Docking Score: -7.1</p>

Representative Docking Poses from Group V Molecules

Molecule	Pose 1	Pose 2
<p>36</p>	 <p>Docking Score: -11.2</p>	 <p>Docking Score: -8.7</p>

6. Selected Poses from MD simulations of ligand-G2E6 complex

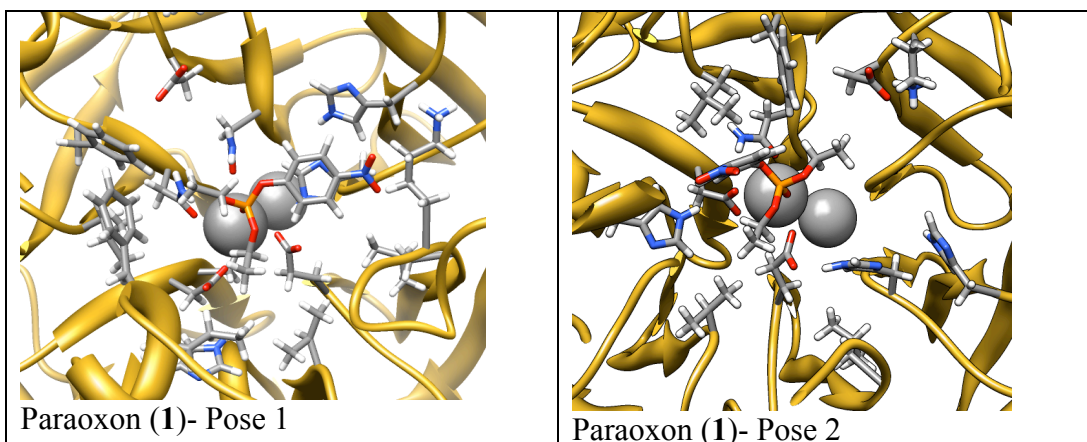
After analysis of the various docking poses for different OP ligands bound into the active-site snapshots, subsequent MD simulations were performed on select calcium-bound receptor-ligand complexes obtained from the docking simulations. A similar minimization protocol was utilized as described for the initial G2E6 model; the only difference was the inclusion of a moderate, flattened parabolic restraint on the calcium-phosphoryl oxygen bond coordinate, from 2.5 to 4.0 Å, to allow for enhanced relaxation of the ligand-receptor contacts prior to the possible dissociation of substrate. This was found to improve on the sub-optimal treatment of receptor flexibility in the docking protocol, and resulted in a reduction in the number of dissociative poses. A total of 4 ns of unrestrained MD simulations were performed on each ligand-receptor complex. A series of coordinate snapshots was extracted from the production MD trajectory from the terminal 1.5 ns of simulations, at 10 ps intervals, from which individual trajectories were generated for the unbound ligand, free receptor, and complex. Poisson-Boltzmann (MM-PBSA)³ and Generalized Born (MM-GBSA)⁴ simulations were performed on these snapshots, using the *sander* module to calculate individual components of the free energy for each component as in eq 1. From the individual results, the overall free energy of binding was calculated using eq 2.

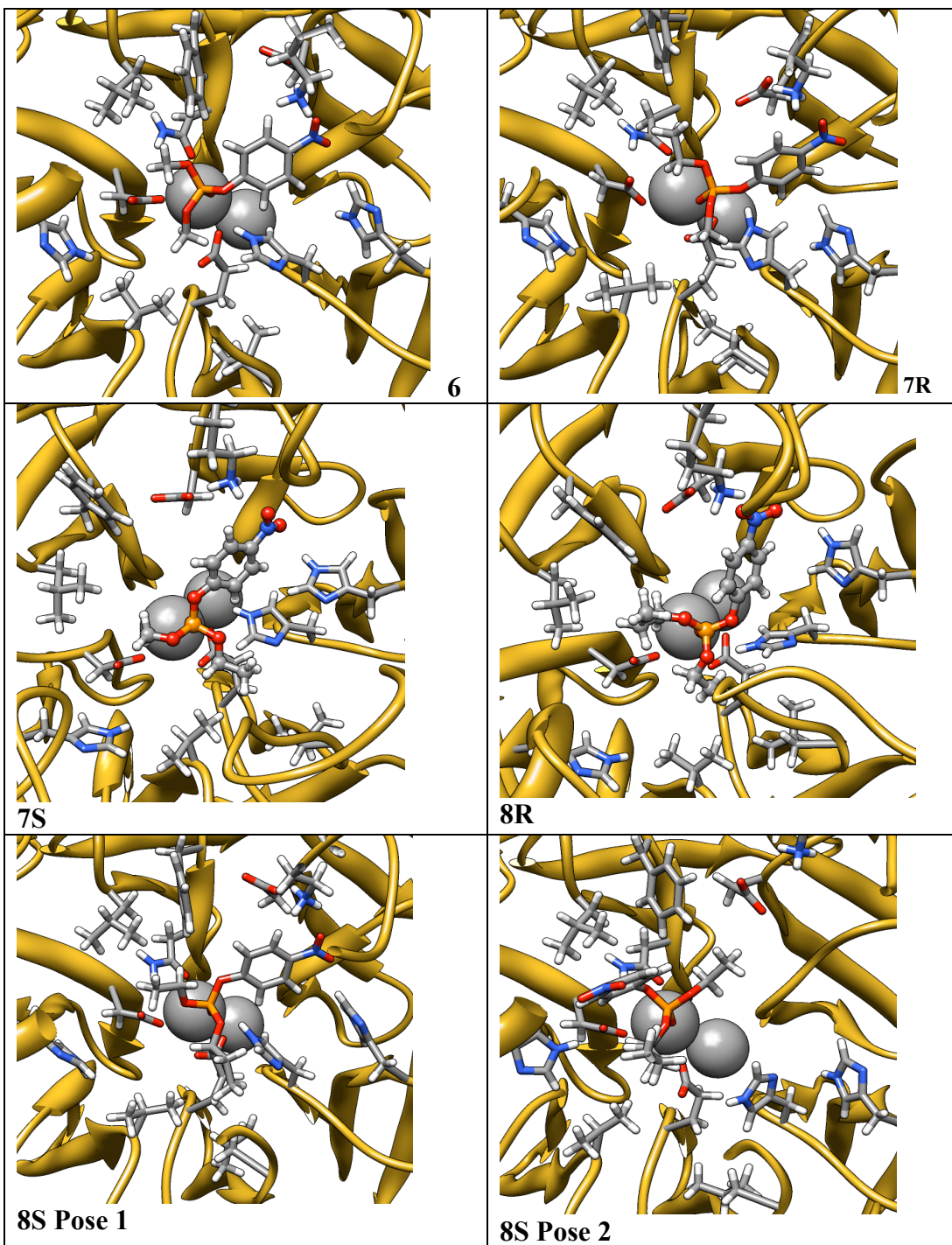
$$G = G_{\text{hyd}} + E_{\text{MM}} - TS_{\text{solute}} \quad (1)$$

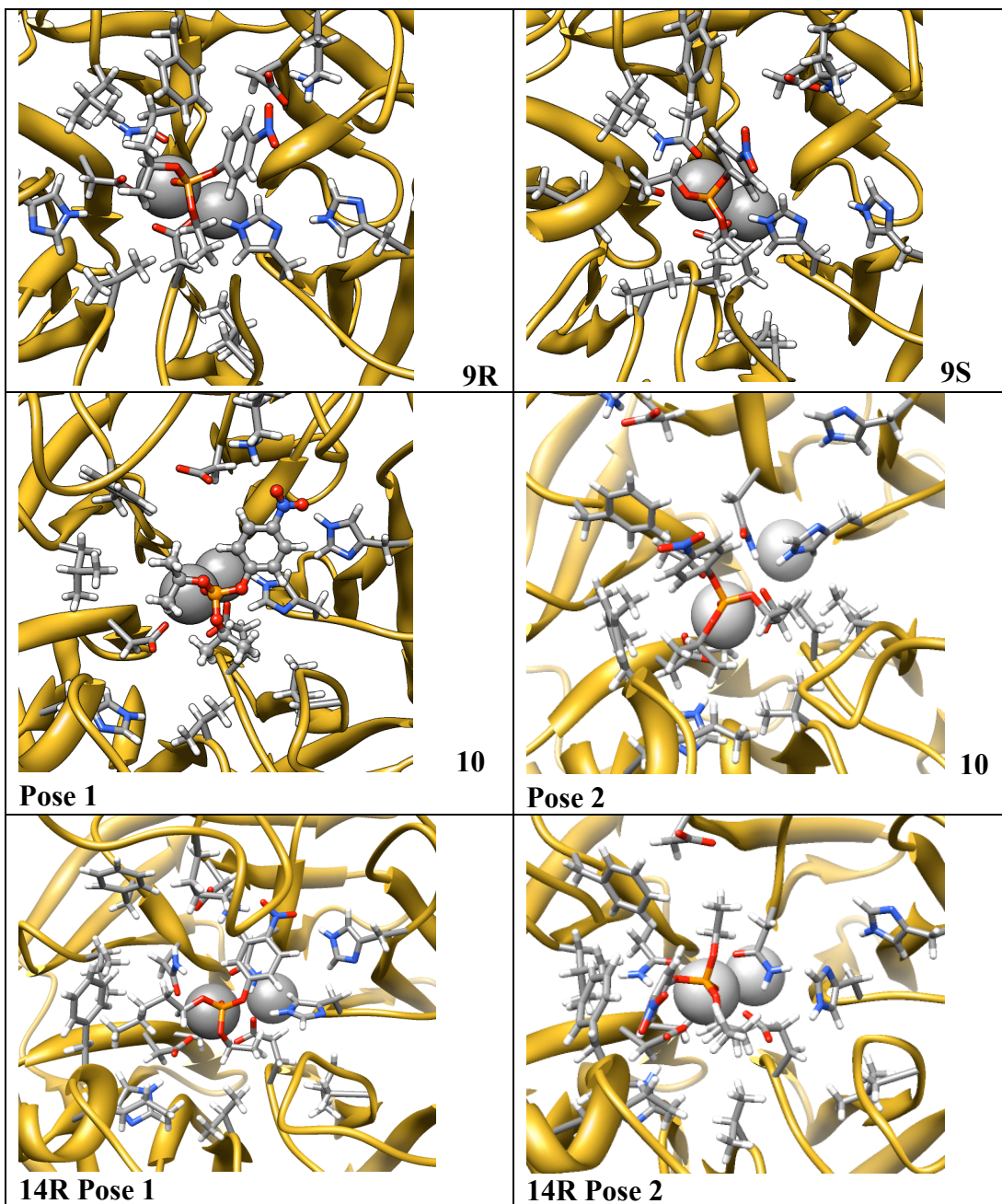
$$\Delta G_{\text{bind}} = G_{\text{complex}} - (G_{\text{receptor}} + G_{\text{ligand}}) \quad (2)$$

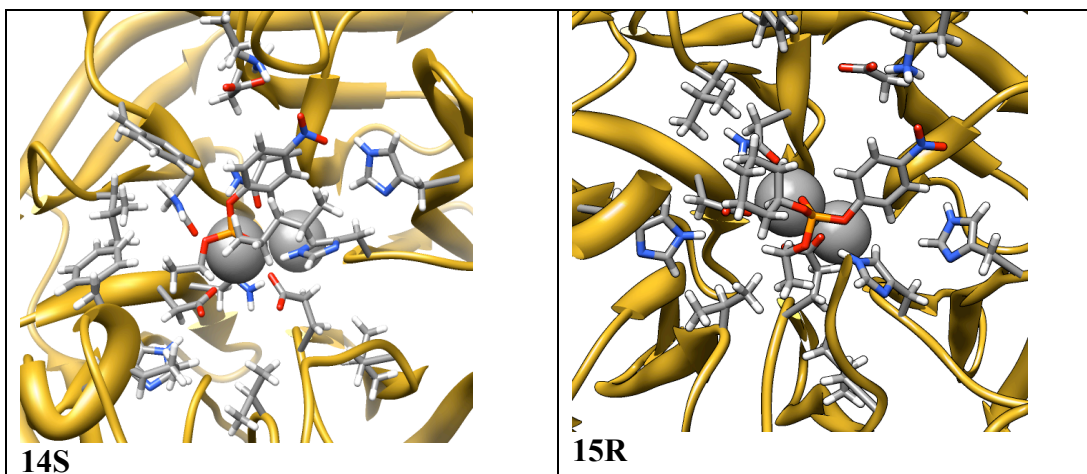
The non-polar (SA) terms were estimated using the MSMS algorithm⁵ using the equation $G_{\text{SA}} = \gamma \text{SASA} + \beta$, with γ and β set to 0.00542 kcal/(mol Å²) and 0.92 kcal/mol, respectively, and using a probe radius of 1.4 Å for estimating the solvent accessible surface area. For the polar (G_{polar}) energy terms, the Generalized Born and Poisson-Boltzmann methods were both utilized as implemented in the AMBER software package. In the GB calculations, dielectric constants of 1 and 78.5 were utilized with AMBER mboni2 radii. The TS_{solute} term represents temperature and solute entropy, and in these calculations this term was omitted. As the binding energies were only compared within ligand families, the effect of entropy changes was estimated to be minimal. Such methods have been employed in estimating binding energies for organic molecules with good agreement with experimental data.^{6,7}

Group I









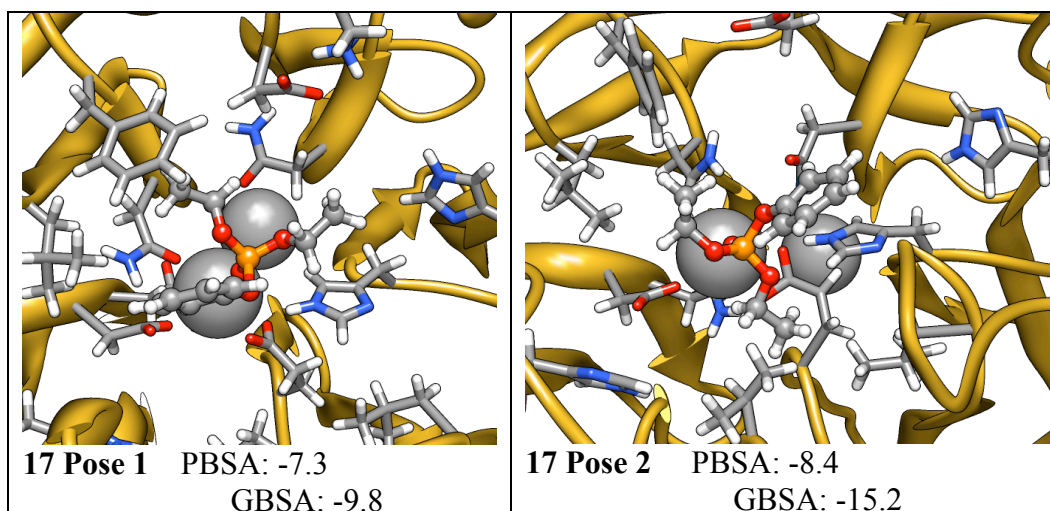
The energies obtained for poses of the group I molecules are shown in Table S1. The energy trend is consistently favorable for the orientation with the leaving group pointing toward the H115/H134/K192 region of the active site pocket.

Table S1. Energies determined for bound poses of the group I molecules bound in the G2E6 model of PON1, for the two primary orientations obtained. (MM-PBSA/MM-GBSA, respectively, in kcal/mol)

Molecule:	Leaving Group Orientation:	
	H115/K192 Pocket	H285 Pocket
Paraoxon (1)	-17.5/-20.5	-13.4/-17.9
6	-13.4/-17.7	a
7R	-16.2/-20.8	a
7S	-14.6/-28.0	a
8R	-20.4/-23.1	a
8S	-22.8/-28.4	-13.1/-21.1
9R	-15.7/-19.7	a
9S	-20.1/-28.8	a
10	-19.1/-25.7	-18.7/-20.3
14R	-20.3/-33.4	-15.1/-22.0
14S	-18.6/-28.8	a
15R	-28.3/-31.5	a

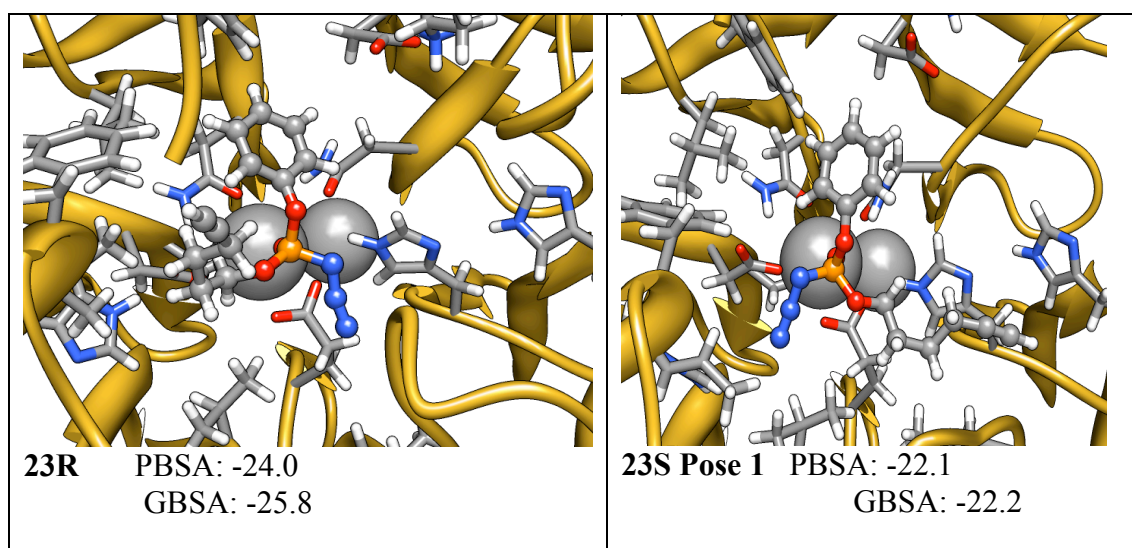
a - No pose determined in this pocket

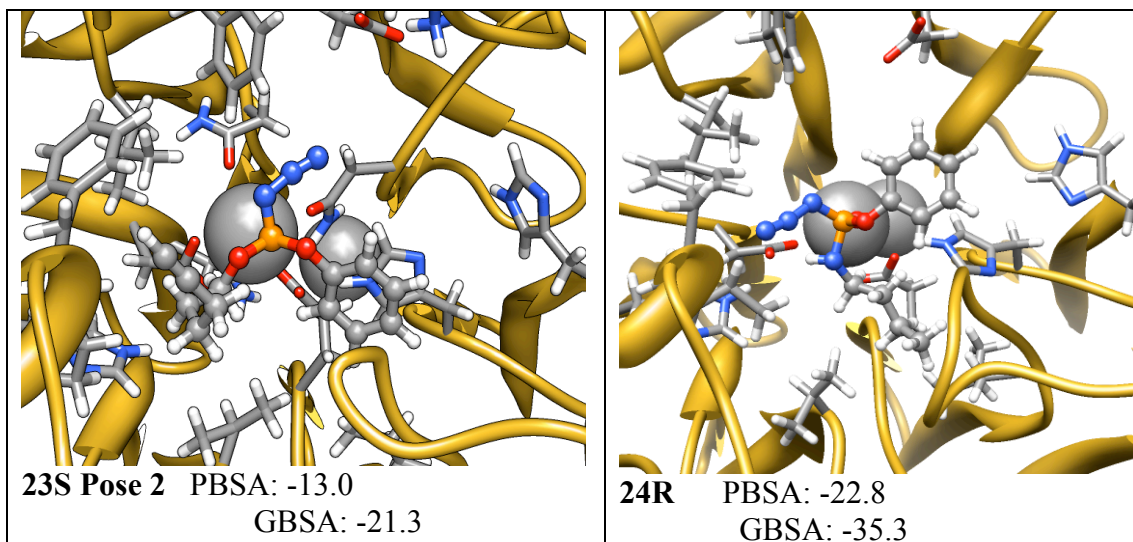
Group II



For the group II molecules, the lack of any electrostatic interactions with either pocket reduced the overall binding energies compared with paraoxon, but the poses do appear to be generally similar to those for the group I molecules.

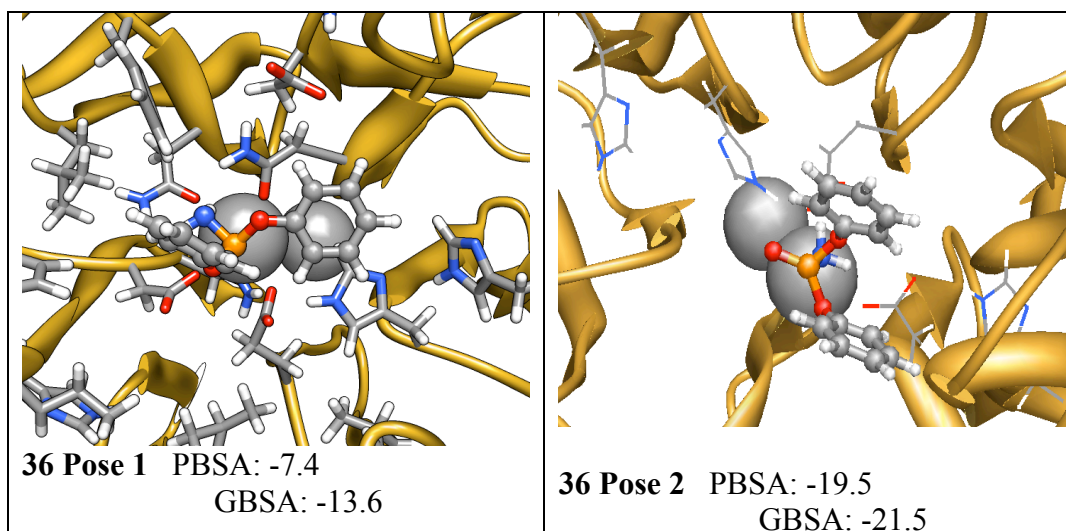
Group III





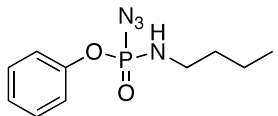
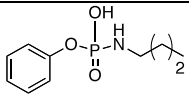
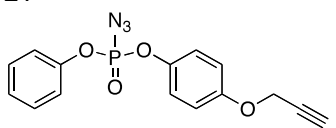
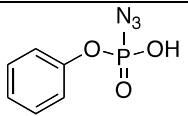
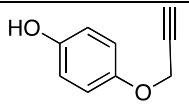
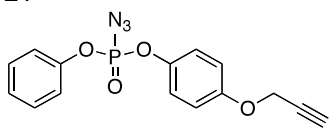
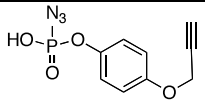
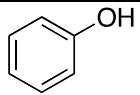
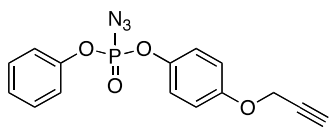
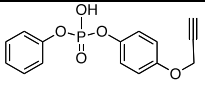
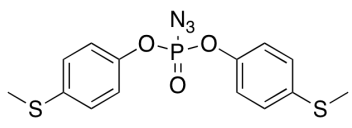
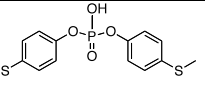
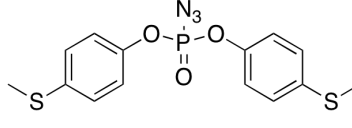
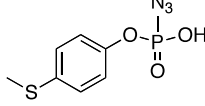
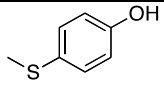
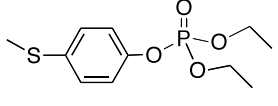
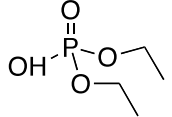
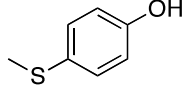
For the group III molecules the energetic preference was again similar, with electrostatic interactions observed between the azide and active site residues, specifically the aspartates and histidine 115. The leaving group is again positioned for hydrolysis by bases in proximity to D269 or E53.

Group V



7. The $\Delta H_{298, \text{hydrol}}$ for the hydrolysis of representative ligands from each group of molecules by water was computed using density functional theory (DFT – B3LYP/6-31G*) using the Gaussian03 suite of programs.^{8,9}

Molecule	Hydrolysis Products	ΔH_{hydrol} kcal/mol	Comment
1 			-6.9 Favorable
10 			-6.8 Favorable
8 			-6.8 Favorable
9 			-6.6 Favorable
23 			-4.9 Favorable
23 	HN ₃		+11.4 Unfavorable
24 			-3.9 Favorable

24		HN ₃		+12.6	Unfavorable
27				-4.5	Favorable
27				-5.4	Favorable
27			HN ₃	+12.1	Unfavorable
29			HN ₃	+11.6	Unfavorable
29				-5.4	Favorable
32				-4.6	Favorable

8. References

1. K. Law, R. A. Acey, C. R. Smith, R. Cameron, D. A. Benton, S. Soroushian, R. Eckenrod, R. Stedman, K. A. Kantardjief, K. Nakayama. *Biochem. Biophys. Res. Commun.* **2007**, 355, 371-378.
2. M. Blum, F. Löhr, A. Richardt, H. Rüterjans, G. C-H Chen *J. Am. Chem. Soc.* **2006**, 128, 12750-12757.
3. R. Luo, L. David, M. K. Gilson. *J. Comput. Chem.* **2002**, 23, 1244-1253.

4. J. Weiser, P. S. Shenkin, W. C. Still. *J. Comput. Chem.* **1999**, *20*, 217–230.
5. M. F. Sanner, A. J. Olson, J. Spehner. *Biopolymers* **1996**, *38*, 305-320.
6. R. C. Rizzo, T. Aynechi, D. A. Case, I. D. Kuntz. *J. Chem. Theory. Comput.* **2006**, *2*, 128-139.
7. B. Kuhn, P. Gerber, T. Schulz-Gasch, M. Stahl. *J. Med. Chem.* **2005**, *48*, 4040-4048.
8. (a) D. A. Becke. *J. Chem. Phys.* **1993**, *98*, 5648-5656. (b) C. Lee, W. Yang, R. G. Parr. *Phys. Rev. B* **1998**, *37*, 785-789.
9. Gaussian 03, Revision C.02, Frisch, M. J.; Trucks, G. W.; Schlegel, H. B.; Scuseria, G. E.; Robb, M. A.; Cheeseman, J. R.; Montgomery, Jr., J. A.; Vreven, T.; Kudin, K. N.; Burant, J. C.; Millam, J. M.; Iyengar, S. S.; Tomasi, J.; Barone, V.; Mennucci, B.; Cossi, M.; Scalmani, G.; Rega, N.; Petersson, G. A.; Nakatsuji, H.; Hada, M.; Ehara, M.; Toyota, K.; Fukuda, R.; Hasegawa, J.; Ishida, M.; Nakajima, T.; Honda, Y.; Kitao, O.; Nakai, H.; Klene, M.; Li, X.; Knox, J. E.; Hratchian, H. P.; Cross, J. B.; Bakken, V.; Adamo, C.; Jaramillo, J.; Gomperts, R.; Stratmann, R. E.; Yazyev, O.; Austin, A. J.; Cammi, R.; Pomelli, C.; Ochterski, J. W.; Ayala, P. Y.; Morokuma, K.; Voth, G. A.; Salvador, P.; Dannenberg, J. J.; Zakrzewski, V. G.; Dapprich, S.; Daniels, A. D.; Strain, M. C.; Farkas, O.; Malick, D. K.; Rabuck, A. D.; Raghavachari, K.; Foresman, J. B.; Ortiz, J. V.; Cui, Q.; Baboul, A. G.; Clifford, S.; Cioslowski, J.; Stefanov, B. B.; Liu, G.; Liashenko, A.; Piskorz, P.; Komaromi, I.; Martin, R. L.; Fox, D. J.; Keith, T.; Al-Laham, M. A.; Peng, C. Y.; Nanayakkara, A.; Challacombe, M.; Gill, P. M. W.; Johnson, B.; Chen, W.; Wong, M. W.; Gonzalez, C.; and Pople, J. A.; Gaussian, Inc., Wallingford CT, 2004.